The role of papain-like cysteine proteases of tomato in pathogen defense

Inaugural–Dissertation

zur
Erlangung des Doktorgrades

der Mathematisch-Naturwissenschaftlichen Fakultät

der Universität zu Köln

vorgelegt von

Muhammad Ilyas

aus Faisalabad (Pakistan)

Köln, Juni 2014

Diese Arbeit wurde am Max-Planck-Institut für Züchtungsforschung in Köln, in der Arbeitsgruppe von Dr. Renier van der Hoorn, Abteilung Molekulare Phytopathologie (Direktor: Prof. Dr. Paul Schulze-Lefert) angefertigt.

Berichterstatter:	Prof. Dr. Paul Schulze-Lefert
	Prof. Dr. Ute Höcker
	Dr. Matthieu H. A. J. Joosten
Prüfungsvorsitzender:	Prof. Dr. Ulf-Ingo Flügge
Tag der Disputation:	22 Juni 2012

To my parents & family
To my Shaista
To my 'Colonian princess' Zoha Khan

Publications

1. Ilyas, S., **Ilyas, M.,** Van der Hoorn, R. A. L., and Mathur, S. **(2013)** Selective conjugation of proteins in mining the active proteome through click-functionalized magnetic nanoparticles. **ACS Nano** 7, 9655-9663.

2. Hörger A. C., **Ilyas, M**., Stephan, W., Tellier, A., Van der Hoorn, R. A.L and Laura E. Rose. **(2012)** Balancing selection at the tomato *RCR3* gene family maintains variation in strength of pathogen defense. **PLoS Genetics** 8, e1002813.

3. Lozano-Torres, J., Wilbers, Ruud H. P., Gawronski, P., Boshoven, J., van't Klooster, J. W., H., Baranowski, L., **Ilyas, M.,** Van der Hoorn, R. A.L., Schots, A., de Wit, Pierre J. G. M., Bakker, J., Goverse, A., and Smant G. **(2012)** Dual *Cf-2*-mediated resistance in tomato requires a common virulence target of two plant pathogens. **Proc. Natl. Acad. Sci. USA** 109, 10119-10124.

4. Bozkurt, T., Schornack, S., Win, J., Shindo, T., **Ilyas, M.,** Oliva, R., Cano, L., Jones, A. M. E., Huitema, E., Van der Hoorn, R. A. L, and Sophien Kamoun**, (2011)** *Phytophthora infestans* effector AVRblb2 prevents focal secretion of a plant immune protease. **Proc. Natl. Acad. Sci. USA** 108, 20832-20837.

5. Kaschani, F., Shabab, M., Bozkurt, T., Shindo, T., Schornack, S., Gu, C., **Ilyas, M.,** Win, J., Kamoun, S., and Van der Hoorn, R. A. L. **(2010)** An effector-targeted protease contributes to defense against *Phytophthora infestans* and is under diversifying selection in natural hosts. **Plant Physiol.** 154, 1794-1804.

6. Van der Hoorn, R. A. L., Gu, C., **Ilyas, M.,** Kolodziejek, I., Kumari, S., Misas- Villamil, J. C., Pruzinska, A., Richau, K., Shabab, M., Shindo, T., Wang, Z. and Kaschani, F. **(2010)** Mining the active proteome in plant-pathogen interactions. In: Biology of Plant-Microbe Interactions, Volume 7. H. Antound, T. Avis, L. Brisson, D. Prevost, and M. Trepanier, eds. International Society for Molecular Plant-Microbe Interactions, St. Paul, MN.

7. Song, J., Win, J., Tian, M., Schornack, S., Kaschani, F., **Ilyas, M.,** Van der Hoorn, R. A. L., and Kamoun, S. **(2009)** Apoplastic effectors secreted by two unrelated eukaryotic plant pathogens target the tomato defense protease RCR3. **Proc. Natl. Acad. Sci. USA** 106, 1654-1659.

List of figures

Abbreviations

35S	double 35S promoter of CaMV
%	percent
::	fused to (in the context of gene fusion constructs)
°C	degree Celsius
3´	three prime end of a DNA fragment
5´	five prime end of a DNA fragment
ABPP	activity-based protein profiling
AF	apoplastic fluid
Avr	avirulence
Bio	biotin
bp	base pair(s)
BSA	bovine serum albumin
BTH	benzothiadiazole
cDNA	complementary DNA
C.f	*Cladosporium fulvum*
dH_2O	deionised water
DNA	deoxyribonucleic acid
dNTP	deoxynucleosidetriphosphate
dpi	day-post-infection
dpt	day-post-treatment
DTT	dithiothreitol
E-64	(2S,3S)-3-(N-{(S)-1-[N-(4-guanidinobutyl)carbamoyl]3-methylbutyl}carbamoyl) oxirane-2-carboxylic acid
EDTA	ethylenediaminetetraacetic acid
ER	endoplasmic reticulum
Fig.	Figure
HR	hypersensitive response
HRP	horseradish peroxidase
kb	kilobase(s)
kDa	kiloDalton(s)
LE	leaf extract
M	molar (mol/l)
min	minute(s)
mM	millimolar
MM	Money Maker
mRNA	messenger RNA
N	amino-terminal
NPC	no-probe control
OD	optical density
PAGE	polyacrylamide gel-electrophoresis
PBS	phosphate buffered-saline
PCD	programmed cell death
PCR	polymerase chain reaction
pH	negative decimal logarithm of the H^+ concentration
PIP1	*Phytophthora* inhibited protease I

PLCPs	papain-like cysteine proteases
PR	pathogenesis related
Pst	*Pseudomonas syringae* pv. *tomato*
pv.	Pathovar
PVDF	Polyvinylidene fluoride
PVX	Potato Virus X
qRT-PCR	quantitative reverse-transcriptase polymerase chain reaction
R	resistance
Rcr3	Required for *C. fulvum* resistance 3
rcr3-3^{pim}	rcr3- S. pimpinellifolium
Rcr3^{chil}	Rcr3-S. chilense
Rcr3^{hab}	Rcr3-S. habrochaites
Rcr3^{lyc}	Rcr3- S. lycopersicum
Rcr3^{pim}	Rcr3- S. pimpinellifolium
Rh	rhodamine
RNA	ribonucleic acid
RNAi	RNA interference
rpm	rounds per minute
RT-PCR	reverse transcription-polymerase chain reaction
RuBisCO	ribulose-1,5-bisphosphate carboxylase/oxygenase
SA	salicylic acid
SDS	sodium dodecyl sulphate
sec	second(s)
SP	signal peptide
TBS	Tris buffered saline
T-DNA	transfer DNA
TMV	Tobacco Mosaic Virus
TRV	Tobacco Rattle Virus
VIGS	virus-induced gene silencing
Vir	virulence
WT	wild-type
μ	micro

Abstract

Recognition and induction of plant immune responses by microbial pathogens is a dynamic process that requires signalling mechanisms associated with defense. Tomato is a host for the fungus *Cladosporium fulvum* and the oomycete *Phytophthora infestans*. The *Cf2* resistance gene of tomato confers recognition of the *Avr2* avirulence gene of *Cladosporium fulvum*. The *Avr2* gene encodes a small secreted protein that inhibits the cysteine proteases Rcr3 and PIP1 in the apoplast of tomato leaves. The perception mechanism involving PIP1 is not yet fully understood. Rcr3, on the other hand, is required for *Cf2*-mediated perception of Avr2. This indirect perception mechanism is consistent with the guard model, which predicts that Rcr3 is a virulence target of Avr2, guarded by the *Cf2* resistance gene product. The higher abundance of PIP1 compared to Rcr3, however, suggests that Rcr3 is rather a decoy that only functions in Avr2 perception. Here we show that silencing of *PIP1* in the transgenic tomato enhances *C. fulvum* susceptibility, whereas *rcr3* mutant plants do not show increased susceptibility in the absence of *Cf2*, consistent with the decoy model.

Rcr3 and PIP1 are also inhibited by Epic1 and Epic2B, which are secreted cystatin-like proteins produced by *P. infestans* during infection. Epics are not recognized through the Rcr3-Cf2 perception system, but *Cf2/rcr-3-3* mutant plants are more susceptible for *P. infestans* when compared to *Cf2/Rcr3* plants, suggesting a role for Rcr3 in *P. infestans* resistance in the absence of Epic recognition. Here we found that *Cf0/rcr3-3* mutant plants are also more susceptible to *P. infestans* when compared to *Cf0/Rcr3* plants. The *Cf0/Rcr3* plants are even more resistance when compared to *Cf2/Rcr3* plants indicating that other genetic factors in addition to *Rcr3* contribute to *P. infestans* immunity.

In the last part of this thesis we studied the role of natural variation in Rcr3 and PIP1 in the interaction with Avr2, Epic1 and Epic2B. We show that part of the diversity observed in Rcr3 plays a role in differential interactions with the effectors and may be important in pathogen recognition. In contrast, only slight phenotypic differences could be observed between allelic variants of PIP1, which may be due to conservation of PIP1 function.

In conclusion, the role of Rcr3 and PP1 in immunity and observed natural variation in Rcr3 and PIP1 affecting interactions with inhibitors illustrate an interesting protease-inhibitor arms race at the plant-pathogen interface.

Zusammenfassung

Die Erkennung und darauffolgende Aktivierung der pflanzlichen Immunabwehr durch mikrobielle Pathogene ist ein dynamischer Prozess, der auf Signalmechanismen basiert, die mit der Immunantwort assoziiert sind. Die Tomate ist eine Wirtspflanze für den Schimmelpilz *Cladosporium fulvum* und den Eipilz *Phytophthora infestans*. Das Resistenzgen *Cf2* in Tomaten ist an der Erkennung des Avirulenzfaktors Avr2, der von *C. fulvum* produziert wird, beteiligt. Das *Avr2*-Gen kodiert für ein kleines, sekretiertes Protein, das im Interzellularraum des Tomatenblattes die Cysteinproteasen Rcr3 und PIP1 inhibiert. Der Erkennungsmechanismus, an dem PIP1 beteiligt ist, ist bislang noch ungeklärt, über die Rolle von Rcr3 im Erkennungsmechanismus von *C. fulvum* sind jedoch mehr Kenntnisse vorhanden. Rcr3 wird für die indirekte Erkennung von Avr2 über das Resistenzgen Cf2 benötigt. Dieser indirekte Erkennungsmechanismus ist konform mit der sogenannten „Guard-Hypothese" („Wächter-Hypothese"), nach welcher Rcr3 ein Zielmolekül des Virulenzfaktors Avr2 ist und gleichzeitig durch das Resistenzprotein Cf2 „bewacht" wird. Die Dominanz von PIP1 im Interzellularraum der Tomatenpflanze verglichen mit Rcr3 spricht jedoch mehr dafür, dass Rcr3 eigentlich die Rolle eines Lockmittels innehat, das die Erkennung von Avr2 ködert. Die Ergebnisse dieser Arbeit zeigen, dass Stillegung des *PIP1*-Gens die Anfälligkeit transgener Tomatenpflanzen gegenüber Infektion mit *C. fulvum* verstärkt, wohingegen mutierte Pflanzen, die kein funktionelles Rcr3 besitzen (*rcr3-3* Genotyp), in Abwesenheit von Cf2 keine erhöhte Anfälligkeit besitzen, was konform mit der „Decoy-Hypothese" („Köder-Hypothese") ist.

Rcr3 und PIP1 können auch durch Epic1 und Epic2B, zwei cystatinartige Virulenzfaktoren, die vom Eipilz *P. infestans* während einer Infektion produziert werden, inhibiert werden. Diese Epic-Proteine werden nicht über den Rcr3-Cf2-Erkennungsmechanismus erkannt. Jedoch sind Pflanzen mit *Cf2/rcr-3-3* Genotyp im Vergleich zu Pflanzen mit *Cf2/Rcr3* Genotyp anfälliger gegenüber *P. infestans*. Dies lässt auf eine Beteiligung von Rcr3 bei der Abwehr von *P. infestans* ohne Erkennung der Epic-Proteine schließen. Desweiteren zeigen die Ergebnisse dieser Arbeit, dass Pflanzen mit dem Genotypen *Cf0/rcr3-3* ebenfalls anfälliger gegenüber *P. Infestans* im Vergleich zu Pflanzen mit dem Genotypen *Cf0/Rcr3* sind und *Cf0/Rcr3*-Pflanzen sogar noch ein höheres Maß an Resistenz aufweisen als Pflanzen mit dem Genotypen *Cf2/Rcr3*. Dies deutet darauf hin, dass neben *Rcr3* weitere genetische Faktoren am

Abwehrmechanismus von *P. Infestans* beteiligt sind.

Der letzte Teil dieser Arbeit befasst sich mit der natürlichen Sequenzvariation, die *Rcr3* und *PIP1* zu eigen ist, und deren Auswirkung auf die Interaktion mit Avr2, Epic1 und Epic2B. Die Ergebnisse dieser Studie zeigen, dass ein Teil dieser Variation im *Rcr3*-Gen eine Rolle bei der Interaktion mit den genannten Effektoren spielt und daher eine wichtige Funktion bei der Pathogenerkennung innehaben könnte. Im Gegensatz dazu hat die Sequenzvariation des *PIP1*-Gens nur geringe Auswirkungen auf den Phänotypen. Dies ist möglicherweise auf starke Konservierung der Funktion von PIP1 zurückzuführen.

Zusammenfassend veranschaulichen die Rolle, die Rcr3 und PIP1 in der pflanzlichen Immunabwehr innehaben, sowie die Sequenzvariation, die beiden Proteinen zu eigen ist und die Auswirkungen auf die Wechselwirkung mit Effektoren hat, wie bedeutend der Wettstreit von Proteasen und deren Inhibitoren bei der Interaktion von Pflanzen und ihren Pathogenen ist.

Chapter 1- Introduction

1.1 The plant immune system

1.1.1 Strategies of plant pathogens

Plants are constantly in contact with a wide range of pathogens from the environment, including bacteria, viruses, fungi, nematodes, insects and oomycetes. These pathogens have adopted different strategies and life styles. Combating these permanent threats is essential for fitness and reproduction of plants. However, the majority of pathogenic attacks fail to cause disease symptoms. The unsuccessful attack is mainly due to the absence of a correct environment provided by the plants for pathogen growth and development. Pathogens may also lack the basic pathogenicity molecules that would enable pathogens to colonise and spread the disease in plants (Heath, 2000). Plant pathogens are generally classified into biotrophic and necrotrophic, depending on their feeding style. While necrotrophic pathogens feed on nutrients derived from dead plant tissues, biotrophic pathogens require living host to colonize (Glazebrook, 2005; Jones *and* Dangl, 2006; Kamoun, 2007). Biotrophic pathogens also tend to be host-specialized since they only infect a few plant species and not a broad host range (Schulze-Lefert and Panstruga, 2011). The reason that biotrophic pathogens are so destructive is because they overcome plant resistance in the field and sometimes jump to a new host. This is a very important feature for pathogen success, although other aspects of life cycles also make them very successful. Other pathogens behave initially as biotrophs and later switch to a necrotrophic life style, and are classified as hemibiotrophs. Pathogens employ different infection strategies including haustoria, a feeding structure of oomycetes and fungi commonly used to invaginate with host cells. Pathogenic bacteria often enter the tissue through natural openings like stomata or wounds and proliferate in the intercellular compartments between host cells (Lipka et al., 2010; Nurnberger *and* Lipka, 2005).

Some plants are not a host for some pathogens. For instance, tomato leaf mould, (*Cladosporium fulvum*) can infect tomato (*Solanum lycopersicum*) but not the related species potato (*Solanum tubersum*). When all individuals in a plant species are resistant to all races of

a particular pathogen, the resistance is called non-host resistance. Non-host resistance represents the most robust and durable form of plant immunity and has been proposed to comprise of successive layers including constitutive plant barriers as well as inducible reactions (Lipka et al., 2010; Nurnberger and Lipka, 2005; Thordal-Christensen, 2003). Most living organisms express effective defenses against pathogens to enhance their probability of survival and reproduction. These defenses include protective layers like the cuticle in plants, which serve as constitutive barriers against pathogen penetration.

1.1.2 PAMP-triggered immunity (PTI)

If a pathogen successfully overcomes constitutive plant defense barriers they are often recognized by pattern recognition receptors (PRRs) in the plasma membrane. PRRs perceive slowly evolving, highly conserved microbial molecules, the microbe-associated molecular patterns (MAMPs), sometimes also called pathogen-associated molecular patterns (PAMPs) or herbivore-associated molecular patterns (HAMPs). MAMPs are common and essential for microbe viability and exist in both pathogenic and non-pathogenic microbes. MAMP recognition is the first inducible layer of the plant immune system (Bent and Mackey, 2007; Chisholm et al., 2006; Dodds *and* Rathjen, 2010; Hogenhout *and* Bos, 2011; Jones *and* Dangl, 2006). MAMPs are indispensable for the pathogen and well-studied examples are lipopolysaccharides (LPS), flagellin, and elongation factor Tu (EF-Tu) from bacteria; chitin, and xylanase from fungi and cell wall β-glucan, Pep-13 and heptaglucosides from oomycetes (Boller *and* Felix, 2009; Schwessinger *and* Zipfel, 2008). PRRs receptors are characterized by the presence of an extracellular ligand-binding domain, a single membrane spanning domain and an intracellular kinase-signaling domain (Lipka et al., 2007). The best studied PRR is the membrane-associated receptor-like kinase (RLK) FLS2 (FLAGELLIN-SENSING 2) of Arabidopsis, which recognizes a fragment of bacterial flagellin (Gómez-Gómez *and* Boller, 2000). This 22 amino-acid peptide (flg22) is highly conserved at the amino terminus of flagellin (Felix et al., 1999). Another PRR is the receptor-like kinase EFR (EF-Tu Receptor), which is only present in Arabidopsis and recognizes elongation factor EF-Tu (Zipfel et al., 2006). Furthermore, the LysM-RLK CERK1 in Arabidopsis and CEBiP in rice are PRRs that perceive the fungal cell wall component chitin (Petutschnig et al., 2010). MAMPs perception induces rapid ion fluxes across the plasma membrane and production of reactive oxygen

species (ROS) and nitric oxide (NO) production. The activation of mitogen-activated protein (MAP) kinase cascades leads to signals to the plant-cell nucleus, culminating in transcriptional reprogramming of defense-related genes, and the induction of PTIs (Asai et al., 2002; Chinchilla et al., 2007; Chisholm et al., 2006; Lipka et al., 2007; Mészáros et al., 2006). The activation of basal defense responses upon PAMP-perception in compatible plant-pathogen interactions is very weak to stop infection. Nonetheless, many plant pathogens deploy PAMP perception mechanism for basal plant immune responses (Nurnberger *and* Lipka, 2005).

1.1.3 Effectors and Effector-triggered immunity (ETI)

Successful pathogens employ effector proteins to manipulate their host. A really interesting concept is that effectors are essentially acting as plant proteins; they function inside the plant cell, and operate as plant protein in the host even though the genes are encoded in the microbial genome (Kamoun, 2007; Kamoun and Smart, 2005). The current plant paradigm in the field is that studying effectors is important for understanding parasitism by bacteria, oomycetes, virus nematodes, and insects. Successful pathogens evolved strategies to suppress PTI by secreting effector molecules into the plant cell. These strategies include of receptor signaling, vesicle trafficking and modification of the organelle function. However, effectors can also help pathogens with spreading, nutrition uptake or manipulation of host development (Dodds and Rathjen, 2010).

In turn, plants possess resistance (R) proteins that specifically recognize effectors and trigger immune responses that results in resistance (Chisholm et al., 2006). This Effector-triggered immunity (ETI) is referred to as the second layer of plant immunity. ETI is often associated with programmed cell death at the site of pathogen infection (hypersensitive response, HR). Resistance proteins are divided into the following categories. NB-LRR resistance proteins form the largest resistance protein family, which contains a nucleotide binding domain (NB) and a leucine-rich repeat domain (LRR). The LRR domain has a conserved structure and is involved in specific protein-protein interactions. Based on the N-terminal domain, NB-LRR proteins are subdivided into coiled-coil (CC) and Toll-interleukin-1 receptor (TIR) proteins

(Takken et al., 2006). Examples of NB-LRR proteins are RPM1, RPS2 and RPS5, which recognize bacterial effectors AvrRpm1, AvrRpt2, and AvrPphB respectively.

The second largest family of resistance proteins contains extracellular leucine-rich repeats. These resistance proteins are divided into two subclasses: receptor-like proteins (RLPs) and receptor-like kinase (RLKs). RLPs contain an extracellular LRR domain and a transmembrane region; whereas RLKs also carry an intracellular protein kinase domain. Examples of RLPs are Cf-2, Cf-4, and Cf-9 of tomato which confer recognition of fungal effector Avr2, Avr4 and Avr9 respectively.

1.2 Gene-for-gene interaction

Almost 60 years ago, a pioneering 'gene-for-gene' model of plant disease resistance was proposed by Harold Flor in 1946. In his work with flax and flax rust, he proposed that for each dominant plant-encoded *R* gene there is a corresponding dominant pathogen-encoded *Avr* gene. Avirulent interactions are incompatible and do not result in disease. A compatible interaction, which results in disease, occurs when there is either no plant *R* gene or pathogen *Avr* gene. Gene-for-gene interactions have been defined for numerous plant-pathogen interactions including viruses, fungi, bacteria and nematodes (Flor, 1971; Sidhu, 1987).

Perhaps due to the unusual host specialization, several gene-for-gene interactions have been studied with respect to obligate biotrophic pathogens (Flor, 1956; Rairdan and Moffett, 2007). Especially in crop plants like barley, flax, rice, tomato and potato, gene-for-gene interaction gained a great deal of attention, because they were used for breeding resistant crops. Pathogen *Avr* genes are isolate-specific and encode structurally diverse effector proteins. *R* gene-mediated immunity is also called ETI. Once an effector protein is recognized, the infected plant cell then initiates a so-called hypersensitive response (HR), which bears hallmarks of programmed cell death. The sacrifice of attacked cells deprives the pathogen of nutrients and access to other cells, preventing the establishment of an infection (Nimchuk et al., 2003)
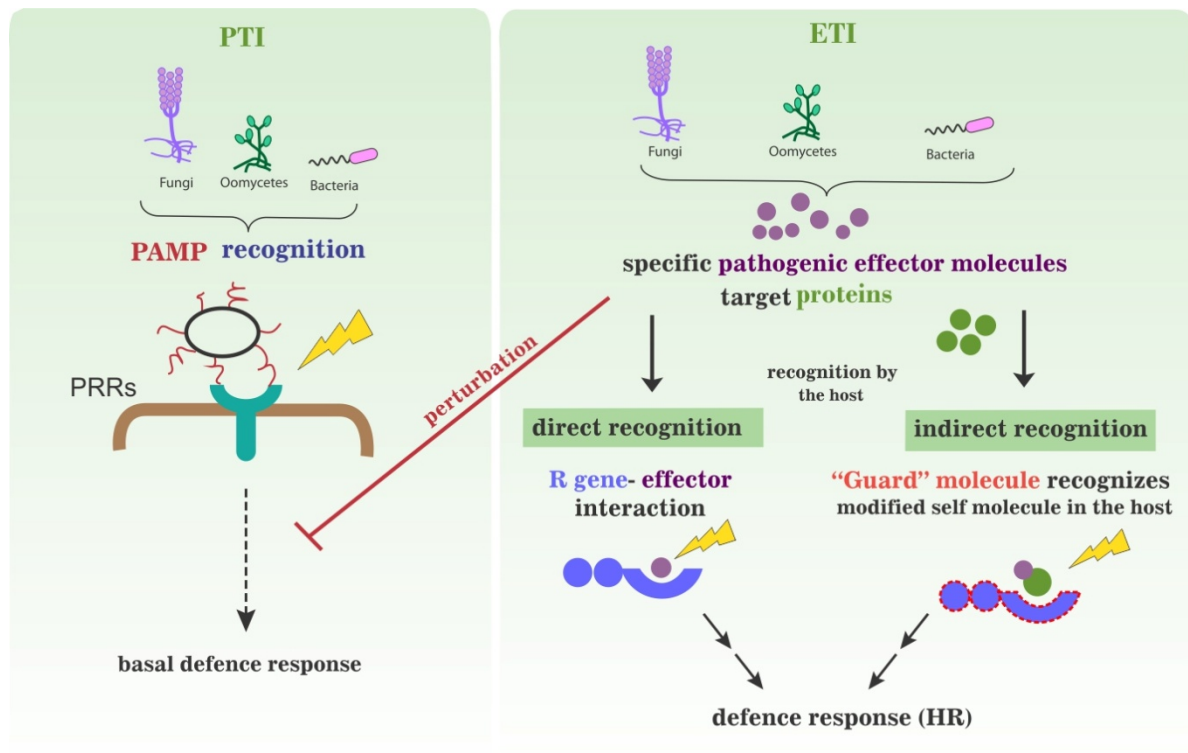
Figure 1 | Schematic overview of the two layers in plant innate immunity

1.2.1 Direct recognition

The simple biochemical interpretation of the gene-for-gene model suggests that *Avr/R* gene products interact directly and trigger HR. However, direct binding of plant resistance proteins to their cognate effector proteins has been experimentally verified in only a few cases. For instance, physical interaction between the rice (*Oryza sativa*) resistance protein Pi-ta and its cognate effector protein AvrPita from the fungal pathogen *Magnaporthe grisea* was demonstrated in yeast-two-hybrid and *in vitro* binding assays (Jia et al., 2000). *Pi-ta* encodes a cytoplasmic NB-LRR protein and *AvrPita* encodes a putative metalloprotease. Remarkably, single amino acid substitutions in LRR domain in the plant R protein abolished interaction between the two proteins, indicating that Pi-ta binds Avr-Pita via its LRR domain (Jia et al., 2000). There is an important limitation to effector perception mechanisms based on direct recognition. The direct recognition of Avr/R components implies that plants must carry an array of *R* genes to confer recognition of

millions of microbes. Since effectors are diverse and show only marginal similarity, millions of *R* genes would be required for the detection of effectors (Göhre et al., 2008; Hogenhout *and* Bos, 2011). However the *A. thaliana* Col-0 genome encodes only 149 NB-LRR proteins (Meyers et al., 2003). Therefore direct recognition is most likely not the common mode of recognition.

1.2.2 Indirect recognition

With the advancement of knowledge in the late 90s, another model for effector perception was proposed. This model was put forward by Van der Biezen *and* Jones (1998). According to this model, some resistance proteins act as 'guard' and monitor the modification of host targets by effectors. Many later examples supported the guard hypothesis. For example, in the *Pseudomonas syringae-Arabidopsis* system, two effector proteins, AvrRpml and AvrB, modify a common target, RIN4 (RPM1 INTERACTING PROTEIN 1), a plasma-membrane associated protein that negatively regulates basal defense responses (Desveaux et al., 2007). Hyperphosphorylation of RIN4 by AvrRpml or AvrB is recognized by the R protein RPMl (resistance to *P*. *syringae* pv. maculicola 1), which activates HR (Mackey et al., 2002). In this scenario, pathogen virulence factor targets are guardees protected by R proteins ("guards"). Several possible scenarios were predicted in favor of the guard hypothesis (Dangl *and* Jones, 2001; Jones *and* Dangl, 2006). The single guard (R protein) can recognize unrelated effectors targeting the same host protein (guardee). For instance, the RPM1 'guards' RIN4 which is manipulated by two effectors; AvrB and AvrRpm1 (Mackey et al., 2002). Another possible scenario is that the multiple NB-LRR proteins (guards) evolve to monitor the same host target. For instance, both RPM1 and RPS2 guard RIN4, and recognition is activated by cleavage of RIN4 by AvrRpt2 (Mackey et al., 2003). Another well-characterized example of the guard model involves R protein Cf2 of tomato. Tomato plants carrying Cf2 recognize the perturbation of defense-related host protein Rcr3, which is manipulated by Avr2, a small protein secreted by *C. fulvum.*
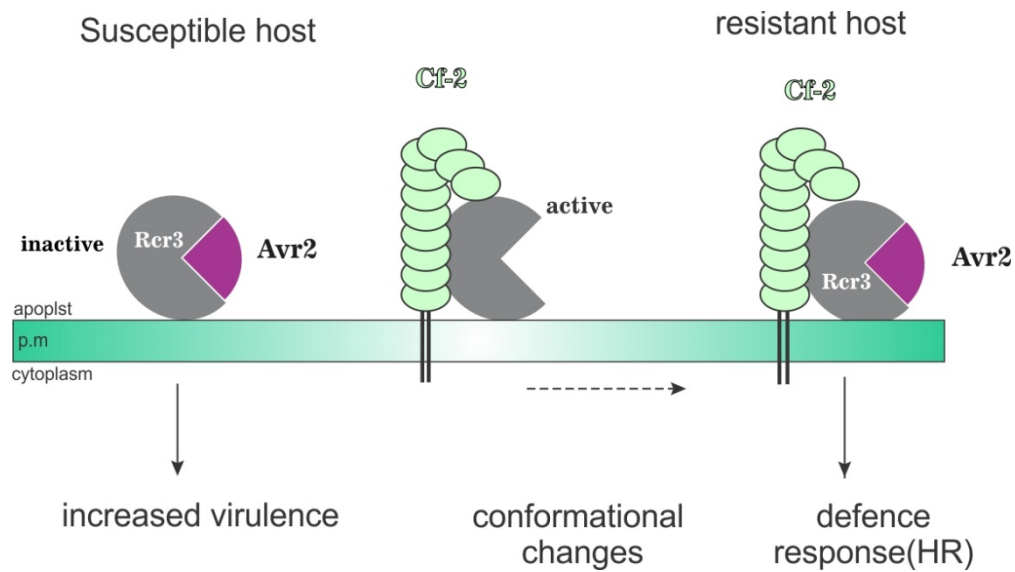
Figure 2 | Schematic representation of the Avr2-Rcr3-Cf-2 interaction

The pathogen *C. fulvum* secretes the effector Avr2 into the tomato apoplast. This protease inhibitor targets the plant protease Rcr3, which is thereby inactivated. In resistant hosts, the LRR protein Cf-2 gets activated upon putative conformational changes in Rcr3, which are caused by Avr2-binding. p.m (plasma membrane).

This indirect recognition of Avr2 by Cf2 leads to HR and resistance (Dangl *and* Jones, 2001; Rooney et al., 2005) (Fig. 3). Cf2 and Rcr3 are also required for the recognition of Gr-VAP1 (Venom Allergen-like Protein 1) from plant parasite nematode *Globodera rostochiensis*. Like Avr2, Gr-VAP1 binds to and inhibits Rcr3, and also this is recognized in a Cf2-dependent manner leading of HR (Lozano-Torres et al., 2012). Thus the plant immune receptor *Cf2* displays a dual resistance specificity that provides protection to tomato plants against a leaf mold fungus and a root-parasitic nematode. The dual resistance specificity of *Cf2* by guarding a common virulence target of unrelated pathogens illustrates the power of indirect recognition of pathogen-derived molecules.

The decoy hypothesis

In addition to Rcr3, Avr2 also inhibits PIP1. Rcr3 and PIP1 are closely related, salicylic acid-induced PLCPs in the tomato apoplast which dominate protease activity during defense. Since PIP1 is probably over 100-fold more abundant when compared to Rcr3, a decoy model has been proposed (van der Hoorn and Kamoun, 2008). According to this model, a host protein that mimics the operative target of an effector acts as a decoy and participate solely in effector perception (van der Hoorn *and* Kamoun, 2008). The absence of a role of Rcr3 in the absence of perception is supported by the fact that *Cf0/Rcr3* and *Cf2/rcr3* mutant plants were equally susceptible for *C. fulvum* (Dixon 2000). Three more examples have been described to support the decoy model: RPS2-RIN4-AvrRpt2 in Arabidopsis, Bs3-pBs3-AvrBs3 in pepper and Prf-Pto-AvrPto in tomato (van der Hoorn *and* Kamoun, 2008).

Decoys may have evolved independently or through a duplication of the target molecule. Since its actual function in the cell would be redundant with that of the real pathogen target and selective constraints would be relaxed, the mimic would thus simply contribute in effector perception. This is how decoy might have evolved. The decoy hypothesis is not in agreement with all data. However, for example, RIN4, has a guard-independent function in PAMP-triggered immunity (Kim et al., 2005), Additionally, mutant *rcr3* plants show enhanced susceptibility when infected with *P. infestans* suggesting an additional role of *Rcr3* in plant immune responses, even though *Cf2* does not confer recognition during *P infestans* infection (Song et al., 2009). As these assays demonstrate roles of guardee independent of R proteins, they cannot be merely decoys.
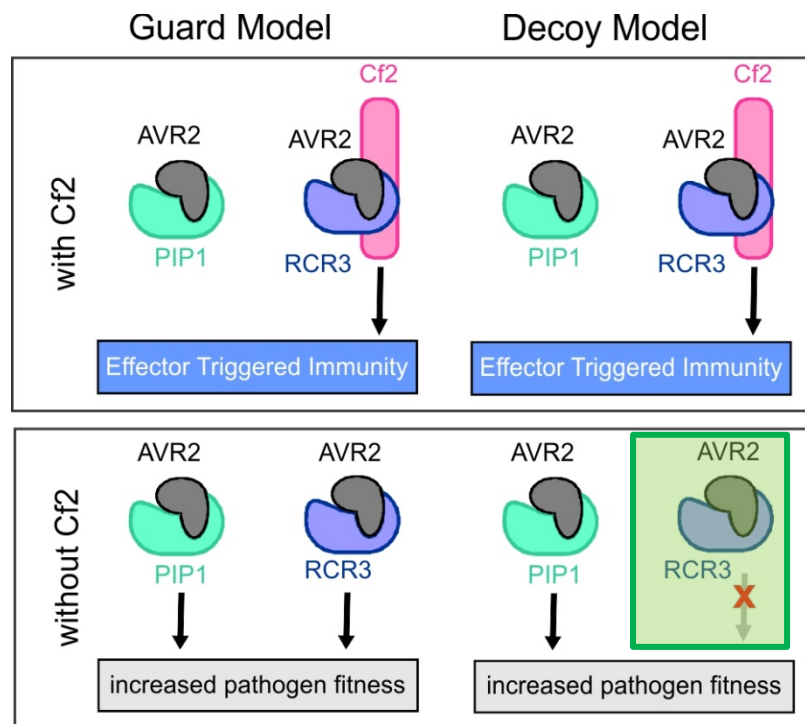
Figure 3 | Schematic overview of guard and decoy model for Avr2-Rcr3-Cf2

In the presence of the R protein (Cf2) top, the situation is identical between the guard and decoy hypothesis. However, in the absence of Cf2 (bottom) inhibition of Rcr3 contributes to pathogen fitness in the guard model but not in the decoy model.

1.2.3 *Cladosporium fulvum*-tomato pathosystem

C. fulvum (syn. *Passalora fulva*) is an asexual extracellular fungal pathogen that causes leaf mold disease on tomato. When conidia contact leaves they germinate and a runner hyphae grows in various directions over the leaf surface to penetrate open stomata. The hyphae enter through stomata and grow in the extracellular space of leaves for the major part of the life cycle (Bond, 1938; de Wit, 1977; Lazarovits and Higgins, 1976). The hyphae increases in diameter and grows in close contact with host cell while acquiring nutrients from the apoplast. Within the 10-14 days after the penetration, conidiophores emerge from the stomata carrying conidia. These conidia generally spread by wind and water splash. During this compatible interaction the fungus grows successfully and causes disease. During incompatible interactions the runner hyphae enters stomata but growth is arrested after two days because death of adjacent mesophyll cells (de Wit, 1977).

 The tomato-*C. fulvum* pathosystem has been extensively studied for 'gene-for-gene' interactions (Joosten and de Wit, 1999). To date four avirulence genes (*Avr)* has been cloned designated as *Avr2*, *Avr4*, *Avr4E* and *Avr9*. These avirulence genes encode small cysteine rich proteins that are secreted during infection. Their recognition is mediated in tomato by cognate R proteins, Cf2, Cf4, Cf4E and Cf9 respectively. Our current knowledge on how effector proteins are recognized and activate the defense by Cf proteins is very limited. For instance, host proteins that interact with Cf proteins before and after their activation by effectors are not known. Furthermore, it is also not known whether direct effector binding is required for effector recognition.

Silencing of *Avr2* in *C. fulvum* compromises virulence on tomato (van Esse et al., 2008). Other studies showed that heterologous expression of Avr2 in tomato promotes *C. fulvum* colonization and increases susceptibility to race 2 of *C. fulvum* (van Esse et al., 2008). Besides Avr2, other Ecp (Extracellular proteins) proteins play a role during infection Avr4 and Ecp6 contain chitin-binding motifs (Bolton et al., 2008; van den Burg et al., 2006). Avr4 is a chitin-binding lectin that protects fungal cell walls against hydrolysis by plant chitinases (van Den Burg et al., 2006). Recently, the abundantly secreted *C. fulvum* LysM domain–containing effector Ecp6 was shown to be required for full virulence (Bolton et al., 2008). Ecp6 proteins suppress the chitin-triggered host immunity by scavenging chitin fragment released during infection (de Jonge et al., 2010).

1.2.4 *Phytophthora infestans*-tomato pathosystem

Oomycete plant pathogens cause great economic losses of important crops such as potato and tomato (Haas et al., 2009). *P. infestans* belongs to the biotrophic oomycete plant pathogens and causes late blight, a devastating disease that causes a severe threat to food security. Potato late blight caused the Irish *potato famine* in 1840s. After landing of zoospores on the leaf surface, spores germinate and germ tubes form an appressorium that perforates the cuticle mediated by a structure called the penetration peg. Hyphae grow between mesophyll cells and penetrate host cells using haustoria. The haustoria invaginate the plasma membrane and enable the oomycete to acquire nutrients and facilitate the delivery of effector molecules to manipulate host functions. After successful infection, the plant tissue necrotizes, and sporangiophores and sporangia develop through the stomata to complete the life cycle (Fig 4).
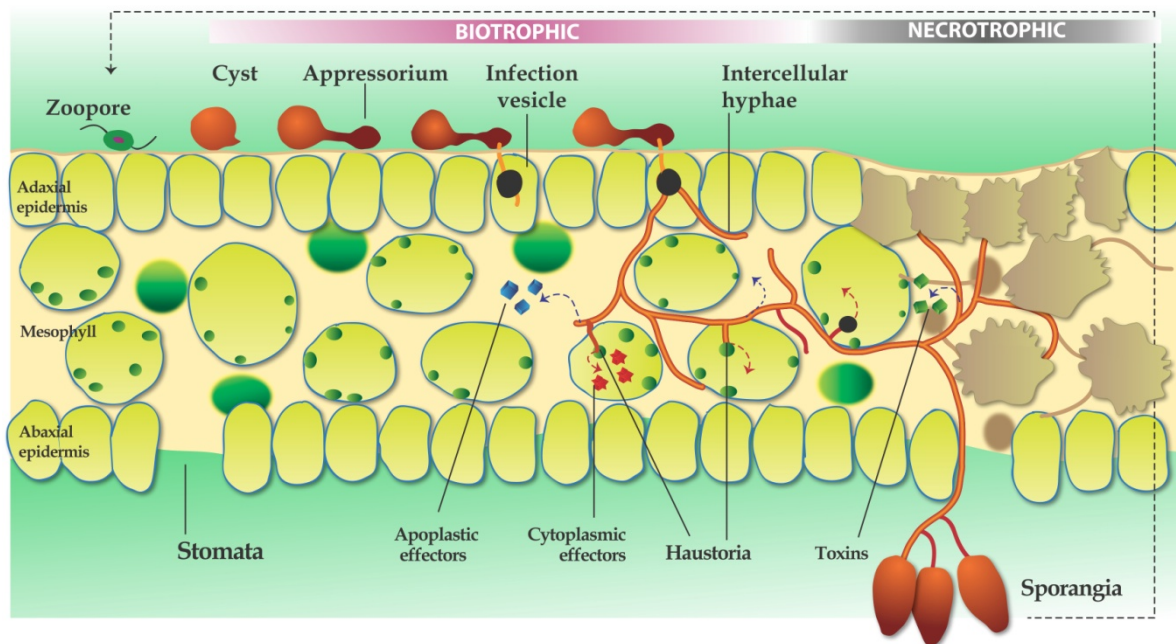
Figure 4 | Schematic illustration of infection cycle of the *P. infestans*

After landing of a spore on the plant leaf surface, an appressorium is formed which further develops into a penetration peg. The fungus attempts to penetrate the cuticle and cell wall of a single epidermal cell. In a compatible interaction, the fungus invaginates with the plasma membrane and forms a haustorium. The infection cycle is reinitiated with the formation of new sporangiophores that emerge from sporangia, spreading of new spores on other plant part.

P. infestans genome has been sequenced and this enabled the genome-wide identification of potential effector repertories (Haas et al., 2009; Kamoun, 2007). *P. infestans* secretes an array of effectors. Effectors are classified according to their presumed location into apoplastic and cytoplasmic effectors. Apoplastic effectors encounter hydrolytic host enzymes, such as proteases and glucanases and many pathogenesis-related proteins (van Loon et al., 2006). The cytoplasmic effectors are also known as host translocated effectors and often contain a highly conserved RxLR amino acid motif. There are 79 RxLR effectors in the *P. infestans* genome, which are highly expressed at 2-3 day-post infection (Haas et al., 2009; Halterman et al., 2010; Rehmany et al., 2005; Vleeshouwers et al., 2011). The CRN (Crinkler) effector family contains a conserved LFLAK amino acid motif. Some CRN effectors induce a necrotic phenotype ('crinkling') when ectopically expressed in plants (Haas et al., 2009). Both RxLR

and LFLAK motifs are required for translocation of effectors inside the cytoplasm of the host cell (Dou et al., 2008; Kamoun, 2007; Schornack et al., 2010).

P. infestans also secretes dozens of apoplastic effectors during infection. Several of these are protease inhibitors. EPI1 and EPI10 are secreted kazal-like serine protease inhibitors that inhibit the apoplastic subtilase protease P69B of tomato (Tian et al., 2005; Tian et al., 2004). In addition Epic1 and Epic2B are cystatin-like protease inhibitors that inhibit apoplastic Cys proteases, Rcr3, (Rooney et al., 2005), PIP1 (Tian et al., 2007), and C14 (Kaschani et al., 2010). C14 silenced plants are more susceptible for *P. infestans* indicating a role for C14 in pathogen defense (Kaschani et al., 2010). Interestingly, the RXLR effector AVRblb2 suppresses focal secretion of C14 around haustoria (Bozkurt et al., 2011). These findings illustrate that *P. infestans* evolved two distinct classes of apoplastic and cytoplasmic effectors that are structurally divergent and target the same plant defense components.

1.2.5 Papain-like cysteine proteases (PLCPs)

Rcr3, PIP1 and C14 are all papain-like cysteine proteases (PLCPs). PLCPs play crucial roles in plant-pathogen interactions (Shindo and Van Der Hoorn, 2008). PLCPs belong to clan CA, and family C1A of the proteases (http://merops.sanger.ac.uk). The name 'papain- like' is based on the high homology to papain, a protein which accumulates in papaya tree upon wounding (Brömme, 2001). PLCPs are usually 23-30 kDa in size and it has 21% beta sheets and 25% alpha helices. PLCPs have a catalytic cysteine residue to cleave peptide bonds in protein substrates. This catalytic cysteine is part of a catalytic triad, consisting of a cysteine, an asparagine and a histidine residue, situated in the middle of a cleft that binds the substrates through specific interactions (Drenth et al., 1968). PLCPs are produced as pre-pro proteases with an N-terminal auto-inhibitory domain (prodomain), which covers the substrate binding groove and needs to be proteolytically removed for protease activation (Taylor et al., 1995).

Activity-based protein profiling (ABPP) is a key technology to study PLCP activity. The probe DCG-04, is a biotinylated version of E-64, a mechanism-based inhibitor of papain-like cysteine proteases (PLCPs) (Greenbaum et al., 2000; Rooney et al., 2005; Shabab et al., 2008; van der Hoorn et al., 2004). ABPP with DCG-04 on apoplastic fluids of BTH-treated tomato plants resulted in the identification of seven PLCPs (Rcr3, PIP1, C14, CYP3, ALP, CatB1 and

CatB2) that belong to four distinct subfamilies. On the above mentioned PLCPs, only Rcr3, PIP1 and C14 will be introduced in this thesis.

Rcr3 and PIP1 are defense-related proteases because upon *C. fulvum* inoculation, the mRNA abundance of *Rcr3* is upregulated (Krüger et al., 2002) and also it has also been reported that *PIP1* is upregulated upon *P. infestans* infections (Tian et al., 2007). Interestingly, Rcr3 and PIP1 are both inhibited by Avr2, a small cysteine-rich effector protein secreted by *C. fulvum* (Rooney et al., 2005; Shabab et al., 2008). *P. infestans* EPICs also inhibit Rcr3 and PIP1 (Song et al., 2009; Tian et al., 2007). EPICs are cystatin-like proteins. EPICs are expressed at early biotrophic stages during infection of tomato or potato (Haas et al., 2009; Tian et al., 2007).

The C14 protease is similar to the C-terminal granulin domain containing RD21 protease in Arabidopsis. C14-like proteases accumulate in the vacuole and in vesicles and can act as a peptide ligase (Hayashi et al., 2001; Wang et al., 2008; Yamada et al., 2001). C14 is inhibited by chagasin-like RIP1 protein secreted by *P. syringae* (Kaschani and van der Hoorn, unpublished). Silencing of C14 proteases in *N. benthamiana* increases the susceptibility to *P. infestans* (Kaschani et al., 2010). Sequencing of alleles of these seven PLCPs in ten wild tomato species revealed that both PIP1 and Rcr3 are under diversifying selection, whereas the other PLCPs are under conservative selection (Shabab et al., 2008). However, C14 is under diversifying selection in natural host of *P. infestans* (Kaschani et al., 2010). The observation that induction and higher accumulation of plant proteases during plant-pathogen interaction is highlight the role of plant proteases in pathogen defense (Yamada et al., 2001).

1.2.6 Natural variation at *Rcr3*

Studies on natural variation at the *Rcr3* locus revealed that this gene exhibits a high level of inter- and intraspecific nucleotide diversity. Particularly the number of nonsynonmyous polymorphisms is elevated compared to neutral standards or other tomato papain-like cysteine proteases (Shabab et al. 2008, Hörger et al., 2012). Considering the dual function of Rcr3 as pathogen target and guardee during the plant immune response, the observed level of diversity may be involved in the interaction with different pathogen effectors or in the interaction between Rcr3 and its guard Cf2.
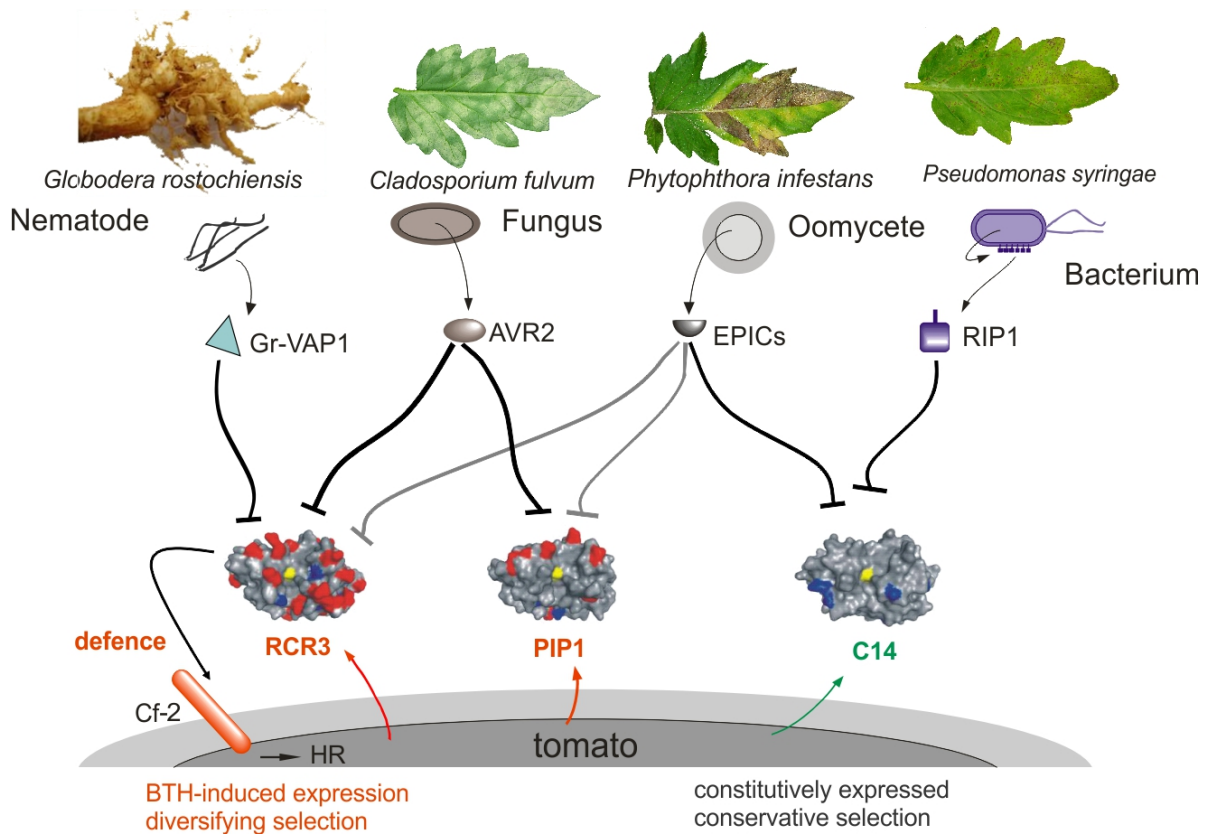
Figure 5 | Pathogen target different host proteases in tomato

C. fulvum Avr2 targets specific proteases Rcr3 and PIP1, *P. infestans* Epic1 and Epic2B target Rcr3, PIP1 and C14, RIP1 from *Pseudomonas syringae* targets C14. *G. rostochiensis* Gr-VAP1 targets Rcr3.

Previous studies reported differences in interaction with the *C. fulvum* effector Avr2 caused by a single amino acid substitution N194D (Shabab et al. 2008, Hörger et al., 2012). Furthermore, the amino acid polymorphisms I206K, Q222E and S330A affect the interaction with guard Cf-2 (Hörger et al., 2012). Nevertheless, there is even more diversity at *Rcr3*, which cannot be explained by differential interaction with Avr2 and Cf-2. Rcr3 also interacts with Epics and the role of variant residues on the interaction with Epics is addressed in this thesis.

1.3 Aims of this thesis

1.3.1 What is the role for *Rcr3*, *PIP1* and *C14* in pathogen defense?

In the absence of *Cf-2*, does *Rcr3* contribute to defense (guard model) or not (decoy model)? What is the contribution by *PIP1*? Is *PIP1* a virulence target of *C. fulvum* or also for other pathogens like *P. infestans*, and *P. syringae*? What is the function of *C14*? These questions will be addressed by reverse genetics in tomato.

1.3.2 What is the role of the variant residues in PIP1 and Rcr3?

Are some of the Rcr3 and PIP1 alleles insensitive for inhibition by Avr2, EPICs and RIP1 or some alleles show enhanced sensitivity? These questions will be addressed by testing Rcr3 and PIP1 alleles and mutants in inhibition assays.

Chapter 2- Results

2.1 Generation of *Rcr3^{pim}* tomato lines in MM-Cf0 background

To obtain the *pimpinellifolium* allele of wild-type and mutant *Rcr3* in the Money Maker (MM) tomato plants lacking *Cf2,* we performed two crosses between different homozygous lines. Cross-1: *Cf2/rcr3-3^{pim}* x *Cf0/Rcr3^{lyc}* and Cross-2: C*f2/Rcr3^{pim}* x *Cf0/Rcr3^{lyc}*. The *Cf2* and *Rcr3* genes segregated in the F2 populations according to Mendelian laws (Fig. 6A & B). Two plants carrying the *rcr3-3^{pim}* allele from cross-1 (Fig. 6A) and the *Rcr3^{pim}* allele from cross-2 (Fig. 6B) in the absence of the *Cf2* locus were selected in the F2 populations using PCR on genomic DNA using allele-specific primers. The genetic background of the selected plants was confirmed in the F3 and F4 populations together with other three parental lines MM-Cf0 genotypes (*Cf0/Rcr3^{lyc}*), MM-Cf2 (*Cf2/Rcr3^{pim}*) and mutant MM-Cf2 (*Cf2/rcr3-3^{pim}*) by PCR on genomic DNA and sequencing (Fig. 6C). We observed autonecrosis in the F1 and F2 population of cross 1 due to a combination of *Cf2* and *Rcr3^{lyc}*. The *Rcr3^{pim}* is allelic to *Ne*, the allele from *S. pimpinellifolium* that suppresses necrosis in MM-Cf2 plants (Krüger et al., 2002). The *Rcr3^{lyc}* is allelic to *ne* (necrosis) that causes autonecrosis in a Cf2-dependent manner. *Rcr3^{lyc}* (*ne*) triggers necrosis that is recessive which means that only homozygous plants (*Cf2/Rcr3^{lyc}*) exhibit necrotic phenotypes. However, in combination with a mutated allele of *Rcr3^{pim}* (*rcr3-3^{pim}*), *Rcr3^{lyc}* will act as a dominant allele (Krüger et al., 2002). Therefore we expected 9/16 (56%) necrotic and 7/16 (46%) non necrotic plants in the F2 population (Fig. 7). In reality we observed necrosis on 31/54 (57%) plants and no necrosis on 23/54 (43%) plants in the F2 progeny of cross 1 (Fig. 7). This phenotypic ratio confirms that the plants that are heterozygous (*Cf2Rcr3^{lyc}/rcr3-3*) also show necrosis and thus the ratio between necrotic and non-necrotic phenotypes is 9:7. This observation confirms that *Rcr3^{lyc}* is dominant over the *rcr3* mutant allele This is consistent with the observation that F1 is also necrotic.

To confirm the newly generated lines we used Avr2 to trigger HR in the *Cf2/Rcr3^{pim}* plants
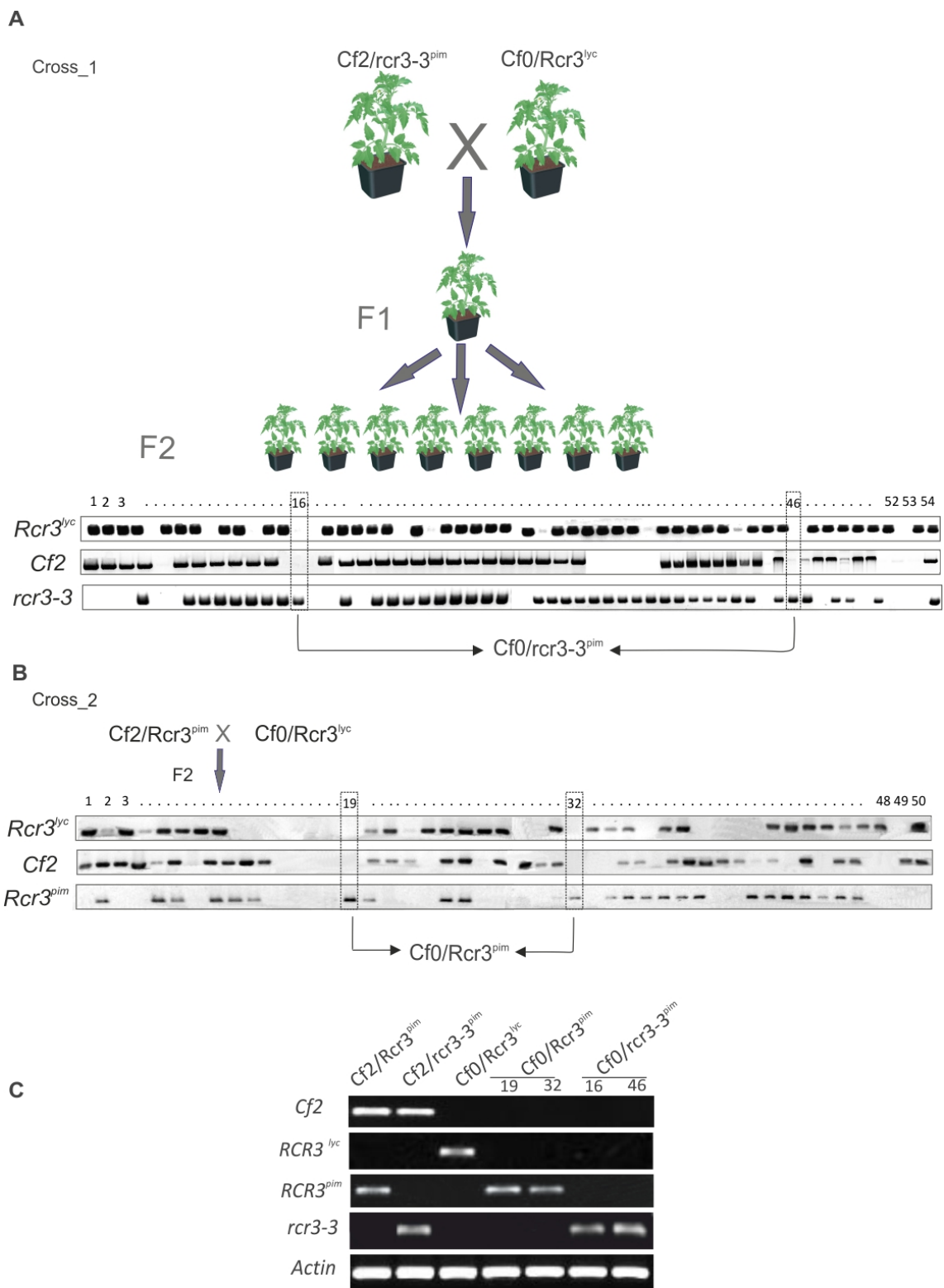
Figure 6 | Selection and confirmation of tomato lines

A- To obtain the *rcr3-3* mutant in tomato lacking the *Cf2* locus, MM-Cf0 (*Cf0/Rcr3^{lyc}*) was crossed with mutant MM-Cf2 (Cf2*/rcr3-3^{pim}*). PCR on genomic DNA with allele-specific primers was used to select two plants (16 & 46) that carry the desired genotype from 54 F2 plants.

B- To obtain the *pimpinellifolium* allele of *Rcr3* in tomato lacking the *Cf2* locus, MM-Cf0 (*Cf0/Rcr3^{lyc}*) was crossed with MM-Cf2 (*Cf2/Rcr3^{pim}*). PCR on genomic DNA with allele-specific primers was used to select two plants (19 & 32) that carry the desired genotype from 50 F2 plants.

C- Confirmation of the genotypes in F3 and F4 generations by PCR on genomic DNA using allele-specific primers. The identity of the PCR fragments was confirmed by sequencing.

Gametes	*Cf2/Rcr3^{lyc}*	*Cf2/rcr3-3*	*Cf0/Rcr3^{lyc}*	*Cf0/rcr3-3*
Cf2/Rcr3^{lyc}	*Cf2/Rcr3^{lyc}*	*Cf2/Rcr3^{lyc}/ rcr3-3*	*Cf0/Cf2/Rcr3^{lyc}*	*Cf0/Cf2/Rcr3^{lyc} rcr3-3*
Cf2/rcr3-3	*Cf2/Rcr3^{lyc}/ rcr3-3*	*Cf2/rcr3-3*	*Cf0/Cf2/Rcr3^{lyc} rcr3-3*	*Cf0/Cf2/rcr3-3*
Cf0/Rcr3^{lyc}	*Cf0/Cf2/Rcr3^{lyc}*	*Cf0/Cf2/Rcr3^{lyc} rcr3-3*	*Cf0/Rcr3^{lyc}*	*Cf0/Rcr3^{lyc}/rcr3-3*
Cf0/rcr3-3	*Cf0/Cf2/Rcr3^{lyc} rcr3-3*	*Cf0/Cf2/rcr3-3*	*Cf0/Rcr3^{lyc}/rcr3-3*	*Cf0/ rcr3-3*

Expected phenotypes: 9/16 necrotic (*Cf2+Rcr3^{lyc}*)   7/16 non-necrotic   1/16 has desired *Cf0/rcr3-3*

Figure 7 | Expected Mendelian segregation of *Cf2* and *Rcr3* genes in the F2 population
Theoretically 9/16 plants (56%) should show the necrotic phenotype due to combination of *Cf2* with *Rcr3^{lyc}* and 7/16 (44%) non-necrotic phenotypes. One out of 16 plants should have the desired *Cf0/rcr3-3* genotype (red). In reality the F2 progeny showed necrosis in 31/54 (57%) plants and no necrosis in 23/54 (43%) plants.

(Rooney et al., 2005). Avr2 of *C. fulvum* only triggered a hypersensitive response in the leaves of *Cf2/Rcr3^{pim}* but not in *Cf2*/*rcr3-3, Cf0/Rcr3^{pim}* , *Cf0/Rcr^{lyc}* or *Cf0/rcr3^{pim}* mutants plants, consistent with Rooney et al., (2005) (Fig. 8). To confirm the *Cf2*/*rcr3-3* lines, the Rcr3^{pim} was produced transiently in *N. benthamiana* by agroinfiltration and co-injected with Avr2 into the leaves of *Cf2/rcr3-3^{pim}* plants. Only the complementation of *Cf2/rcr3-3^{pim}* plants resulted in cell death (Fig. 8). These experiments confirm the identity of the genetic material. These observations demonstrate that all the tested tomato lines have the correct genotypes.

2.2 Selection of overexpression lines for *PIP1*

For generating overexpression lines, MM-Cf0 plants were transformed with the *35S:PIP1-His* construct described earlier (Tian et al., 2007). This construct contains the *PIP1* open reading
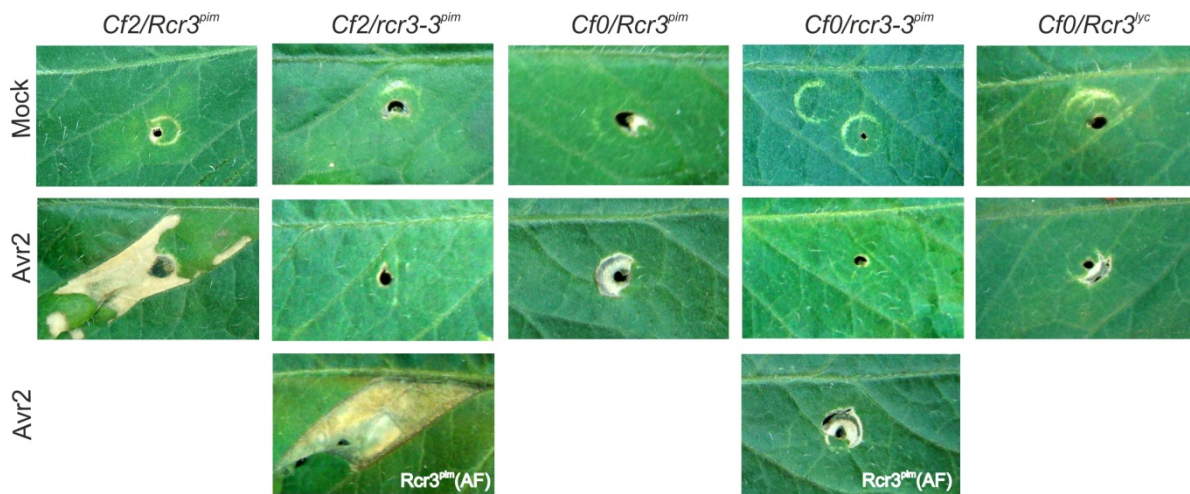
Figure 8 | Phenotypic confirmation of genetic materials by HR assays
Fully expanded leaves of 4-week-old tomato plants carrying *Cf2/Rcr3^{pim}*, *Cf2/rcr3-3^{pim}*, *Cf0/Rcr3^{pim}*,
Cf0/rcr3-3^{pim} and *Cf0/Rcr3^{lyc}* were infiltrated with 1 µM purified Avr2 protein. The apoplastic fluid (AF)
containing Rcr3^{pim}, produced by agroinfiltration in *N. benthamiana* was co-infiltrated with Avr2 protein in both
rcr3-3^{pim} mutant plants (*Cf2/rcr3-3^{pim} Cf0/rcr3-3^{pim}*). The dialysis buffer was infiltrated as negative control into
tomato leaves (Mock). Leaves were photographed at 5 day-post-infiltration.

frame cloned behind a 35S promoter in frame with a C-terminal His tag followed by a nopalin
synthase terminator (T*nos*) from *Agrobacterium tumefaciens* and a neomycin
phosphotransferase II (*nptII*) reporter gene that confers resistance against kanamycin (Fig.
9A). The T-DNA was transformed into tomato cultivar Money Maker (MM-Cf0) by
Agrobacterium-mediated transformation. Overexpression lines were selected in three steps
(Fig. 9B). Kanamycin-resistant transformants were selected with PCR on genomic DNA using
three primer combinations to ensure that the T-DNA insert is intact (Fig. 9C). Primary
transformants were tested for elevated levels of PLCP activity (by ABPP), PIP1 level (using
αPIP1-antibody and αHis antibody). Three primary transformants were selected. The progeny
of the selected primary transformants (T1) were further screened for kanamycin resistance.
The lines were not studied further in the T2 generation because the analysis of *asPIP1* lines
was prioritized (see next page).

2.3 Selection of silenced lines for *PIP1*

To generate *PIP1*-silenced transgenic tomato lines, a construct was made by ligating the 1.1 kb *PIP1* cDNA in the antisense orientation behind the 35S promoter (Fig. 9A). Tomato line Money Maker (MM-Cf0) was transformed by *Agrobacterium*-mediated transformation by the transformation service at The Sainsbury Laboratory John Innes Center Norwich UK. The selection of transformants has been carried out in three steps (Fig. 9B). To confirm the presence of the transgene in the T0 transformants, PCR was performed on genomic DNA using gene-specific and promoter/terminator-specific primer combinations resulting in 34 transgenic plants that carry the *asPIP1* transgene. Transgenic plants selected in T0 were further screened for reduced levels of *PIP1* transcript and PIP1 protein compared to MM-Cf0 tomato plants. In summary a total of three plants exhibiting reduced levels of PIP1 protein and transcript were selected in T1 (Fig. 9C).

To measure PIP1 protein levels in *asPIP1* in the T2 generation, AF was used for immunoblotting using the PIP1 antibody. The PIP1 protein level is reduced in almost all lines and four plants showed strongly reduced level of PIP1 protein when compared with BTH-treated control plants (Fig. 9E, upper panel). Finally, out of 20 plants tested by ABPP and western blot, six plants showing reduced PIP1 expression were selected for generating stable homozygous plants in subsequent generations. To validate the *PIP1* transcript level in *asPIP1* lines, real-time quantitative PCR was carried out using cDNA of *asPIP1* and control plants. The transcript level of *PIP1* was determined relative to the constitutively expressed tomato *Actin* gene (*SlACT*). This analysis showed a 70-90% reduction of transcript levels in each transgenic plant when compared to control, non- transgenic plants (Fig. 10A). To investigate co-silencing of *C14* and *Rcr3*, we also performed the real-time quantitative PCR on cDNA. The transcript level for *C14* and *Rcr3* remained unaltered in all tested plants (Fig. 10B & C). This data demonstrates that there is no co-silencing of *Rcr3* and *C14.* Reduced *PIP1* levels had no effect on plant growth and development.

Thirty seeds from *asPIP1* were sown per tested line in the T2 generation and all PIP1 transgenic plants were sprayed with benzothiadiazole (BTH) to identify the plants with low
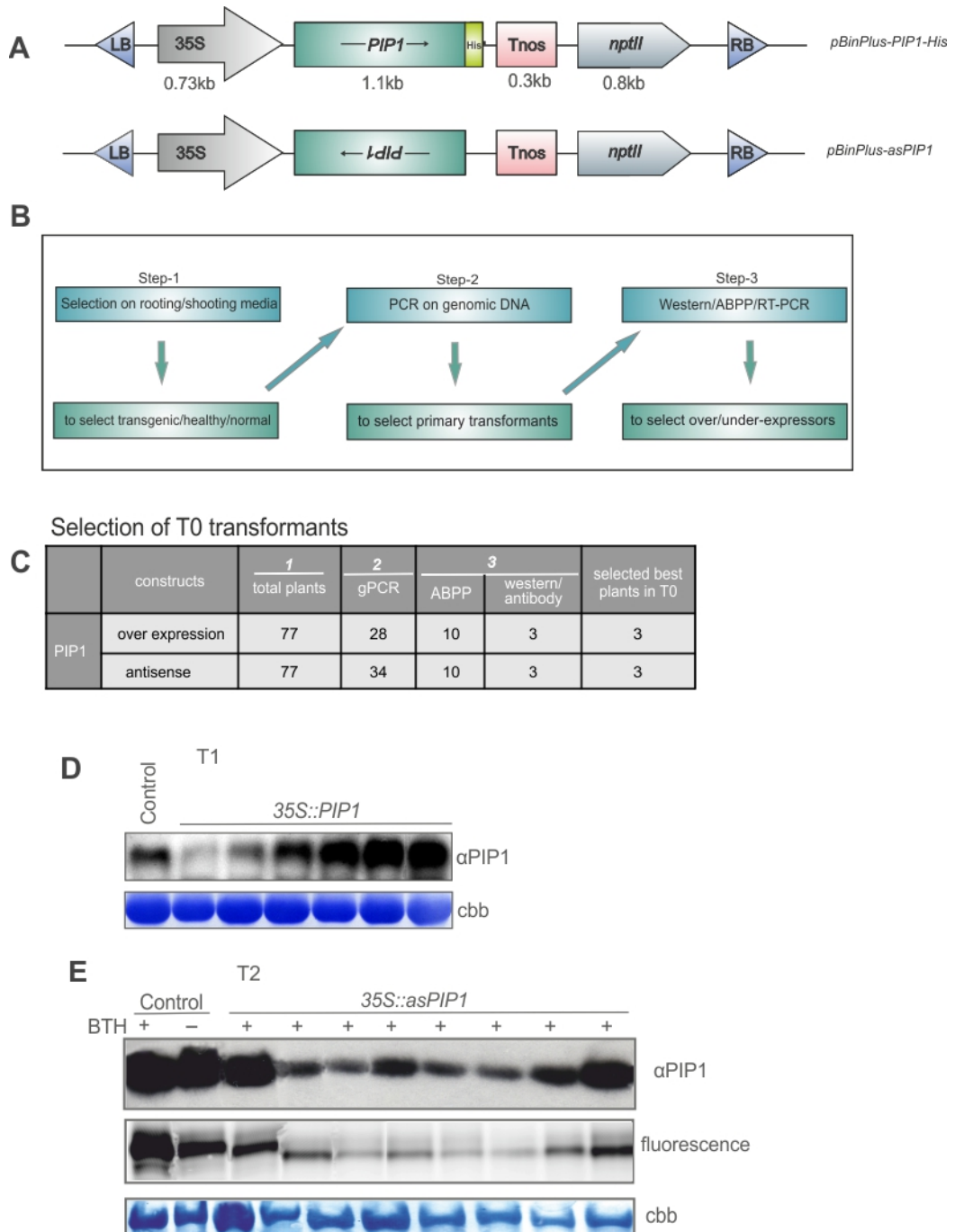
Figure 9 | Selection of overexpression and silenced lines for *PIP1*

A- Schematic representation of T-DNA constructs used for *Agrobacterium*-mediated transformation of tomato. For PIP1 overexpression lines 35S-driven constructs were generated expressing PIP1 carrying a C-terminal His tag. The PIP1 reverse complement sequence was used to generate antisense PIP1 lines. For C14 overexpression lines, full length C14 was used driven by 35S promoter.

B- Screening of transgenic tomato lines. 35S-driven constructs of PIP1 and C14 were transformed into tomato line MM-Cf0 by *Agrobacterium*-mediated transformation. Screening has been performed in three steps. Through tissue culture using rooting /shooting media in glass jars healthy, normal and light green plants were selected (step1) Plants carrying the transgenes were selected by PCR on genomic DNA (step 2) were identified   using western blotting, activity-based protein profiling (ABPP) and quantitative real-time PCR on cDNA (step3).

C- Summary of the selection of transformants. Primary transgenic lines were selected with PCR on genomic DNA. The three best overexpressing and silenced transgenic plants were selected by ABPP and western blotting in the T0 generation.

D- PIP1 overexpression plants. The total leaf extract was isolated of four-week-old transgenic tomato plants in the T1 generation. Non-transgenic parental plant was used as control. Samples were analyzed on acrylamide protein gel with PIP1 antibody and coomassie staining (RuBisCo).

E- PIP1 antisense lines. Transgenic *asPIP1* plants and control tomato plants were sprayed with water or benzothiadiazole (BTH) in the T2 generation. Apoplastic fluid (AF) was isolated from four-week-old plants. AF was labeled with fluorescent DCG-04 and labeled proteins were detected by fluorescence scanning of the protein gel, western blotting with PIP1 antibody (middle panel) and coomassie staining (P69B).

PIP1 level, even upon induction of *PIP1* expression by SA signaling (Shabab et al., 2008).

To estimate the PLCP activity in transgenic lines, we performed ABPP, a tool to visualize the reduced levels of PLCPs activities indicate that *PIP1* is silenced in the T2 transgenic plants (Fig. 9E, middle panel).
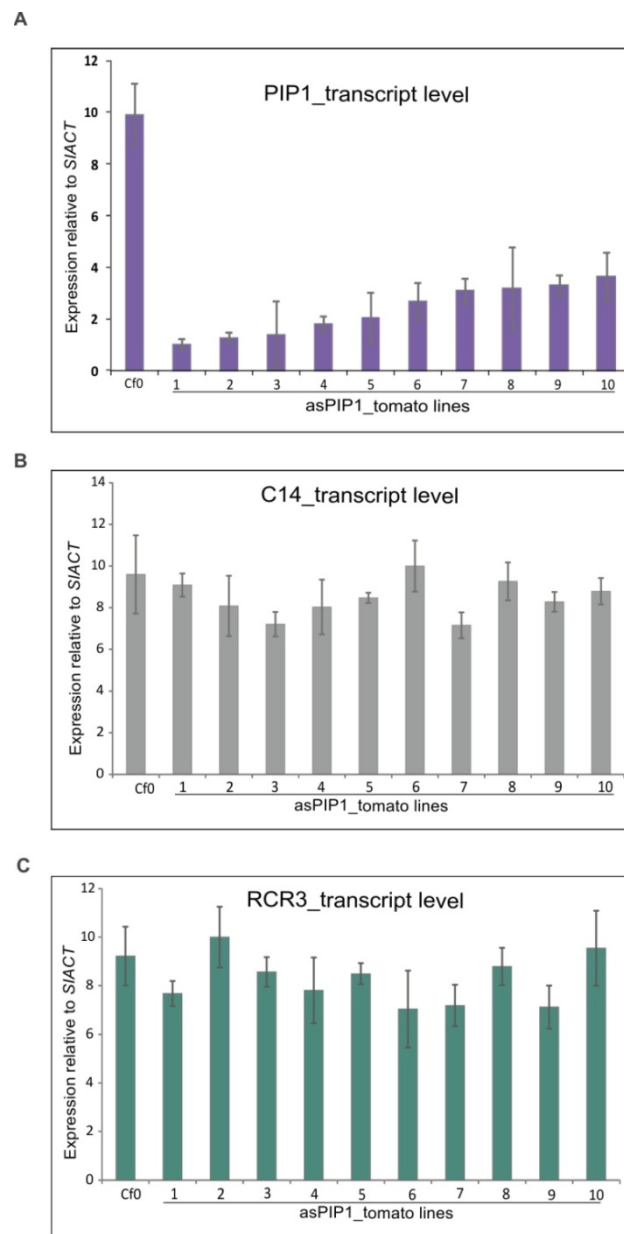
Figure 10 | Transcript levels in *asPIP1* lines

Transcript levels of *PIP1* (A) *C14* (B) and *Rcr3* (C) in *asPIP1* lines. RNA was isolated from leaves of two-week-old plants and used for cDNA synthesis and quantitative real time PCR. The *PIP1* transcript level relative to tomato *Actin* transcript level is significantly reduced in *asPIP1* plants (plant 1-10) when compared to the MM-Cf0 control. In contrast, transcript levels of *C14* and *Rcr3* are not affected in the *asPIP1* lines. Error bars represent SEM, 9= *n*) leaves of three independent plant. Similar results were obtained from three independent experiments.

2.4 Selection of overexpression and silenced lines for *C14*

For generating overexpression and silenced lines, MM-Cf0 plants were transformed with the *35S:C14* construct described earlier in Shabab et al., (2008) (Fig. 11A). The T-DNA was transformed into the tomato line Money Maker (MM-Cf0) by *Agrobacterium*-mediated transformation (Matthew Smoker, The Sainsbury Laboratory, Norwich UK). Overexpression lines were selected in three steps (Fig. 11B). Kanamycin-resistant transformants were selected by PCR on genomic DNA using three primer combinations to ensure that the transgenes are present in the correct orientation. Primary transformants were tested for elevated levels of PLCP activity (by ABPP), and C14 level (using αC14 antibody, Fig. 11C). Three primary transformants were selected for overexpression C14. Interestingly three other plants were selected because they showed reduced C14 protein level, presumably caused by co-suppression (Charrier et al., 2000). The progeny of selected primary transformants (T1) were further selected for kanamycin resistance to select homozygous lines.

The C14 overexpression and silenced lines showed an altered phenotype compared to non-transgenic plants. C14 overexpressing plants were smaller in height and darker in color when compared to non-transgenic plants, where csC14 plants showed height and color in between the MM-Cf0 non-transgenic and C14 overexpressing plants. Since C14 has been described as a cold or abiotic/biotic stress related protein (Avrova et al., 1999; Drake et al., 1996; Harrak et al., 2001; Schaffer and Fischer, 1988), over- or under-expression of C14 may cause growth retardation. These lines were not studied further because the analysis of *asPIP1* lines was prioritized.
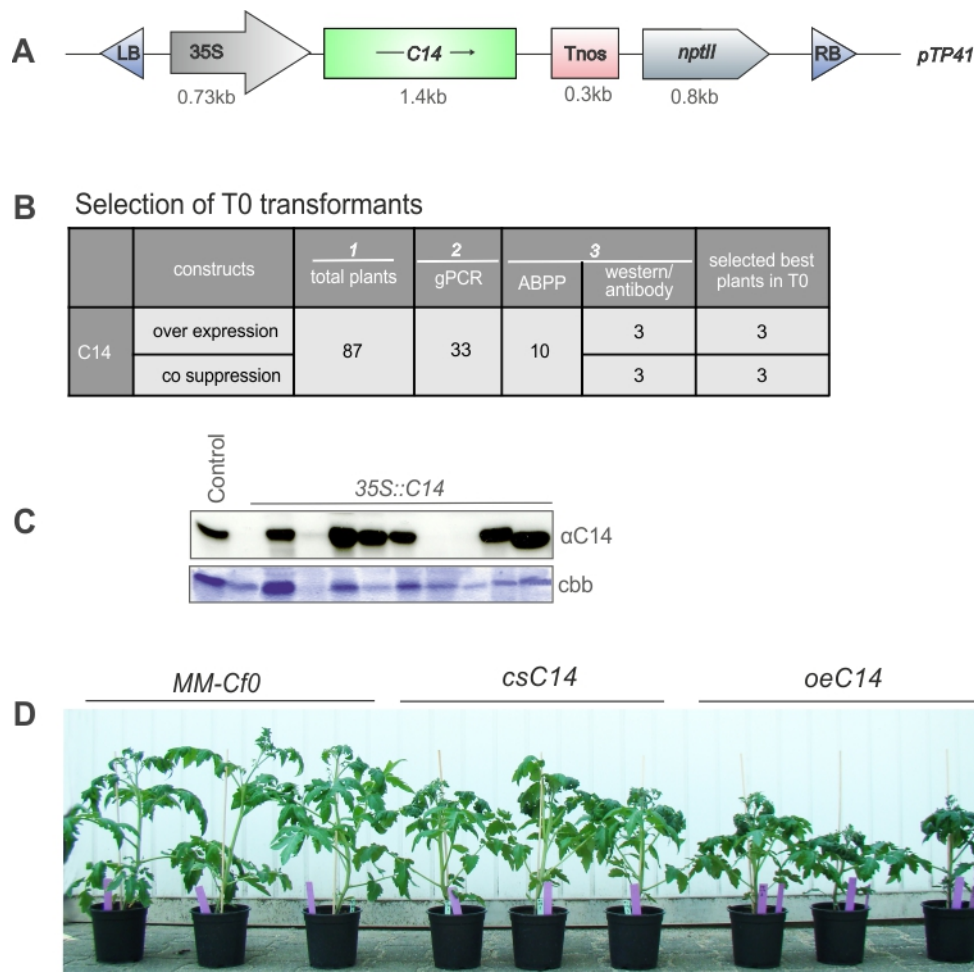
Figure 11 | Selection of overexpression and co-suppression lines for *C14*

A- Schematic representation of the T-DNA construct used for *Agrobacterium*-mediated transformation of tomato. For C14 overexpression lines, full length C14 was used driven by the 35S promoter.

B- Summary of the selection of transformants. Primary transgenic lines were selected by PCR on genomic DNA. The three best overexpressing and co suppressed transgenic plants were selected by ABPP and western blotting in the T0 generation.

C- C14 overexpressing lines. Apoplastic fluid (AF) was isolated of four-week-old transgenic *35S:C14* tomato plants in the T1 generation. Non-transgenic parental plants were used as control. Samples were analyzed on protein gels with C14 antibody and coomassie staining (P69B).

D- Reduced growth of C14 overexpression and silencing lines. Pictures were taken of Money Maker Cf0 control, co-suppression C14 (cs) and C14 overexpression plants (oe) of 6-week-old-plants

2.5 Role of *Rcr3* and *PIP1* in *Cladosporium fulvum*-tomato interactions

2.5.1   *Rcr3^{pim}* contributes to immunity to *Cladosporium fulvum* in *Cf2* plants

To setup a quantitative *C. fulvum* disease assay, we inoculated 4-week-old *Cf2/Rcr3^{pim}* and *Cf2/rcr3-3^{pim}* tomato lines with *C. fulvum* race 5 expressing Avr2. The *Cf2/rcr3-3^{pim}* tomato line does not have a functional *Rcr3^{pim}* due to presence of a premature stop codon (Krüger et al., 2002). To determine fungal biomass during infection, transcript levels of *C. fulvum* glyceraldehyde-3-phosphate dehydrogenase (*Cf-GAPDH*) were measured relative to tomato *Actin (SlACT)* at different days-post-inoculation. *Cf-GAPDH* transcript levels appear at 8dpi and develop 5-15 fold until 14 dpi on *Cf2/rcr3-3^{pim}* plants (Fig. 12A). These transcript levels reflect the visible fungal growth on the lower side of the tomato leaves. No fungal mycelium was visible in the first week, but then gradually developed until the lower side of the leaf was covered (Fig. 17B). In contrast, no *Cf-GAPDH* transcript levels were detected on *Cf2/Rcr3^{pim}* plants, consistent with the absence of fungal growth. Additionally, we tested the expression levels of fungal *Actin* (*Cf-actin*) and *Avr9*, relative to tomato *Actin* (*SlACT*). The transcript level of *Cf-Actin* was similar as of *Cf-GAPDH* in *Cf2/Rcr3^{pim}* and *Cf2/rcr3-3^{pim}* tomato lines (Fig. S1A, upper). The transcript level of *Avr9* relative to tomato *Actin* was higher in *Cf2/rcr3-3^{pim}* and in *Cf2/Rcr3^{pim}* tomato line, the expression level maintained the same level for all time points analyzed (Fig. S1B, upper).

2.5.2 *Rcr3^{pim}* does not affect susceptibility in the absence of *Cf2*

The guard model implies that *Rcr3* is a virulence target of *C. fulvum*. In order to investigate if *Rcr3^{pim}* contributes to immunity in the absence of *Cf2*, we inoculated tomato lines lacking the *Cf2* locus carrying *Rcr3^{pim}* or *rcr3-3^{pim}* (Section 4.1) with conidia of *C. fulvum* race 5 expressing Avr2. The transcript level of *Cf-GAPDH* for all time points analysed in *Cf0/Rcr3^{pim}* and *Cf0/rcr3-3^{pim}* plants clearly shows that both genotypes are susceptible to the same level (Fig. 13A). An indistinguishable increase of transcript levels was observed for fungal *Actin* (*Cf-actin*) and *Avr9* (Fig. S1A & B, middle). The transcript levels also correlate with development of symptoms (Fig. 13B). These data indicate that in the absence of *Cf2*, *Rcr3^{pim}* does not contribute to immunity against *C. fulvum.*
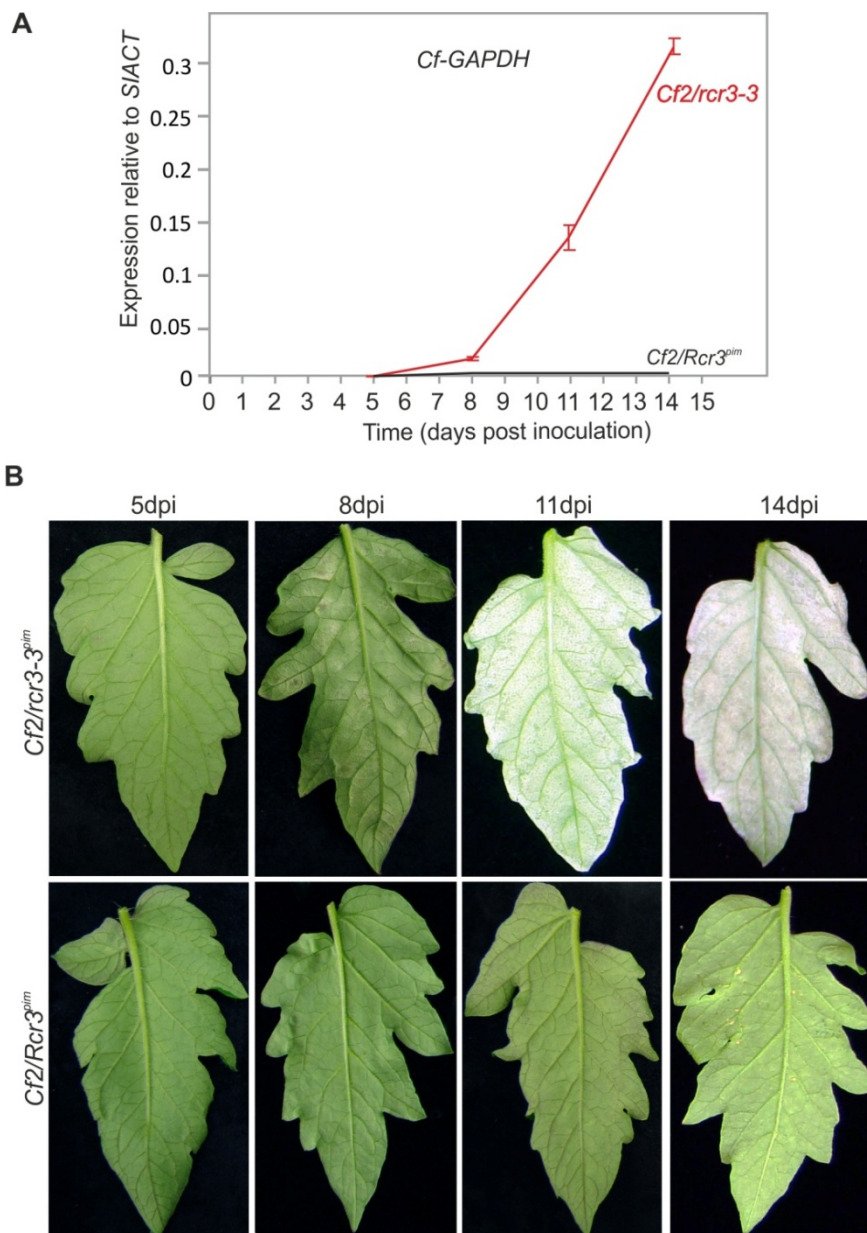
Figure 12 | Fungal transcript levels correlate with disease development
A- Transcript levels of *C. fulvum* glyceraldehyde-3- phosphate dehydrogenase (Cf-*GAPDH*) relative to tomato *Actin* (*SlACT*) upon inoculation of tomato lines with *C. fulvum* race 5, which produces Avr2. RNA was isolated from three leaflets taken from 2nd, 3rd and 4th compound leaflets of three independent tomato plants at different days-post-inoculation (dpi). Error bars represent (SEM) of nine samples taken of three independent plants. Similar results produced from three independent experiments.
B- Developing symptoms upon inoculation of tomato plants with *C. fulvum* race 5. Pictures were taken at 5, 8, 11 and 14 dpi and representative pictures are shown.
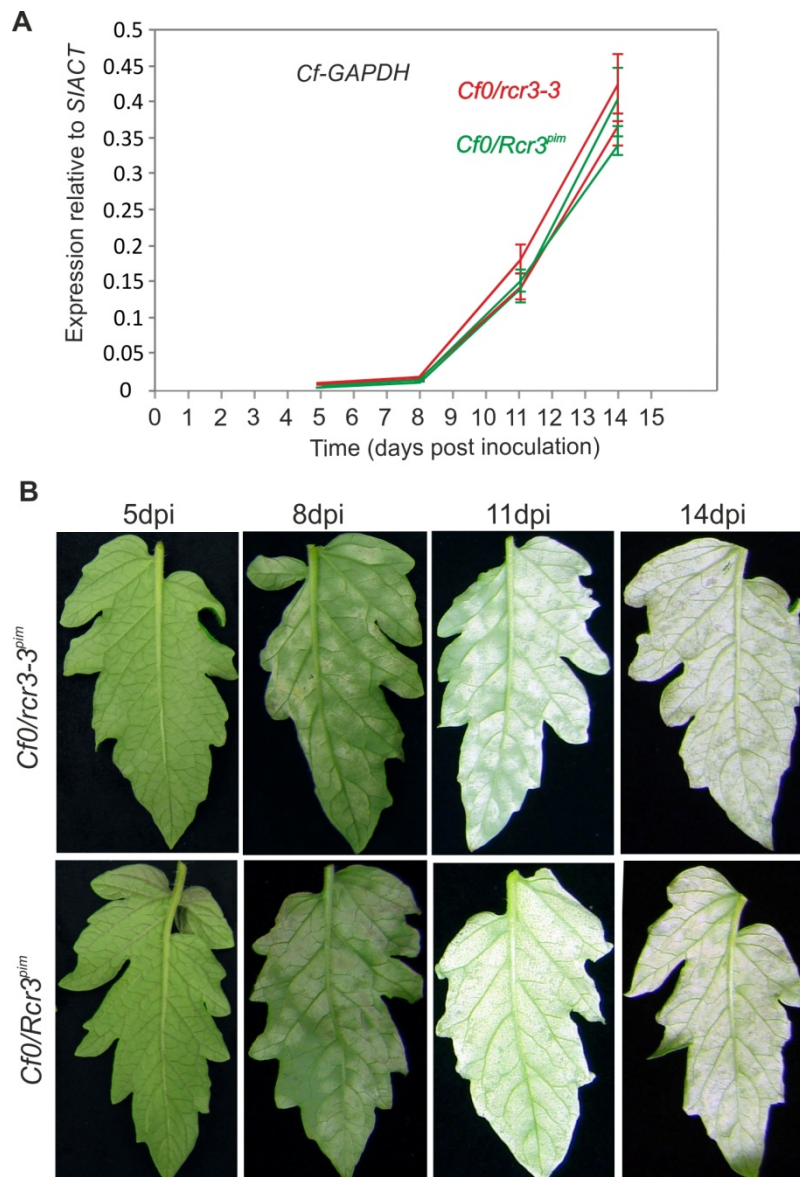
Figure 13 | *Rcr3^pim* does not affect susceptibility in the absence of *Cf2*

A- Transcript levels of *C. fulvum GAPDH* relative to tomato *Actin* upon inoculation of tomato lines with *C. fulvum* race 5, which produces Avr2. RNA was isolated from three leaves taken from 2nd, 3rd and 4th compound leaflets of three independent tomato plants at different days-post-inoculation (dpi). Two independently selected tomato genotypes (19 & 32, green lines) and (16 & 46, red lines) were used for inoculations. Error bars represent (SEM) of 9 samples taken from three independent plants. The experiment was repeated three times with similar results.

B- Developing symptoms upon inoculation of tomato plants with *C. fulvum* race 5. Pictures were taken at 5, 8, 11 and 14 dpi and representative pictures are shown.

2.5.3 *PIP1* contributes to immunity against *Cladosporium fulvum*

To determine the role of *PIP1* during *C. fulvum* infection, we inoculated *asPIP1* and non-transgenic control plants with race 5 of *C. fulvum.* Importantly the transcript level of *Cf-GAPDH* in *asPIP1* lines is 3-5 fold higher than that of the parental MM-Cf0 line (Fig. 14A). The difference in transcript level is prominent at later stages (11-14 dpi) in *asPIP1* plants when compared with non-transgenic control plants. A similarly enhanced transcript level of fungal *Actin* (*Cf-actin*) and *Avr9* was observed when compared to tomato *actin* (*SlACT*) in *asPIP1* plants (Fig. S1 A & B, lower). The development of disease symptoms at 5-8 dpi is slower, but later at 11-14 dpi, the disease symptoms were rapidly enhanced and mycelium spreaded on the full leaf. The development of disease symptoms correlate with transcript levels of *Cf-GAPDH* (Fig. 19B) Overall these data demonstrate that the silencing of *PIP1* enhances disease susceptibility indicating that *PIP1* contributes to immunity against *C. fulvum* and is therefore a genuine virulence target for *C. fulvum.*
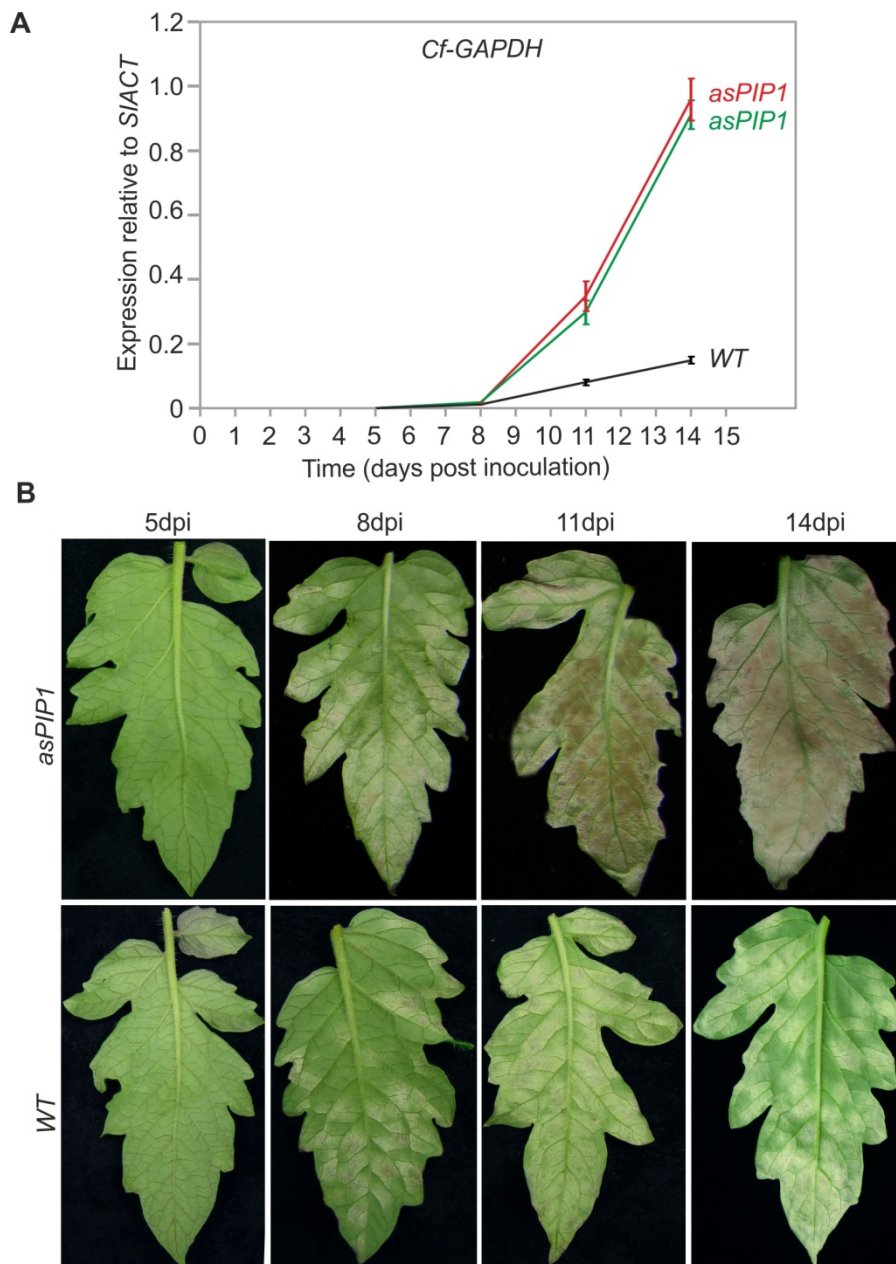
Figure 14 | *PIP1* contributes to immunity against *C. fulvum*
A- Transcript levels of *C. fulvum GAPDH* relative to tomato *Actin* upon inoculation of tomato lines with *C. fulvum* race 5, which produces Avr2. RNA was isolated from three leaves taken from 2nd, 3rd and 4th compound leaflets of three independent tomato plants at different days-post-inoculation (dpi). Two independently selected tomato *asPIP1* plants (green & red) were used for inoculations. Error bars represent (SEM) of 9 samples taken from three independent plants for RNA isolation. Similar results were produced from three independent experiments.
B- Developing symptoms upon inoculation of tomato plants with *C. fulvum* race 5. Pictures were taken at 5, 8, 11 and 14 dpi and representative pictures are shown.

2.6 Role of *Rcr3* in *Phytophthora infestans*-tomato interactions

2.6.1 *Rcr3^{pim}* contributes to defense against *P. infestans* in the presence of *Cf2*

To confirm whether *Rcr3^{pim}* contributes to tomato defense against *P. infestans*, we conducted disease assays using standard zoospore inoculation on detached leaves of 4-week-old tomato plants. Infection assays demonstrated that *Cf2/rcr3-3^{pim}* is more susceptible when compared to *Cf2/Rcr3^{pim}* (Fig. 15A), consistent with the literature (Song et al., 2009). The difference of lesion growth rate between *Cf2/Rcr3^{pim}* and *Cf2/rcr3-3^{pim}* was statistically significant at P<0.01 level (Table S1). Enhanced necrosis was observed in *Cf2/rcr3-3^{pim}* compared to *Cf2/Rcr3^{pim}* plants (Fig. 15B). We also used transgenic strain of *P. infestans* 88069td, a strain expressing the red fluorescent dimer RFP marker (known as tdtomato) to monitor the spread of hyphae in infected leaves to discriminate the level of susceptibility. The hyphal growth in *Cf2/rcr3-3^{pim}* mutant plants is significantly enhanced when compared with *Cf2/Rcr3^{pim}* lines (Fig. 15C). Taken together, these experiments confirm that *Cf2* tomato plants lacking *Rcr3^{pim}* (*Cf2/rcr3-3^{pim}*) exhibited enhanced susceptibility to *P. infestans* compared to tomato carrying *Rcr3^{pim}* (*Cf2/Rcr3^{pim}*) consistent with the literature (Song et al., 2009).

### 2.6.2 *Rcr3^{pim}* contributes to defense against *P. infestans* in the absence of *Cf2*

Song et al., (2009) and the results described in the section above show that *Rcr3^{pim}* contributes to defense against *P. infestans* on tomato plants carrying the *Cf2* gene. Here we addressed whether *Rcr3^{pim}* contributes to defense independently of *Cf2*. To test this we used *Cf0/Rcr3^{pim}* and *Cf0/rcr3-3^{pim}* tomato plants described in section 2.1. *P. infestans* disease assays were performed using standard zoospore inoculation on detached leaves of 4-week-old tomato plants. The *Cf0/Rcr3^{pim}* plants were significantly less susceptible when compared to *Cf0/rcr3-3^{pim}* plants (Fig. 16).

The difference of lesion growth rate between the *Cf0/Rcr3^{pim}* and *Cf0/rcr3-3^{pim}* was statistically significant at the *P*< 0.01 level (Table S1). Disease-associated necrosis was less in *Cf0/Rc3^{pim}* plants when compared to *Cf0/rcr3-3^{pim}* plants (Fig. 16B). Furthermore, hyphal
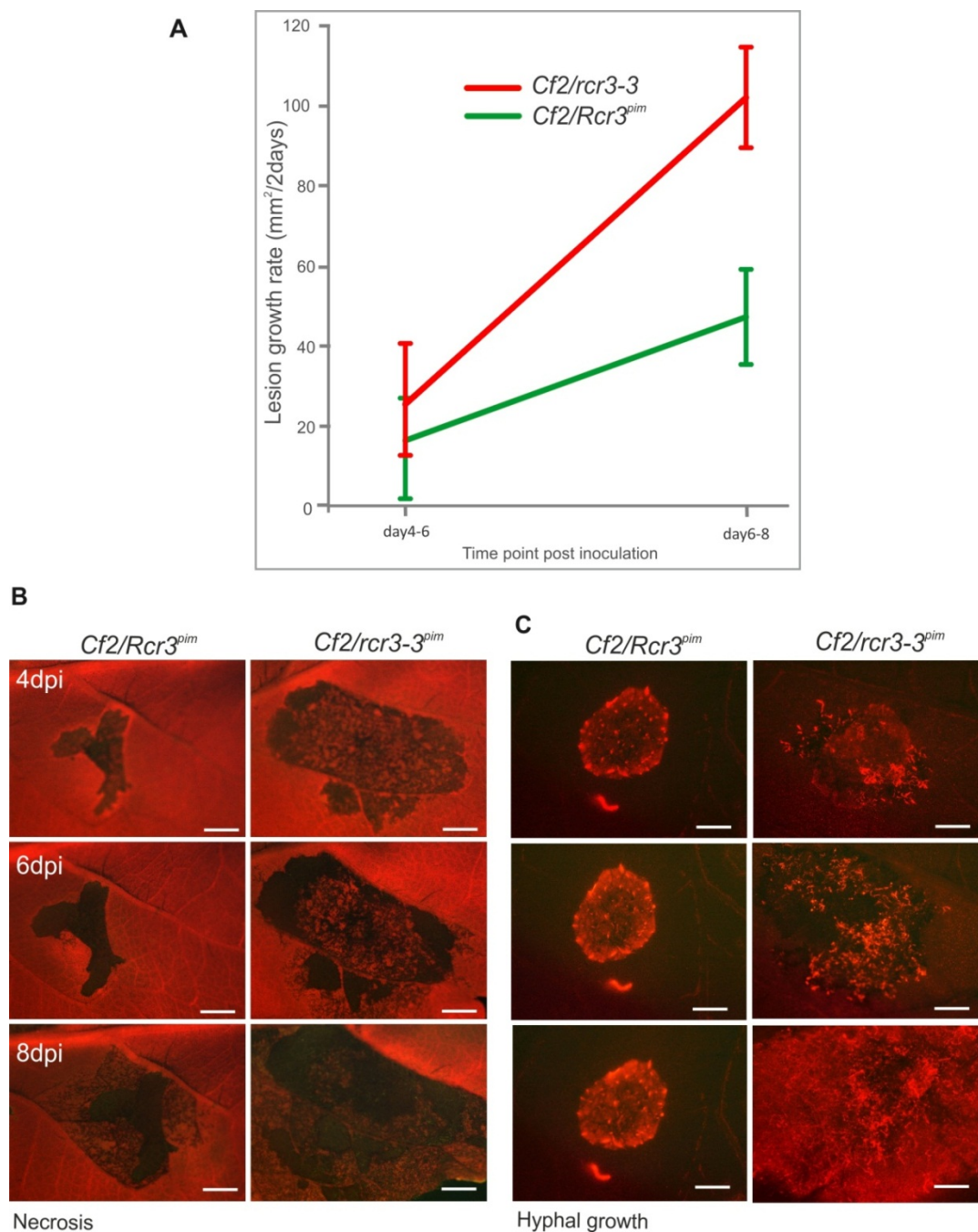
Figure 15 | *Rcr3^pim* in the presence of *Cf2* contributes to defense against *P.infestans*
A- Lesion growth area was measured at 4, 6 and 8 days-post-infection and pairwise subtracted. The experiment was repeated three times with similar results. Error bars represents (SEM) of 24 lesion growth measurements.
B- Necrosis on tomato upon *P.infestans* infection. Pictures were taken of infected leaf area to visualize disease-associated necrosis using Leica microscopy with identical settings for each time point.
C- Hyphal growth on tomato infected by transgenic *P. infestans* strain 88069td (tandem dimer tomato RFP) was documented using the DSR filter (Leica microscope). Pictures were taken at 4, 6 and 8 days-post-infection.
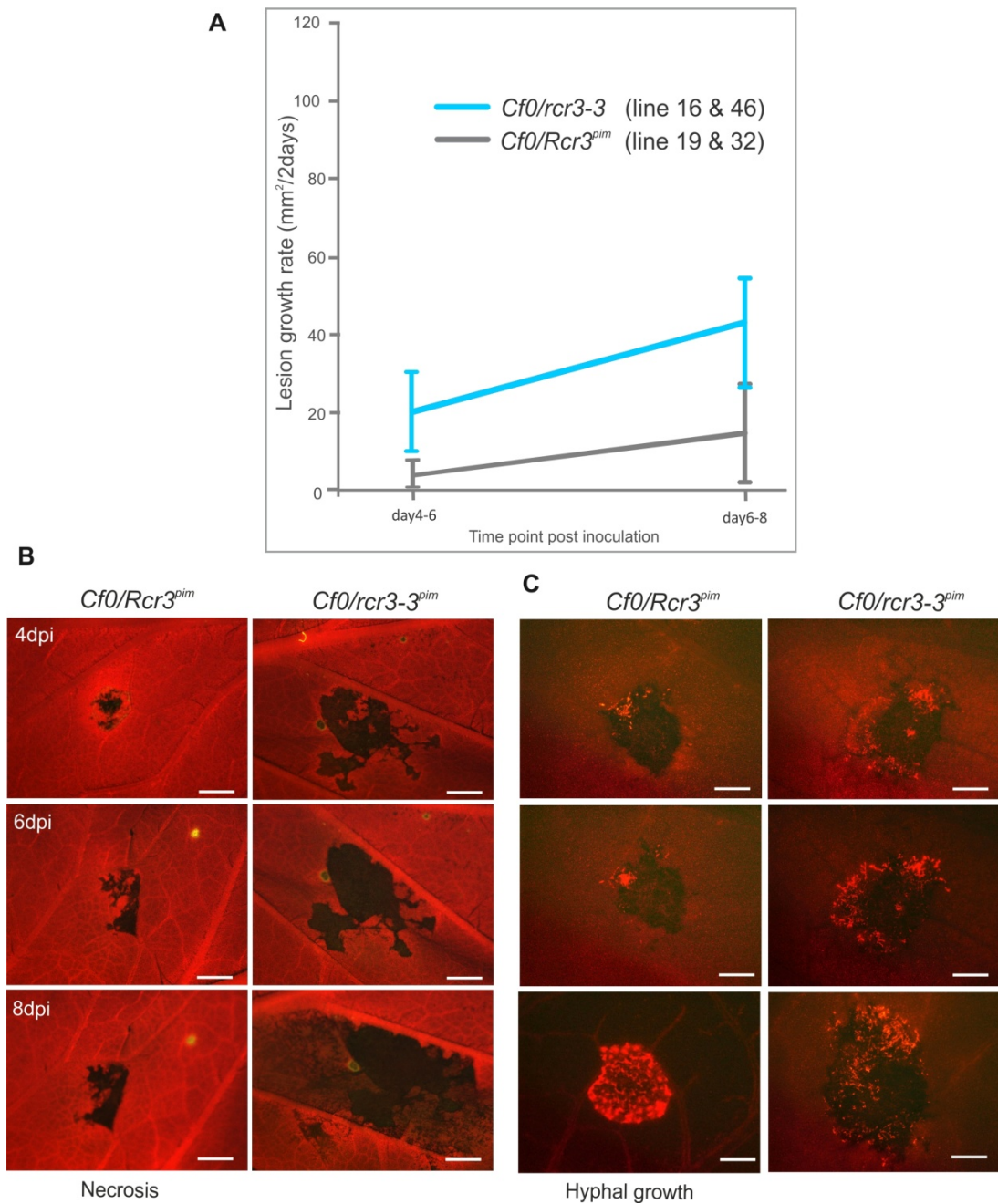
Figure 16 | *Rcr3^pim* in the *Cf0* background contributes to defense against *P. infestans*
A- Lesion growth area was measured at 4, 6 and 8 days-post-infection and pairwise subtracted. The experiment was repeated three times with similar results. Error bars represents (SEM) of 24 lesion growth measurements.
B- Necrosis on tomato upon *P.infestans* infection. Pictures were taken of infected leaf area to visualize disease-associated necrosis using Leica microscopy with identical settings for each time point.
C- Hyphal growth on tomato infected by transgenic *P. infestans* strain 88069td (tandem dimer tomato RFP) was documented using DSR filter (Leica microscope). Pictures were taken at 4, 6 and 8 days-post-infection.

growth in *Cf0/Rcr3^{pim}* plants showed significantly compromised susceptibility to *P. infestans* when compared to *rcr3-3^{pim}* mutant lines (Fig. 16C). In summary, these observations demonstrate that *Cf0* tomato plants carrying the *rcr3-3^{pim}* mutant (*Cf0/rcr3-3^{pim}*) exhibited enhanced susceptibility to *P. infestans* compared *Cf0* tomato lines carrying *Rcr3^{pim}* (*Cf0/Rcr3^{pim}*) (Fig. 16A).

2.6.3 Absence of *Cf2* increases *Rcr3^{pim}* -dependent resistance to *P. infestans*

To determine the extent to which the genetic background contributes to immunity to *P. infestans*, we performed *P. infestans* infections on *Cf2/rcr3-3^{pim}*, *Cf0/rcr3-3^{pim}*, *Cf2/Rcr3^{pim}* and *Cf0/Rcr3^{pim}*. Zoospores were used for inoculation on detached tomato leaves of 4-week-old plants. Pictures were taken at single time points to avoid damage caused by UV light. Interestingly the tomato line carrying *Cf2* (*Cf2/rcr3-3^{pim}*) was more susceptible when compared with *Cf0/rcr3-3^{pim}* (Fig. 17A). Likewise the sporulation symptoms on *Cf2/rcr3-3^{pim}* showed significantly enhanced susceptibility to *P. infestans* compared to *Cf0/rcr3-3^{pim}* line (Fig. 17B). Unexpectedly, we discovered that *Cf0/Rcr3^{pim}* tomato lines showed increased resistance against *P. infestans* (Fig. 17B & C). This indicates that the *Cf0* locus contributes to immunity to *P. infestans* in the presence of *Rcr3^{pim}*.
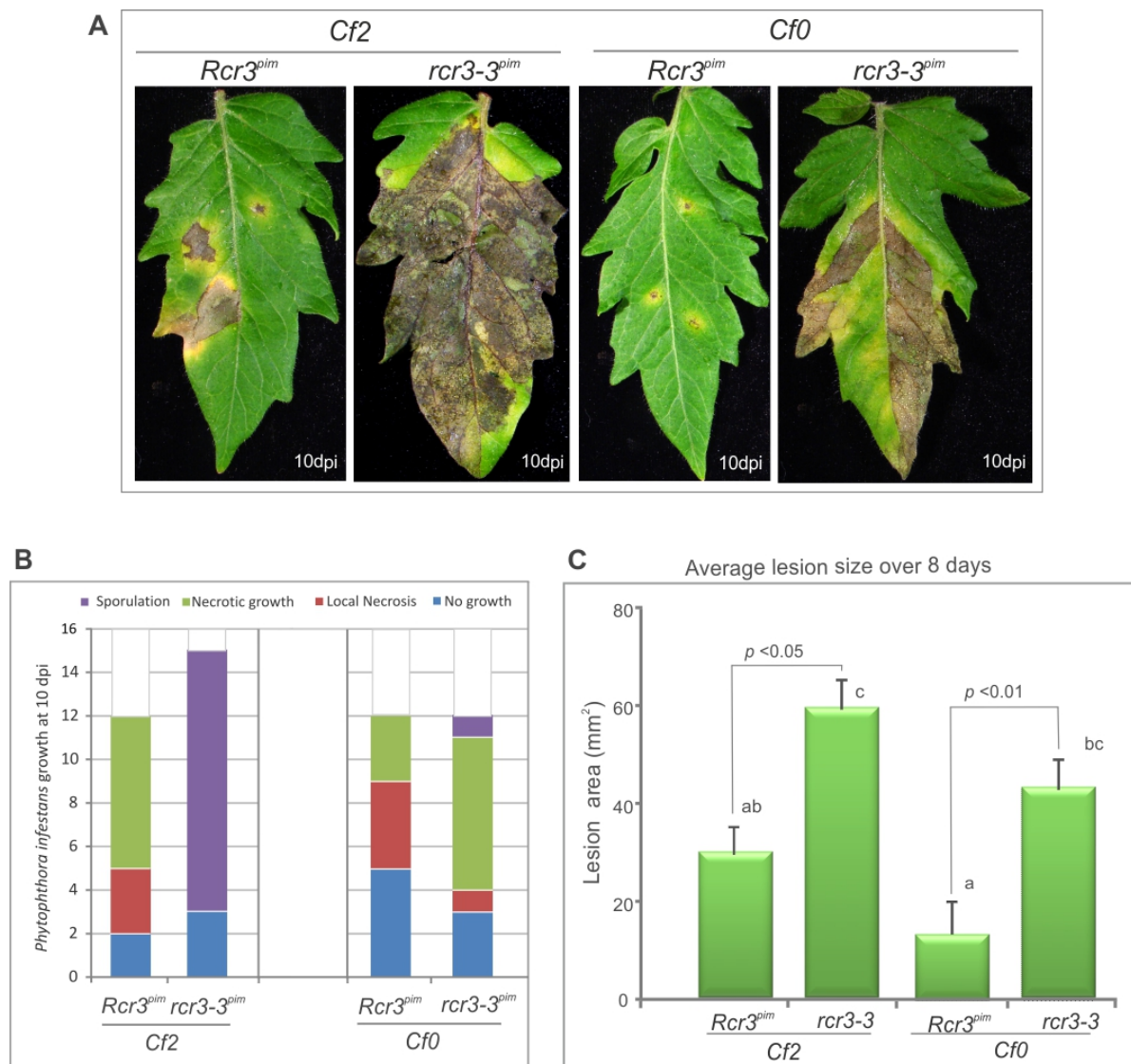
Figure 17 | Effect of genetic background on loss of *Rcr3^pim*^

A- Colonization of *P. infestans* on detached leaflets of on 5-week-old tomato plants. Pictures were taken at 10 days post inoculation.

B- A histogram of symptoms upon *P. infestans* infection. Disease progression symptoms were scored at 10 dpi by monitoring *P. infestans* growth at each inoculation site.

C-Absence of Cf2 increases Rcr3^pim^ -dependent resistance to *P. infestans*. Average lesion area was analyzed by SPSS statistical software. ANOVA analysis and Tukey test were performed for *P*-values. Error bars represent (SEM=24*n*) lesion area measured at 8dpi of three independent inoculated detached leaves. The virulence assay was repeated three times with similar results.

2.7 Functional consequences of sequence variance in Rcr3 and PIP1

2.7.1 Natural variation in Rcr3 affects inhibition by pathogen-derived inhibitors

Previous studies have shown that *Rcr3* exhibits high levels of inter- and intraspecific nucleotide and amino acid diversity (Shabab et al. 2008, Hörger et al., 20212, Hörger 2011). Part of this diversity plays a role in differential interaction of Rcr3 with the *C. fulvum* effector Avr2 and the R protein Cf-2. Similarly, differential interaction with the *P. infestans* effectors Epic1 and Epic2B has been shown to underlie this observed diversity at the *Rcr3* locus (Hörger, 2011). The amino acid polymorphisms N9S, G27A, Q94E, H148N, R151Q and D283N appear to be significantly associated with these phenotypic differences with H148N and D283N having reciprocal effects allowing inhibition by Epic2B and preventing inhibition by Epic1(Hörger 2011).

Three wild-type Rcr3 alleles from *S. lycopersicum* (*Rcr3^lyc^*), *S. chilense* (*Rcr3^chil^*) and *S. habrochaites* (*Rcr3^hab^*) (Fig. 19B & C) were successfully expressed in *N. benthamiana* using agroinfiltration and could be labeled with fluorescent DCG-04 (MV201) inhibited by the universal cysteine protease inhibitor E-64 indicating that they are all active proteases (Fig. 19A & D, 20 and 21). All except one tested Rcr3 variants were inhibited by Avr2 (Fig. 19D, 20, Table 1). The one allele which was insensitive to inhibition by Avr2 (Rcr3^chil^) carries the N194D substitution, which has previously been demonstrated to play a role in the interaction with Avr2 (Shabab et al. 2008, Hörger et al., 2012). Inhibition assays with Epic1 and Epic2B showed that wild-type Rcr3^lyc^ and Rcr3^chil^ can be inhibited by Epic2B and not by Epic1, while wild-type Rcr3^hab^, which differs from Rcr3^lyc^ and Rcr3^chil^ at the amino acid positions 148, 151, 267 and 283, can also be inhibited by Epic1 (Fig. 19D, 20, Table 1). These results are consistent with previous findings (Hörger 2011). We next studied the role of these variant residues in more detail by site-directed mutagenesis. To disentangle the effect of the single polymorphisms, the following Rcr3 mutants have been generated, cloned into a binary
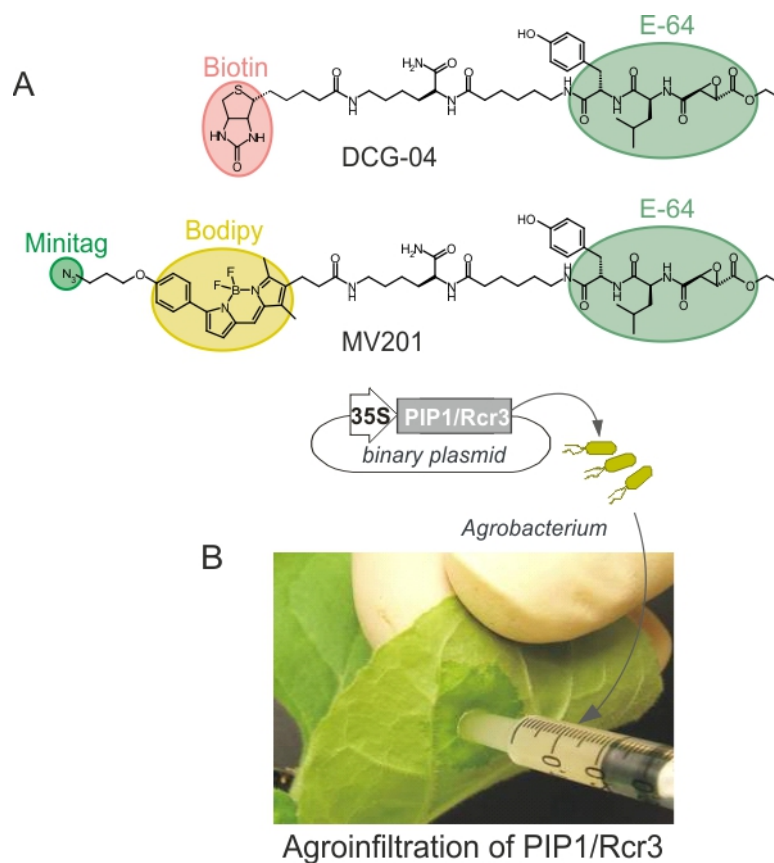
Figure 18 | Fluorescent DCG-04 structure scheme for agroinfilteration
A- Structure of activity-based probes for PLCPs. DCG-04 has a biotin tag to visualize the biotinylated protein using streptavidin and MV201 has two reporter tags BODIPY and azide. Both carry the epoxide reactive group to label the catalytic Cys.
B- PIP1/Rcr3 was produced by agroinfiltration**.** The PIP1/Rcr3 ORFs of wild tomato species were cloned into binary vectors transformed into *Agrobacterium tumefaciens* and produced in *N. benthamiana*. Apoplastic fluid (AF) was harvested at 4-5 days after infiltration.

vector, expressed in *N. benthamiana* and tested for interaction with Epic1 and Epic2B using inhibition assays based on ABPP: $Rcr3^{lyc\_H148N/R151Q}$, $Rcr3^{lyc\_Q267H}$, $Rcr3^{lyc\_D283N}$, $Rcr3^{lyc\_S330A}$, $Rcr3^{hab\_N148H/Q151R}$, $Rcr3^{hab\_H267Q}$, $Rcr3^{hab\_N283D}$, $Rcr3^{hab\_A330S}$. Additionally, the following Rcr3 mutants were available for these assays: $Rcr3^{lyc\_H148N}$, $Rcr3^{lyc\_R151Q}$, $Rcr3^{hab\_N148H}$ and $Rcr3^{hab\_Q151R}$ (Hörger, unpublished results). The mutants however showed in part a different behavior from the wild-type constructs (Fig. 20, Table 1). Most of the mutants in the *S. lycopersicum* background were behaving like the wild-type and could be inhibited by Epic2B, but not by Epic1. The $Rcr3^{lyc\_H148N}$ mutant however, can be
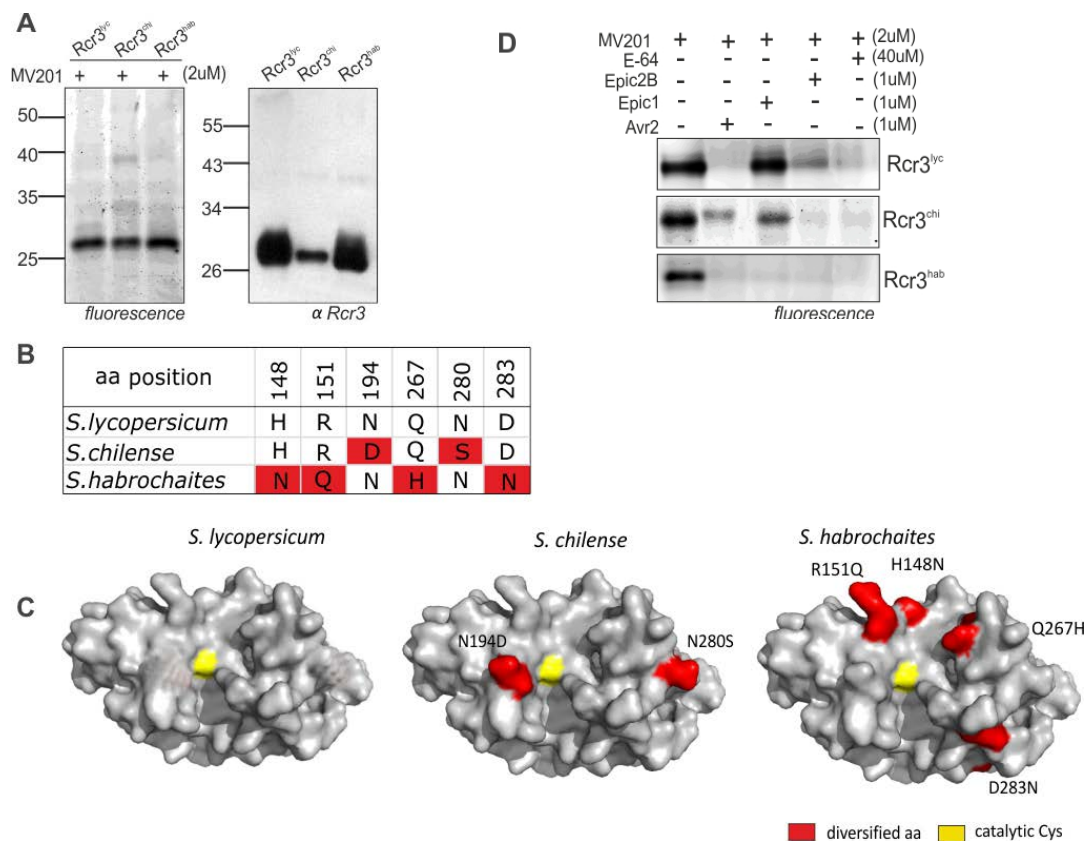
Figure 19 | Rcr3 variants from wild tomato species

A- Apoplastic fluids extracted from infiltrated *N. benthamiana* plants contain active Rcr3. Left panel: Labeling of AFs containing Rcr3 by MV201. Right panel: Detection of Rcr3 in AFs using αRcr3.

B- Summary of variant residues (red) in the protease domain of Rcr3 from three wild tomato relatives.

C- Structural models of Rcr3. Position of variant residues is highlighted in red and the catalytic cysteine in yellow.

D- Differential inhibition activity of *C. fulvum* and *P. infestans* effectors regarding inhibition of all tested natural Rcr3 variants. Preincubation of effector (1μM) protein with AF-containing Rcr3 for 30 minutes was followed by MV201 (2μM) labeling for two hours at room temperature. The lower blue panel (coomassie) represents the loading control

inhibited by Epic1 and therefore shows *S. habrochaites*-like behavior suggesting that N148 is the most likely residue interacting with Epic1. The pattern observed at the reciprocal mutants in the *S. habrochaites* background is not consistent with this finding. Unlike *S. habrochaites*, most of the mutants could be inhibited by Epic2B, but not by Epic1 suggesting that it is not only amino acid position 148 determining the interaction between Rcr3[hab] and both Epics.

Rcr3 combining protein haplotypes and inhibition data														
aa position	148	151	194	267	280	283	330	inhibited by						
								E-64	Avr2	Epic1	Epic2B	Epic2B^{L2V}	Epic2B^{N3D}	Epic2B^{K67N}
S.lycopersicum	H	R	N	Q	N	D	S	+	+	−	+	(+)	(+)	+
S.chilense	H	R	D	Q	S	D	S	+	−	−	+	n.t.	n.t.	n.t.
S.habrochaites	N	Q	N	H	N	N	A	+	+	+	+	+	+	+
lyc_H148N	N	R	N	Q	N	D	S	+	+	+	+	+	+	+
lyc_R151Q	H	Q	N	Q	N	D	S	+	+	−	+	+	+	+
lyc_H148N/R151Q	N	Q	N	H	N	D	S	+	+	(+)	+	+	+	+
lyc_Q267H	H	R	N	Q	N	D	S	+	+	(+)	+	−	−	+
lyc_D283N	H	R	N	Q	N	N	S	+	+	−	+	(+)	+	+
lyc_S330A	H	R	N	Q	N	D	A	+	+	−	+	−	+	+
hab_N148H	H	Q	N	H	N	N	A	+	+	(+)	+	+	(+)	+
hab_Q151R	N	R	N	H	N	N	A	+	+	+	+	+	+	(+)
hab_N148H/Q151R	H	R	N	H	N	N	A	+	+	+	+	(+)	(+)	(+)
hab_H267Q	N	Q	N	Q	N	N	A	+	+	−	(+)	+	+	+
hab_N283D	N	Q	N	H	N	D	A	+	+	−	+	+	+	+
hab_A330S	N	Q	N	H	N	N	S	+	+	−	+	−	−	−

Table 1 | Overview of all tested Rcr3 protease domain haplotypes and their phenotype in inhibition assays with pathogen-derived effectors and their mutants. The protein sequence of *S. lycopersicum* is used as a reference. In the haplotype matrix, amino acid polymorphisms in the natural variants are indicated with red and the mutated amino acid positions in the site-directed mutants with green.
+ = phenotype present, (+) = weak phenotype, - = phenotype absent, n.t. = not tested

All Rcr3 mutants and wild-type alleles were in addition tested for inhibition by mutants of Epic2B, which have previously been generated in search for the site of interaction of the Epics with their host targets (Hörger, unpublished results). These mutants (Epic2B^{L2V}, Epic2B^{N3D} and Epic2B^{K67N}) are derived from wild-type Epic2B and carry each one amino acid change towards Epic1 (Fig. 20). Rcr3^{lyc} and Rcr3^{hab} could both be inhibited by these three Epic2B mutants, but inhibition of Rcr3^{lyc} by Epic2B^{L2V} and Epic2B^{N3D} appeared to be weaker than inhibition by Epic2B^{K67N} or wild-type Epic2B. The Rcr3^{lyc} mutants H148N, R151Q and H148N/R151Q behaved like wild-type Rcr3^{hab} and could be inhibited strongly by all three Epic2B mutants, while the others showed weaker inhibition similarly to wild-type Rcr3^{lyc}. The Rcr3^{hab} mutants could like wild-type Rcr3^{hab} be strongly inhibited by the Epic2B mutants with exception of Rcr3$^{hab\_N148H/Q151R}$, Rcr3$^{hab\_N148H}$ and Rcr3$^{hab\_A330S}$, which showed weaker or even no inhibition by the Epic2B mutants (Fig. 22, Table 1).
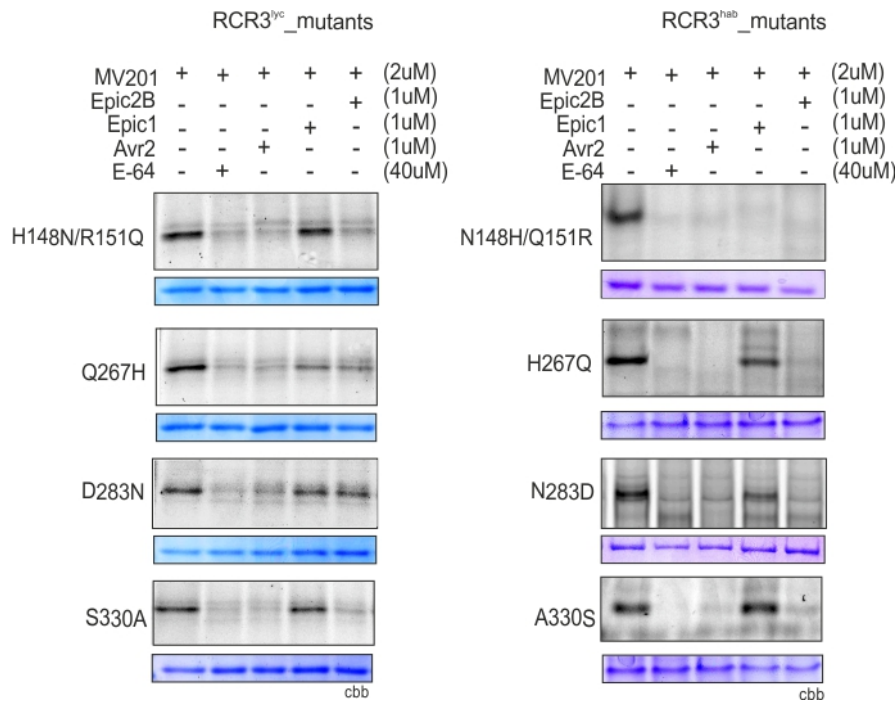
Figure 20 | Differential inhibition activity of *C. fulvum* and *P. infestans* effectors regarding inhibition of all tested Rcr3 mutants. Preincubation of effector (1µM) protein with AF-containing Rcr3 mutants for 30 minutes was followed by MV201 (2µM) labeling for two hours at room temperature. The lower blue panel (coomassie) represents the loading control.
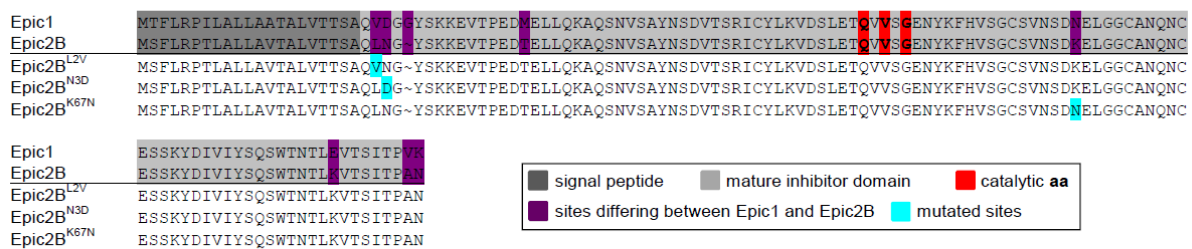
Figure 21 | Protein sequence of Epic1, Epic2B and the Epic2B mutants
Sites on purple background differ between the two Epics, and the positions, which have been mutated in the Epic2B background towards Epic1, are highlighted on light blue background. The two wild-type Epics and the three mutants were expressed in E. coli and purified via fused His-tags.
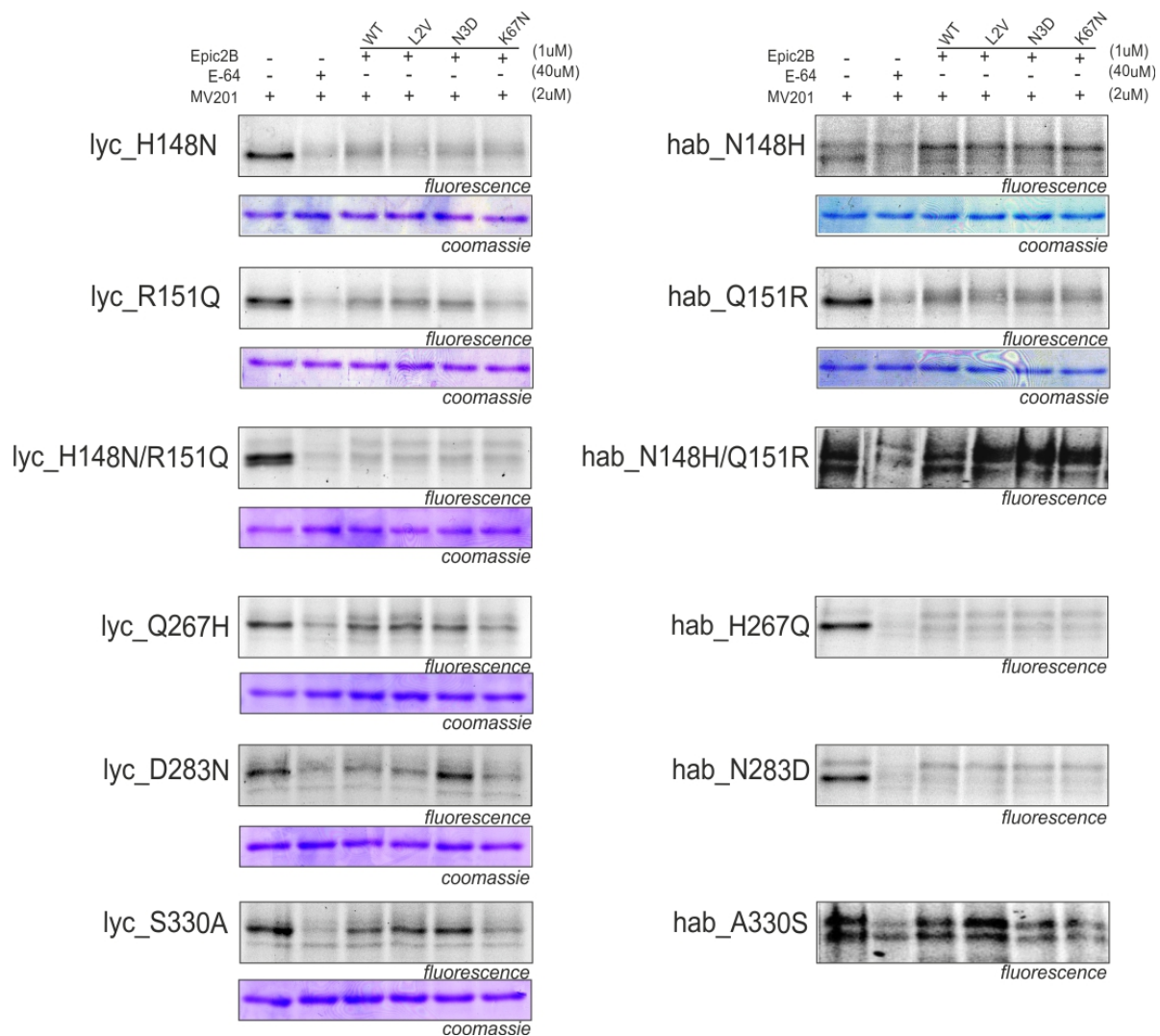
Figure 22 | Differential inhibition activity of mutant Epic2B
The Epic2B mutants were expressed in *E. coli* and purified. Preincubation of mutant Epic2b (1µM) protein with AF-containing Rcr3 for 30 minutes was followed by MV201 (2µM) labeling for two hours at room temperature. The lower blue panel (coomassie) represents the loading control.

To obtain a statistically supported picture of the phenotypic data and to disentangle the effects of single amino acid polymorphisms on the interaction between Rcr3 and Epic1, an association analysis was performed using all 54 natural Rcr3 alleles from the previous association study (Hörger et al. unpublished data) and all Rcr3 variants tested in this study. Similarly to previous findings, the following sites show up to be highly significantly associated with sensitivity to inhibition by Epic1: position 441 (synonymous polymorphism, $R^2 = 0.219$, *P*-value = 3.03 x 10^{-6}), position 442 (amino acid polymorphism H148N, $R^2 =$

0.327, P-value = 1.26 x 10^{-8}) and position 452 (amino acid polymorphism R151Q, R^2 = 0.243, P-value = 9.61 x 10^{-7}). Two additional polymorphic sites are marginally significantly associated: position 280 (synonymous polymorphism, R^2 = 0.162, P-value = 4.18 x 10^{-5}) and position 950 (amino acid polymorphism N283D, R^2 = 0.154, P-value = 6.06 x 10^{-5}). A striking difference in this new dataset is the increased significance of association of the H148N polymorphism with the observed phenotype (Fig. 23). Due to small sample size, association analyses with the Epic2B mutants did not show any significant results.
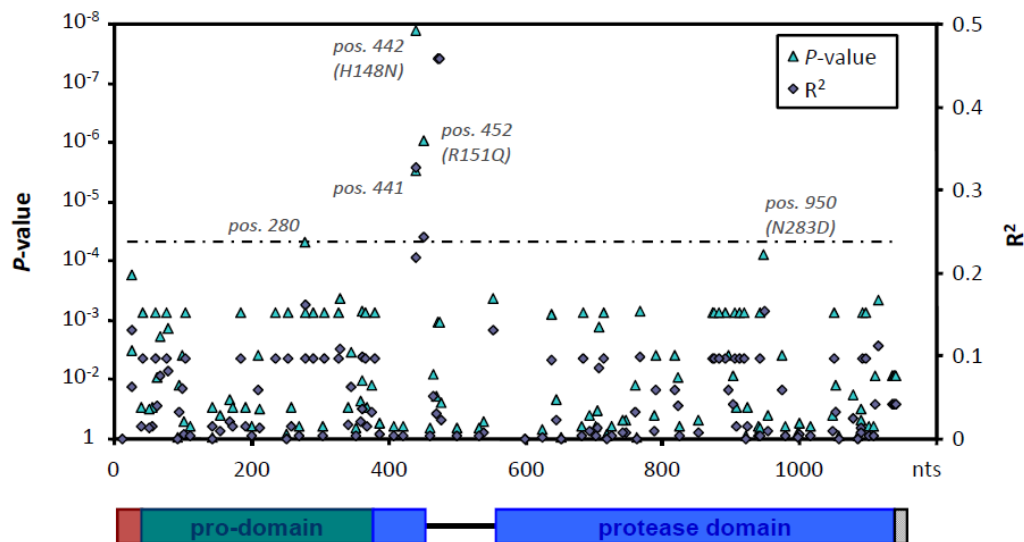
Figure 23 | Association of SNPs along the *Rcr3* locus with inhibition by Epic1 *in vitro*
SNPs were correlated with the observed phenotype using a general linear model. The y-axes on the left hand side show the P-values of the correlation. The y-axes on the right hand side show the correlation coefficient. Values were corrected by the Bonferroni method. The dashed line indicates the significance threshold after Bonferroni correction (0.05). A schematic of the gene is indicated below the x-axis (colored boxes are the exons encoding for signal peptide (red), pro-domain and protease domain).

2.7.2 Natural variation in PIP1 affects inhibition by pathogen-derived inhibitors

The second defense related protease PIP1 exhibits levels of interspecific nucleotide and amino acid diversity, which are decreased in comparison to Rcr3 but increased in comparison to

other PLCPs in the tomato apoplast (Fig. 24 A & B). This variation is largely found at the protein surface surrounding the catalytic center (Fig. 24C). To investigate the role of the observed natural variation in protein function, PIP1 alleles from six different tomato species (*Solanum lycopersicum*, *S. peruvianum*, *S. habrochaites*, *S. pennellii*, *S. cheesmanii and S. chilense*) were cloned into binary vectors, expressed in *N. benthamiana* and tested for interaction with different pathogen effectors as described in chapter 2.7.1.

All five PIP1 constructs were expressed successfully and could be detected through western blot analysis in *N. benthamiana* AFs (Fig. 25B). Furthermore, all alleles could be labeled by DCG-04 and inhibited by E-64 suggesting they are all active proteases (Fig. 25A & C). Subsequently, these natural variants were tested for their interaction with Avr2, Epic1 and Epic2B. The allele originating from *S. cheesmanii* could not be stably expressed in *N. benthamiana* in following rounds of agroinfiltration and was therefore not incubated in inhibition assays. Even though the remaining five tested PIP1 alleles exhibited substantial diversity at the protein level, only slight phenotypic differences could be observed between alleles (Fig. 25C, Table 2). Inhibition assays showed that Avr2 can inhibit all tested PIP1 alleles strongly and Epic2B strongly to moderately, while in contrast Epic1 was not able to inhibit any of the five variants. This dataset comprised only five PIP1 alleles and no significant phenotypic difference between alleles were observed. Therefore no significant association between genotype and phenotype could be obtained for PIP1.

PIP1 combining protein haplotypes and inhibition data												
PIP1 proteases	134	139	223	225	238	241	267	283	314	inhibited by			
										E-64	Avr2	Epic1	Epic2B
S.lycopersicum	M	R	A	N	N	E	D	S	D	+	+	−	+
S.peruvianum	.	.	.	.	S	.	.	.	S	+	+	−	(+)
S.habrochates	.	.	S	.	.	.	H	Y	S	+	+	−	+
S.pennellii	.	.	.	K	.	.	.	.	S	+	+	−	(+)
S.chilense	T	K	.	.	S	.	.	.	S	+	+	−	+

Table 2 | Overview of all tested PIP1 protease domain haplotypes and their phenotype in inhibition assays with pathogen-derived effectors and their mutants

The protein sequence of *S. lycopersicum* is used as a reference. In the haplotype matrix, amino acid polymorphisms in the natural variants are indicated with green. + = phenotype present, (+) = weak phenotype, - = phenotype absent
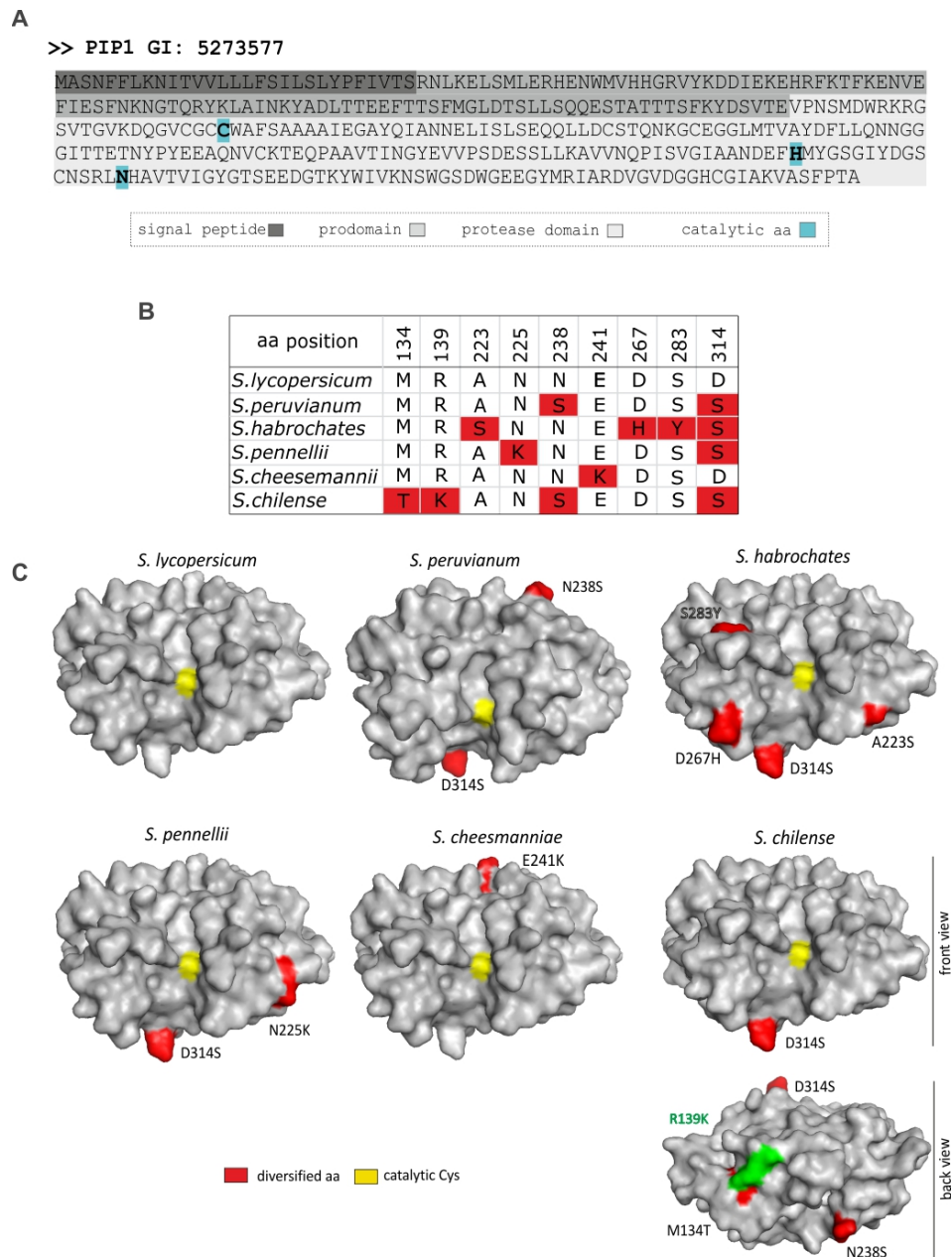
Figure 24 | Full length PIP1 amino acids sequence and variant residues in wild tomato species

A- Protein sequence of PIP1 (*Phytophthora inhibited protease 1*). Different colors represent the signal peptide, (29aa, dark gray), pro-domain, (100aa, medium gray) and functional protease domain (216aa, light gray). Amino acids indicated in bold and cyan background are catalytic residues Cys (C25), His (H159) and Asp (N175).
B- Summary of variant residues (red) in the protease domain of PIP1 from various wild tomato relatives.
C- Structural models of PIP1. Position of variant residues is highlighted in red, catalytic cysteine in yellow and substrate binding cleft front top-to-bottom.
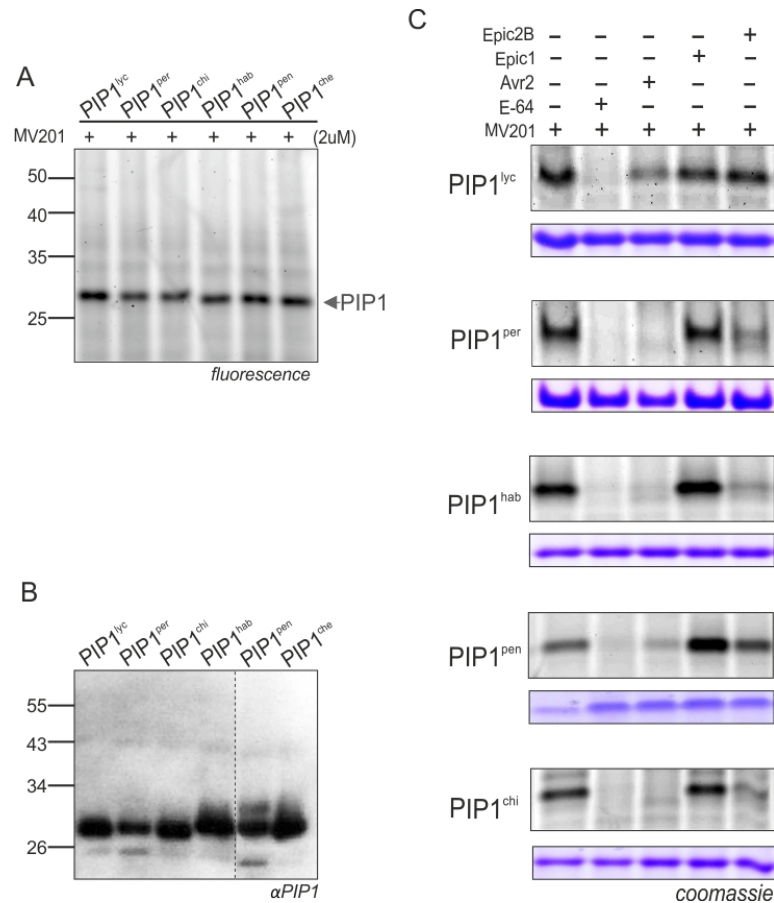
Figure 25 | Characterization and Inhibition of PIP1 by MV201 profiling

A- Labeling of PIP1-containing AF using MV201**.** AF was labeled for two hours with 2 µM of MV201 at pH 6.0 at room temperature. Labeled protein was separated on gel blots and detected using fluorescent scanning. The arrow head indicates the signals of PIP1 at 28-30 kDa.

B- Confirmation of identity by PIP1 antibody**.** The AF of different PIP1 was loaded onto polyacrylamide gel 12 % and proteins were transferred to PVDF membranes. For detecting PIP1 proteins the membrane was incubated with PIP1 antibody, signals were detected using Super Signal Femto/Pico substrate.

C-Unlike Epic1, Avr2 and Epic2B inhibit PIP1 globally**.** PIP1 constructs were transiently expressed in *N. benthamiana* plants using agroinfiltration and AFs containing the different expressed PIP1 variants was isolated. AF was preincubated at pH 6.0 with or without E-64 (40 µM), Avr2, Epic1and Epic2B (1µM) for 30 minutes. MV201 (2µM) was added to label the remaining the noninhibited PIP1 and labeled protein was detected on protein gels using fluorescent scanning.

Chapter 3- Discussion

3.1   General concept of the project

The way how plants recognize pathogens and initiate the defense responses has been subject of intense research of the past decade. In this thesis we investigated the role of PLCPs Rcr3 and PIP1 in immunity against *C. fulvum* and *P. infestans*. We found that *PIP1* but not *Rcr3* contributes to immunity to *C. fulvum* in the absence of *Cf2* consistent with the decoy model. In contrast, *Rcr3* does contribute to *P. infestans* immunity, both in the presence and absence of *Cf2*. We also investigated the role of natural variation in Rcr3 and PIP1 on interaction with *P. infestans* Epics proteins and could identify residues in Rcr3 that affect the interaction with Epic1.

3.2 Dominance of necrotic phenotype caused by *Rcr3^{lyc}*

We observed that autonecrosis induced by *Rcr3^{lyc}* segregates as a dominant gene in the F1 and F2 populations of a cross between *Cf2/rcr3-3^{pim}* and *Cf0/Rcr3^{lyc}* plants. This observation is consistent with previous studies and highlights an interesting aspect of *Rcr3* function. When *Cf2* was introgressed into *S. lycopersicum* by an inter-species cross with *S. pimpinellifolium,* half of the progeny of a backcross to *S. lycopersicum* spontaneously developed necrotic lesions {Langford, 1948 #130}. This phenotype was associated with the presence of *Cf2*, either in a homozygous or heterozygous state, and another gene called *Ne*. Necrotic plants were all homozygous for the *S. lycopersicum* allele *ne* whereas heterozygous plants were not necrotic. Thus the *S. pimpinellifolium* allele *Ne* suppressed the development of necrosis as a dominant gene. *Ne* was later shown to be *Rcr3^{pim}* and *ne* is *Rcr3^{lyc}*. The development of necrosis requires that *Rcr3^{lyc}* levels are relatively high. This also explains that why no *35S::Rcr3^{lyc}* transgenic plants have been recovered in a *Cf2* background (Rooney, H. PhD thesis, 2004). We observed that *Rcr3^{lyc}* segregates as a dominant gene in the F1 and F2 populations of a cross between *Cf2/rcr3-3^{pim}* and *Cf0/Rcr3^{lyc}*. The F1 progeny was necrotic and necrosis segregated in 9/16 in the F2 population. Our observation that *Rcr3^{lyc}* is a dominant gene could be explained since the *Cf2/rcr3-3^{pim}* parent does not contain the

functional $Rcr3^{pim}$. The data indicate that $Rcr3^{pim}$ outcompetes $Rcr3^{lyc}$ function and that $Rcr3^{lyc}$ becomes dominant in the absence of $Rcr3^{pim}$. According to literature, necrosis is partially suppressed in *rcr3-1* mutant plants because *rcr3-1* is also a partial mutant (Krüger et al., 2002). A null mutant *rcr3-3* failed to induce full necrosis. The biochemical interpretation of these genetic interactions is that in the absence of Avr2, $Rcr3^{lyc}$ interacts with Cf2, but this interaction triggers autonecrosis. $Rcr3^{pim}$ would also bind to Cf2 in the absence of Avr2 and outcompete $Rcr3^{lyc}$ binding. This hypothesis would suggest that $Rcr3^{pim}$ has a higher affinity for Cf2 than $Rcr3^{lyc}$, which would be consistent with the coevolution between Cf2 and $Rcr3^{pim}$ in *S. pimpinellifolium*.

3.3   *Cladosporium fulvum*-tomato interactions

3.3.1 Rcr3 is probably a decoy

Our findings support the hypothesis that Rcr3 is a decoy. In the absence of *Cf2*, *C. fulvum* growth was indistinguishable between *Cf0/Rcr3* and *Cf0/rcr3-3* plants (Fig. 12A & B). This data is consistent with previous studies. A previous study did not show significant difference of *C. fulvum* growth between *Cf0/Rcr3^{lyc}* and *Cf2/rcr3-3* plants (Dixon et al., 2000). However, the authors state: 'The tendency of lower disease sensitivity was observed 10 days after infection in *rcr3-3* and *rcr3-2* mutants compared with the Cf0 susceptible control could be caused by the absence of *Rcr3* pathogenicity target'. This remark illustrates strong expectation on a role of *Rcr3* in the absence of *Cf2*. In a second study, *Cf2/rcr3-3* plants were not more susceptible than *Cf2/Rcr3* plants to *C. fulvum* race 2 which does not carry *Avr2* (van Esse et al., 2008). Taken together, these data indicate that Rcr3 has no function in the absence of the Cf2 resistance protein.

3.3.2 PIP1 is an operative target of Avr2

The decoy model implies that besides the decoy, there must be an operative target of the effector. In case of Avr2, PIP1 was our prime candidate. We found that plants silenced for *PIP1* (*asPIP1* plants) are more susceptible than control plants (Fig. 14 A & B). This data indicates that PIP1 contributes to immunity against *C. fulvum* and hence that PIP1 is the

operative target of Avr2, consistent with the decoy model (van der Hoorn and Kamoun, 2008).

Preliminary results indicate that *asPIP1* plants are also more susceptible to *P. syringae* (Ilyas *and* Van der Hoorn unpublished). This would suggest that *PIP1* contributes to basal defense making PIP1 a genuine operative target consistent with the decoy model. Examples to test whether *asPIP1* plants are more susceptible against *P. infestans* remain to be done in future. Although *C. fulvum* produces PLCPs inhibitors, the protection against PIP1 must be incomplete, possibly because these inhibitors are not completely effective. How PIP1 can function against *C. fulvum* is yet unclear. In general, it remains unclear how the apoplastic proteases contribute to immunity. It can be argued that proteases act directly by degrading pathogen-derived proteins or indirectly by regulating a signalling cascade and/or activation other proteins. For example, the apoplastic aspartic protease CDR1 acts in disease resistance signalling against *P. syringae* (Xia et al., 2004). CDR1 triggers SA-dependent *PR* gene expression due to release of small peptides that are thought to function as a mobile signal to activate systemic acquired resistance (SAR). Another example is the apoplastic Cys protease from maize which can trigger *PR* gene expression upon injection into the naïve maize plants, indicating that Cys proteases are sufficient for defense induction even without pathogen infection (van der Linde et al., 2012). As another example, subtilisin-like proteases, termed phytaspases (plant Asp-specific protease), were identified in rice (*Oryza sativa*) and tobacco. Phytaspases have caspase-like activity and regulating immune responses leads to PCD (Chichkova et al., 2010). Overexpression and silencing of the phytaspase gene showed that phytaspase is essential for PCD-related responses to tobacco mosaic virus and abiotic stresses (Chichkova et al., 2010). During *C. fulvum*-tomato interaction, it can be assumed that PIP1 causes damage to pathogen directly by degrading the effector molecules or indirectly by activating other enzymes or inducing signalling cascades. However further understanding of how PIP1 function against *C. fulvum* would highlight the role of PLCPs in pathogen defense.

3.4 *Phytophthora infestans*-tomato interactions

3.4.1 *Rcr3^{pim}* contributes to defense against *P. infestans*

Our data and data of Song et al (2009) shows that *Cf2/rcr3-3^{pim}* plants are more susceptible

when compared to *Cf2/Rcr3^{pim}* plants (Fig. 15 A & B). This suggests that *Rcr3^{pim}* contributes to immunity to tomato plants against *P. infestans*. This result justifies the prediction that the guardee contributes to basal defense.

Like Avr2, Epic2B binds and inhibits Rcr3, but unlike Avr2, Epic2B is a weak reversible inhibitor. Only high concentration causes full inhibition of Rcr3 *in vitro*. The kinetics of this interaction may explain the finding that the Epic2B-Rcr3 complex is not recognized in a Cf2 dependent manner and fails to trigger HR in *Cf2/Rcr3^{pim}* plants. It has been proposed that Epics effector molecules have evolved stealthy inhibitory properties that inhibit the virulence target in the host but avoid being recognized by the plant immune system (Song et al., 2009).

Both *Cf2* and *Rcr3^{pim}* were co-introgressed into the cultivated tomato from the wild relative *S. pimpinellifolium*. It has been assumed that the Rcr3-Epic complex may cause weak activation of *Cf2* and this might be the reason for defense against *P. infestans*. However, no HR induced by Epics was observed in *Cf2/Rcr3^{pim}* plants, and even *PR1a* gene expression was found only in *Cf2/Rcr3^{pim}* plants by injecting Avr2 but not induced by Epics (Song et al., 2009). To confirm that Epics do not trigger immune responses in *Cf2/Rcr3^{pim}* plants, we monitored ROS production on four tomato lines *Cf2/Rcr3^{pim}*, *Cf2/rcr3-3^{pim}*, *Cf0/Rcr3^{pim}* and *Cf0/rcr3-3^{pim}* using purified Avr2, Epic1, Epic2B and flg22, as control. We found that there was no ROS production in either case with Epics but we observed weak generation of ROS in *Cf2/Rcr3^{pim}* tomato leaves when adding Avr2. Furthermore, we performed ion leakage assays on detached tomato leaves of above mentioned four tomato lines, and found that there was no induction of ion leakage in any of the tested tomato lines upon infiltration of Epic1 and Epic2B indicating that Rcr3 and Epics together do not trigger (*Cf2*-mediated) defense. These results indicate that the Rcr3-Epic complex is not recognized in a Cf2-dependent manner. It is possible that, unlike Avr2, Epics create a different conformational change in Rcr3 preventing the recognition by Cf2. The 3D structures of Avr2, Rcr3 and Epics are not known yet. However with the help of comparative modeling, the 3D structures of Rcr3 and the Epics can be predicted. Future studies on the structural identification of Rcr3^{pim}, Avr2 and Epcis will yield a better understanding to determine how Cf2 recognizes conformational changes in Rcr3.

3.4.2 *Rcr3* is a guardee

To investigate whether *Rcr3* can contribute to defense independent of *Cf2*, we performed *P. infestans* inoculation on tomato plants carrying *Cf0/Rcr3^{pim}* and *Cf0/rcr3-3^{pim}*. Notably, we discovered that the *Cf0/Rcr3^{pim}* tomato line shows increased resistance against *P. infestans* when compared to *Cf0/rcr3-3^{pim}* plants (Fig. 16 A & B). These results demonstrate that *Rcr3^{pim}* contributes to defense independent of Cf2. This is consistent with the guard model, which predicts Rcr3 is a virulence target.

However, the observation that *Cf0/Rcr3^{pim}* plants are more resistant to *P. infestans* when compared to *Cf2/Rcr3^{pim}* plants suggests that additional components may have been introgressed during crossing that are causing enhanced resistance in this line (Fig. 17A). In *Cf0/Rcr3^{pim}* infected leaves only local necrosis at the inoculation site was observed while *Cf2/Rcr3^{pim}* plant developed more necrotic growth. Likewise *Cf2/rcr3-3^{pim}* plants showed more sporulation when compared to *Cf0/rcr3-3^{pim}* plants. These results indicate that the loss of *Cf0* locus increases the susceptibility to *P. infestans*.

The *Cf2* locus carries two independent functional genes, *Cf2.1* and *Cf2.2*. These genes differ only with three nonsynonmyous nucleotides and both genes confer resistance (Dixon et al., 1996). A third gene, *Hcr2-2A* (Homolog for *C. fulvum* resistance gene 2) also located at *Cf2* locus but does not confer resistance to *C. fulvum* (Dixon et al., 1998). It can be assumed that the three genes at the *Cf2* locus have been introgressed during crossing between *Cf2/Rcr3^{pim}* and *Cf0/Rcr3^{lyc}* plants in the Cf0 background. The *Cf0* locus contains two *Cf2*-homologs *Hcr2-0A* and *Hcr2-0B* (Dixon et al., 1998). The enhanced disease resistance to *P. infestans* in Cf0 background might therefore be due to the presence of *Hcr2-0A* or *Hcr2-0B* homologs or a suppression of resistance on the *Cf2* locus. We speculate that Epics or another effector molecule from *P. infestans* is recognized by the *Hcr2-0A* or *Hcr2-0B* in *Rcr3^{pim}*-dependent manner. However, these possibilities remain to be tested e.g. by transformation of the *Hcr2-0AB* homologs into *Cf2/Rcr3^{pim}* and *Cf2/rcr3-3^{pim}* tomato lines. ROS and ion leakage assays of Epics in *Cf0/Rcr3^{pim}* were not conclusive. *PR1* gene expression upon injecting Epics along with HR induction assays remains to be done in *Cf0/Rcr3^{pim}* plants. A further understanding of this observation might help the breeding of tomato lines that are resistant to *P. infestans*.
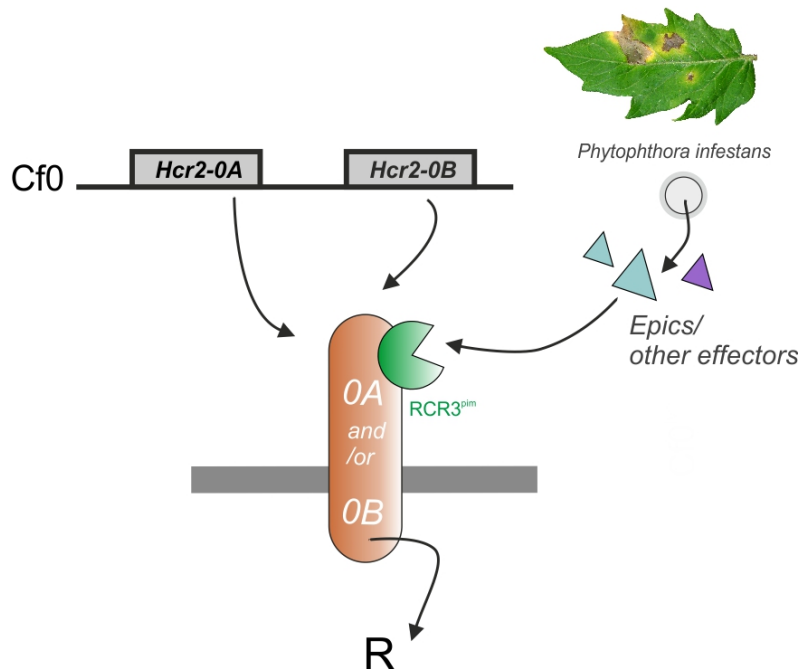
Figure 26 | Model of *P. infestans* recognition and defense induction

P. infestans secretes Epics/putative effectors. These effectors might be recognized by *Rcr3^{pim}* through *Hcr2-0A* and/or *Hcr2-0B*-mediated defense pathway which triggers immunity.

3.4.3 Rcr3- a multitasking role in pathogen-defense

Rcr3 does not contribute to defense against *C. fulvum* but *Rcr3* does contribute against *P. infestans* independent of *Cf2*. Furthermore, in the nematode-tomato interaction *Rcr3* also contributes to defense (Lozano-Torres, et al., 2012). Potato root-nematode *G. rostochiensis* secrets a small protein Gr-VAP1 that physically binds to and inhibits *Rcr3* (Lozano-Torres, et al., 2012). This interaction also triggers a *Cf2*-mediated defense response leading to HR. This is an example of a dual specificity of plant immune receptors that recognize common virulence targets (guardee, *Rcr3*) of effectors of two unrelated pathogens. In this study it has been shown that the number of nematodes in *Cf2/Rcr3^{pim}* was 60% lower compared to *Cf2/rcr3-3^{pim}*. This result demonstrates that *Rcr3^{pim}* also confers resistance to *G. rostochiensis*. Intriguingly, *Cf0/Rcr3^{pim}* plants exhibit more susceptibility compared to *Cf0/rcr3-3^{pim}* suggesting that *Rcr3^{pim}* enhances susceptibility in the absence of *Cf2*. These observations are very different to our *C. fulvum* infection data where in the absence of *Cf2*, *Rcr3* does not

affect the susceptibility. We do not have an explanation for these contrasting phenotypes. However, an important assumption of the guard hypothesis that the host guardees are virulence targets for the Avr protein is supported with the observation that enhanced susceptibility in $Cf0/Rcr3^{pim}$ when compared to $Cf0/Rcr3^{lyc}$ indicating that $Rcr3^{pim}$ is a virulence target. In conclusion, $Rcr3$ act as a guardee and this exemplifies the role of $Rcr3$ and support the guard model in context to tomato-nematode pathosystem.

According to the biochemical properties of effector molecules from unrelated pathogens may enable them to target various host proteins. In fact, it has been demonstrated that *C. fulvum* secretes the protease inhibitor Avr2 that targets at least two different host proteases: Rcr3 and PIP1. Furthermore, it has been shown in addition to Avr2 from *C. fulvum*, effectors Epic1 and Epic2B from an unrelated pathogen of *P. infestans* can target the same host proteins Rcr3 and PIP1 (Song et al., 2009). Similar arguments were used to explain that *P. syringae* effectors AvrRpm1 and AvrRpt2 target the RIN4 protein. The phosphorylation of RIN4 caused by the AvrRpm1 and cleavage by AvrRpt2 causes the activation of the R proteins RPM1 and RPS2 respectively (Chung et al., 2011). These findings support the second prediction of guard model.
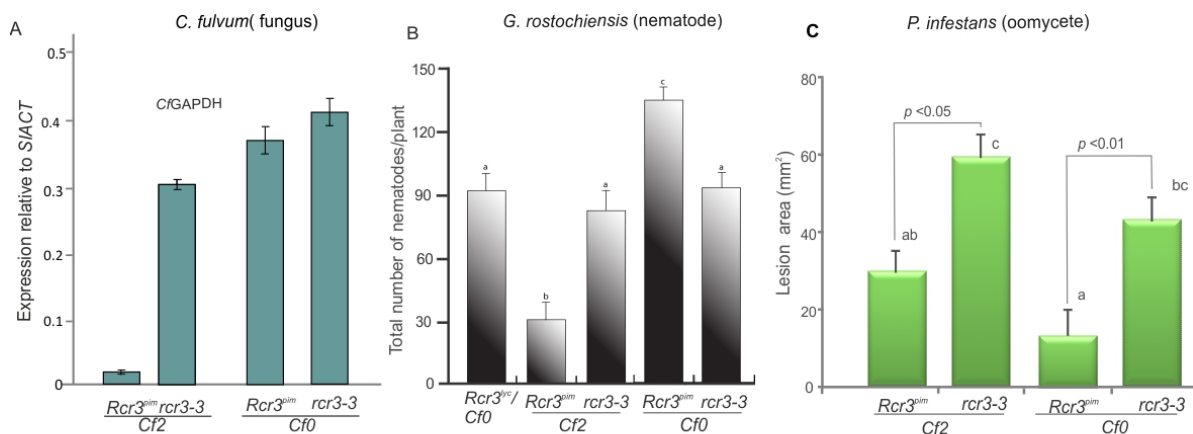
Figure 27 | Role of *Rcr3* during infection with different pathogens
Data were extracted for fungus from results section 2.5.1 and 2.5.2 (**A**), for nematode (Lozano-Torres et al., 2012) (**B**) and for oomycete results section 2.6.3, Fig. 17 (**C**).

This is a very interesting observation: a single host protein (Rcr3) act differently in three pathosystem. In the presence of *Cf2*, *Rcr3* contributes to resistance against all three pathogens, fungus *C. fulvum*, nematode *G. rostochiensis* and oomycete *P. infestans.* In the absence of *Cf2*, *Rcr3* presence does not affect *C. fulvum* growth but enhances *G. rostochiensis* growth and decreases *P. infestans* growth. Therefore *Rcr3* has a multitasking role in immunity.

3.5   Functional consequences of sequence variance in *Rcr3* and *PIP1*

A central concept of host-pathogen evolution is that natural selection promotes diversity at involved loci improving recognition of the pathogen by the host and facilitating evasion of recognition by the pathogen. Antagonistic protein-protein interaction at the plant-pathogen interface can be shaped by diversifying selection of residues that can interfere with protein-protein interactions (Misas-Villamil and van der Hoorn, 2008). There is selection pressure on both the effector and its targets to adapt to a changing environment (van der Hoorn and Kamoun, 2008).

3.5.1 Epic2B seems to be a universal inhibitor of tomato defense related PLCPs

Inhibition assays of three natural Rcr3 variants and site-directed mutants showed that Rcr3 could in general be inhibited by Epic2B and to a lesser extent by Epic1, consistent with previous findings (Song et al. 2009, Hörger 2011) (Table 1, Fig. 19 & 20). A similar pattern could be observed in inhibition assays with five PIP1 alleles. Epic2B showed a varying ability to inhibit PIP1, while Epic1 was not able to inhibit any of the tested PIP1 alleles (Table 2, Fig. 25). These results suggest that Epic2B is a universal inhibitor of defense related PLCPs in tomato, Rcr3 and PIP1, while Epic1 seems to inhibit more selectively. This differential phenotypic behavior of two closely related, very similar effector proteins can have different outcomes of the interaction between host plant and oomycete. Assuming on the one hand that inhibition of defense related proteases is beneficial for the pathogen; *P. infestans* individuals carrying Epic2B would have a fitness advantage on most host plants. Individuals carrying

only Epic1 would in most cases not be able to disturb the proteolytic environment created in the apoplast to prevent pathogen invasion and could therefore not establish a successful infection. If on the other hand inhibition of the host protease would lead to recognition of the pathogen, as it is the case in the Rcr3-Avr2 interaction, pathogens carrying only Epic1 would have a clear fitness advantage. However, since infiltration of Epic1 and Epic2B into different tomato genotypes did not lead to activation of HR, it cannot be assumed that Rcr3 and PIP1 contribute to resistance to *P. infestans* via interaction with Epic1 or Epic2B in a similar manner as in the Avr2-Rcr3-Cf-2 system. These findings suggest that Rcr3 and PIP1 may simply have an important role in the basal defense and inhibition of their proteolytic function is crucial for the pathogen. *P. infestans*, like many oomycetes, is dwelling in rather humid and temperate climates (Agrios book) and it is therefore unlikely that the wild tomato species studied in this thesis, which are distributed in rather dry habitats (Nakazato et al., 2010), have undergone long-term coevolution with this pathogen resulting in specific recognition of pathogen effectors. Since it is a common strategy of plants to create a proteolytic environment during pathogen attack (Shindo and Van Der Hoorn, 2008) , Rcr3 and PIP1 might simply be targeted by the Epics due to structural similarities with proteases *P. infestans* encounters during infection of its natural hosts.

3.5.2 Natural variation in Rcr3 affects inhibition by pathogen-derived inhibitors

Rcr3 exhibits an elevated level of inter- and intraspecific nucleotide and amino acid diversity compared to neutral standards and to other tomato PLCPs. This genotypic diversity has been shown to also translate into phenotypic diversity regarding the interaction with the *C. fulvum* effector Avr2 and the interaction with Cf-2 (Shabab et al. 2008, Hörger et al. unpublished results). However, these aspects of Rcr3 function do not explain the full diversity observed at this gene and previous results suggested that differential interaction between Rcr3 and the *P. infestans* effectors Epic1 and Epic2B accounts for another portion of this diversity (Hörger 2011). These findings are confirmed and further assessed in this thesis. Inhibition assays with three natural Rcr3 variants and site-directed mutants have been performed to decipher the role of particular amino acid polymorphisms which are significantly associated with differential

interaction with Epic1 or Epic2B or both in a reciprocal fashion. The results regarding inhibition by Epic1 support previous findings suggesting that the amino acid position 148 is important in the interaction between Rcr3 and Epic1 (Table 1, Fig. 19, 20 & 23). Rcr3^{lyc} and other Rcr3 variants, which encode Histidine at this position cannot be inhibited by Epic1, while Rcr3^{hab} and the site-directed mutants H148N/R151Q and H148N carrying Asparagine at position 148, are inhibited by Epic1. An association analysis performed with 54 Rcr3 alleles tested in a previous study (Hörger et al. unpublished results, Hörger 2011) as well as the Rcr3 variants tested in the present study confirmed a significant association between sensitivity to inhibition by Epic1 and H148N (Fig. 23).
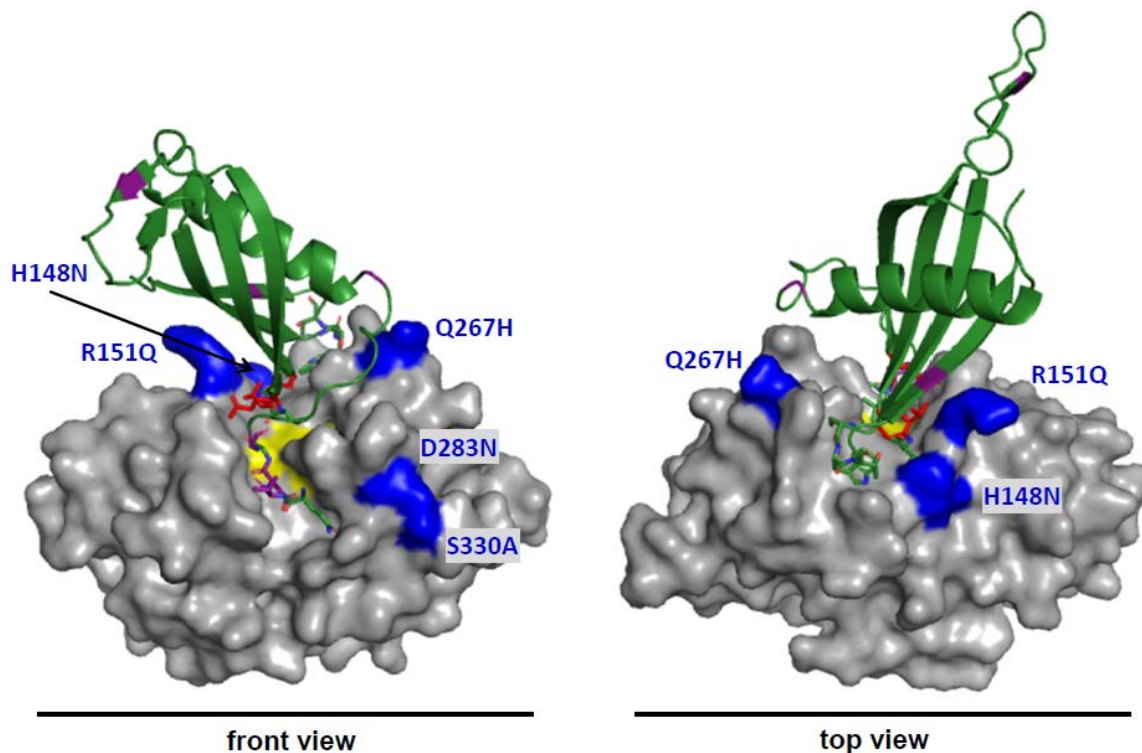
Figure 28 | Putative structural co-model of Rcr3^{lyc} (grey) and *P. infestans* Epic1 (green).
The model was generated based on the C14-Epic1 co-model from Kaschani et al. 2011. The catalytic centre of Rcr3 is shown in yellow. Amino acid residues varying between Rcr3lyc and Rcr3hab, which potentially have an effect on differential behaviour towards inhibition by Epic1, are highlighted in blue. Amino acid residues distinguishing Epic1 and Epic2B are shown in purple and QxVxG motif in Epic1 are highlighted in red.

The structures of Rcr3 and Epic1 have not yet been resolved. However, it is possible to structure modeling (Kaschani and van der Hoorn, 2011). The putative co-model of Rcr3 in complex with Epic1 illustrates the possibility that H148N plays a crucial role in this protein-protein interaction. This residue is located in close proximity to the QxVxG motif of Epic1 (highlighted in red) and replacement of the positively charged Histidine at this position by the polar, uncharged Asparagine may have an impact on sensitivity to inhibition. These findings are consistent with a previous study finding that H148N, R151Q and D283N in the Rcr3 protease domain are significantly associated with sensitivity to inhibition by Epic1 (Hörger 2011). The testing of the here generated mutants allowed to disentangle the effects of different amino acid substitutions and to uncover H148N to be the most likely site of interaction.

It is not clear from previous data and from the results obtained in this thesis whether the interaction between Rcr3 and the Epics plays a role during the tomato-*P. infestans* interaction because it is unknown if *P. infestans* is a coevolving pathogen of wild tomato species. However, the observation that natural variation at the *Rcr3* locus can translate into differences in the interaction with Epics may hint at the significance of this interaction. There is so far no evidence for selective forces generating diversity regarding interaction with these *P. infestans* effectors, but this may be due to the nature of the datasets surveying polymorphism at this locus. Previous evolutionary studies have focused on populations from the species *S. peruvianum*, *S. chilense* and *S. corneliomulleri*, which are native to rather dry habitats (Hörger 2011) and likely do not encounter *P. infestans*, and variation regarding differential interaction with Epic1/2B was rare. The mutation(s) likely affecting the interaction with Epic1 can be found in *S. habrochaites* and *S. lycopersicoides* and an interesting future project would be to study variation in terms of interaction with *P. infestans* effectors within these species.

3.5.3 The inhibition phenotype cannot be recovered in reciprocal mutants

To perform an adequate site-directed mutagenesis approach, not only mutants in *S. lycopersicum* but also the reciprocal mutants in *S. habrochaites* background were generated and tested. In light of the results obtained for the mutants in *S. lycopersicum* background, these reciprocal mutants showed unexpected phenotypic behavior in inhibition assays. While mutants in *S. lycopersicum* background, except for H148N and H148N/R151Q, behaved like wild-type Rcr3^{lyc}, most mutants in *S. habrochaites* background did not behave like the wild-

type. Moreover, N148H and N148H/Q151R could still be inhibited by Epic1 (like Rcr3[hab]), which is unexpected under the assumption that position 148 is the site of interaction. A possible explanation for this finding is epistasis between amino acids within a certain Rcr3 background. Thereby, H148N may have a strong effect on sensitivity to inhibition by Epic1 in *S. lycopersicum* background, but the effect in *S. habrochaites* background may be weaker due to epistatic interactions with other amino acids occurring in Rcr3[hab] (Ortlund et al., 2007). The fact that the associations study did not only uncover H148N to be significantly associated, but also other positions support this hypothesis.

3.5.4 Reciprocal behavior of Epic1 and Epic2B cannot be recovered

One result of a previous study investigating natural variation at Rcr3 found that differential interaction with Epic1 or Epic2B appeared to be reciprocal (Hörger 2011). Rcr3 alleles, which could be inhibited by Epic1, could not be inhibited by Epic2B and vice versa. Association analysis indicated that there is an overlap between the mutations causing sensitivity to inhibition by Epic1 and insensitivity to inhibition by Epic2B. Substitutions H148N and D283N were found to be significantly associated with this reciprocal phenotype. These polymorphisms still show up to be significantly associated with sensitivity to inhibition by Epic1, but association analysis performed for the interaction between Rcr3 and Epic2B did not give clear significant results after adding data obtained for the Rcr3 mutants. One reason for this inconsistency may be epistasis between different sites at Rcr3, which may have been weakened in course of this site-directed mutagenesis approach separating the potential causative sites to disentangle their effects.

3.5.5 The Epic2B mutations L2V and N3D most likely cause the difference between Epic1 and Epic2B

Variation at the target molecules in the host seems to play an important role in protease-inhibitor interactions at the plant-pathogen interface (Shabab et al. 2008, Hörger et al. unpublished results). However, also variation at the second partner in this interaction – the effector – may be involved in its outcome. The results of a previous study finding reciprocal behavior in interactions with Epic1 and Epic2B has led to the idea that one or more of the sites distinguishing Epic1 and Epic2B may be the sites of interaction between Rcr3 and the Epics (Hörger 2011). Based on the putative co-model of Rcr3 and Epic1/2B, putative

candidate sites have been identified and site-directed mutants of Epic2B towards Epic1 have been generated. Inhibition assays with these mutants do not give a clear answer to the question on which residues are responsible for functional differences between Epic1 and Epic2B, but there is a clear tendency showing that the mutations L2V and N3D cause a more Epic1-like behavior of these Epic2B mutants (Table 1, Fig. 22). However, each of these single mutations is not able to recreate the full Epic1 phenotype suggesting that the two sites have additive effects on the inhibitory properties of these effectors.

3.5.6 Natural variation at PIP1 does not affect the inhibition by pathogen-derived inhibitors

When comparing interspecific diversity at different tomato PLCPs not only Rcr3, but another defense related protease, PIP1, exhibit an elevated level of nucleotide and amino acid diversity. The diversity observed at PIP1 is centered around the catalytic site of this protease and might therefore be involved in differential interaction with pathogen-derived protease inhibitors. To test this hypothesis, inhibition assays with Avr2, Epic1 and Epic2B were performed using five PIP1 alleles originating from the cultivated tomato and different wild tomato species. Unlike Rcr3, only minor phenotypic differences between the natural variants were observed. All tested alleles could be strongly inhibited by Avr2 and to varying degrees by Epic2B, but were insensitive to inhibition by Epic1. This lack of observed functional diversity may be due to the experimental setup. Since only five different PIP1 variants were tested, important variation with functional relevance might have been missed. Likewise, it is possible that the variation at PIP1 plays a role for interaction with other pathogen effectors and showed conformity when being tested with only one different effector. On the other hand, the lack of observed functional variation may be due to strong functional conservation of PIP1 and may reflect its importance as protease during the basal defense (Caldwell and Michelmore, 2009). The fact that PIP1 is the most abundant apoplastic protease during the course of infection supports this idea.

3.6 Future prospects

The work described in this thesis has contributed to the understanding of the role of PLCPs PIP1 and Rcr3 in pathogen defense against *C. fulvum* and *P. infestans*. Previous data and

results of this thesis suggest that different, unrelated pathogens target similar host proteins. Rcr3 can adopt multiple roles during the immune defense depending on the pathosystem.

Following research questions can be addressed in future for a better understanding of plant immune responses.

First- How Rcr3 interact with Cf2: in the presence/absence Avr2?

How Cf2 sense the modification of Rcr3 by Avr2 is not yet known. Future experiments could therefore focus on the sites and mode of interaction between Cf2 and Rcr3. Domain-swap (e.g. van der Hoorn et al. 2001) and site-directed mutagenesis approaches along with infiltrations and/or protein-protein interaction studies might thereby help to find interacting sites in Cf2. Co-infiltration of purified Rcr3 instead of AF containing expressed Rcr3 would exclude side effects caused by other components in the apoplast.

Second- -Elucidate the role of variant residues in inhibition assays.

During inhibition assays with Rcr3 variants, potential effects between residues could be identified. It would be necessary to generate mutants carrying specific amino acid residues. These mutants could be used for identifying association regarding inhibition of *Rcr3* alleles by different pathogen effectors.

Third- What is the role of *Hcr2-0A* and *Hrc2-0B* might exhibit together with *Rcr3*?

Cf0/Rcr3 plants are more resistant to *P. infestans* than *Cf2/Rcr3* plants. The *Cf0* locus contains two *Cf2* homologs, *Hcr2-0A* and *Hcr2-0B* (Dixon et al., 1998) which could potentially interact with *Rcr3*. *Rcr3*-mediated disease resistance could be assessed through generation of new tomato genotypes without one or both *Cf2*-homologs or *Cf0* (*Hcr2-0A* or *Hcr2-0B*) in *Cf2/Rcr3* genotypes.

Forth- Would *rcr3* mutation in *asPIP1* show a phenotype for *C. fulvum* infection?

Results of this work show that *asPIP1* lines are more susceptible to *C. fulvum* infection than wild-type *PIP1* plants. Since the *asPIP1* lines have been generated in *Cf0/Rcr3* background, it is possible that there is an effect of *Rcr3* on resistance to *C. fulvum* in these lines. It would be an interesting to assess whether *Rcr3* influences the outcome of the infection in *asPIP1* lines. Silencing of *PIP1* in *rcr3-3* mutant genotypes would contribute to solve this question.

Fifth- Are *asPIP1* plants more susceptible for pathogens (*P. infestans* and *G. rostochiensis*)?

PIP1 seems to be involved in resistance to different unrelated pathogens (*P. syringae* and *C. fulvum)*. These findings suggest that *PIP1* plays a role during the basal defense, if this was indeed the case, *asPIP1* lines should be more susceptible to a larger set of pathogens including oomycetes or nematodes. Infection assays with other pathogens (e.g. *P. infestans* or *G. rostochiensis*) using *asPIP1* plants should give an idea about whether or not *PIP1* likely has a role in the basal defense.

Chapter 4- Materials and Methods

4.1 Materials

4.1.1 Laboratory chemicals and biochemical consumables

Purity grade chemicals and deionised water (Milli-Q Plus Water system, Millipore, Bedford, U.S.A.) were used for preparation of all solutions and media. As dictated by different requirements, solutions and media were autoclaved (20 min, 120°C, 2 x 105 Pa). General laboratory chemicals were supplied from: Applichem (Darmstadt, Germany), Biomol (Hamburg, Germany), Brand (Wertheim/Main, Germany), Duchefa (Haarlem, The Netherlands), Fluka (Buchs, Germany), Merck-Schuchard (Darmstadt, Germany), Roth (Karlsruhe, Germany), Serva (Heidelberg, Germany) and Sigma-Aldrich (Münich, Germany).

4.1.2 Wild tomato lines and other plant materials

All tomato (*Solanum lycopersicum*) work was carried out using cultivar Money Maker (MM), unless otherwise stated (Table 4.1 and 4.2).

Table 4.1 Wild tomato species

	accession No.	tomato species
1		*S. lycopersicum*
2	LA0446	*S. peruvianum*
3	LA1777	*S. habrochaites/hirsutum*
4	LA0716	*S. pennellii*
5	LA0927	*S. cheesmaniae*
6	LA1930	*S. chilense*

Table 4.2   Tomato species

Species	line		characteristics
S. lycopersicum	MM-Cf0 (*Cf0/Rcr3^{lyc}*)		cv Money Maker (MM), no resistance to *C. fulvum* strains tested {Jones, 1993 #281}
	MM-Cf2 (*Cf2/Rcr3pim*)		Near-isogenic to MM-Cf0, *Cf-2* and *Rcr3^{pim}* have been introgressed from *S. pimpinellifolium* followed by successive backcrossing to *S. lycopersicum*
	MM-Cf2 rcr3 (*Cf2/rcr3-3^{pim}*)		MM-Cf2 carrying rcr3-3 mutation causing premature stop codon in *Rcr3^{pim}* (Rooney et al., 2005)
	Cf0/Rcr3^{pim}		generated in this study through crossing
	Cf0/rcr3-3^{pim}		generated in this study through crossing
	MM-Cf0	*35S:PIP1*	generated in this study through transformation
		asPIP1	generated in this study through transformation
		35S:C14	generated in this study through transformation
		csC14	generated in this study through transformation

4.1.3 Bacterial strains

Escherichia coli strain DH10B was used for standard cloning. *Agrobacterium tumefaciens* strain GV3101 was used for *Agrobacterium*-infiltration and plant transformation.

4.1.4 Chemical probes and inhibitors

Epoxide probes DCG-04 (Greenbaum et al., 2000) and MV201 (Richau et al., 2012) were provided by Dr. Matthew Bogyo (Stanford University) and Dr. Herman Overkleeft (Leiden University). All probes were dissolved in DMSO to a stock concentration of 1 mM and stored at -20 °C. Fluorescent probes were always kept in the dark. Chemical inhibitor E-64 was purchased from Sigma. BTH 50WG (Actigard/Bion, 50% wettable granule) was ordered from Ciba.

4.1.5 Plasmids

Following plasmids have been described before: pFK26 (shuttling vector), pTP05 (binary vector), pTP43 (binary *35S: PIP1^{lyc}*), pTP36 (*35S:Rcr3^{lyc}*) (Shabab et al., 2008) and pBinPlus (*35S:Rcr3^{pim}-His*) (Song et al., 2009).

Table 4.3 Cloning procedure of tomato proteases into agroinfiltration vectors

gene	species	primers	cloned into *pFK26* using	cloned into *pTP05* using	binary clone
PIP1-His	*S. pennellii*	r070 & r270	*Nco*I-*Bam*HI	*Hin*dIII- *Bam*HI	*pIM01a*
PIP1-His	*S. peruvianum*	r070 & r270	*Nco*I-*Bam*HI	*Hin*dIII- *Bam*HI	*pIM02a*
PIP1-His	*S. cheesmaniae*	r070 & r270	*Nco*I-*Bam*HI	*Hin*dIII- *Bam*HI	*pIM03a*
PIP1-His	*S. chilense*	r070 & r270	*Nco*I-*Bam*HI	*Hin*dIII- *Bam*HI	*pIM04a*
PIP1-His	*S. habrochates*	r070 & r270	*Nco*I-*Bam*HI	*Hin*dIII- *Bam*HI	*pIM05a*
RCR3-His	*S. chilense*	r072 & r271	*Nco*I-*Xho*I	*Xba*I-*Sal*I	*pIM06a*
RCR3-His	*S. habrochates*	r072 & r271	*Nco*I-*Xho*I	*Xba*I-*Sal*I	*pIM07a*

4.1.6 Materials generated by site-directed mutagenesis (SDM)

Parent plasmids of pTP25 (*Rcr3^{lyc}*) generated by Twinkal Pansuriya (Plant Chemetics Lab, Max Planck Institute for Plant Breeding Research Cologne Germany), pIM07a (*Rcr3^{hab}-His,* in shuttling vector pFK26) and pSK6.1 (*Epic2B*) generated by Selva Kumari Plant Chemetics Lab, Max Planck Institute for Plant Breeding Research Cologne Germany) were used for site-directed mutagenesis. Primers used for generating the mutants are summarized in table 4.8.

Table 4.4   Site-directed-mutagenesis constructs generated for RCR3 and Epic2B

SDM-constructs	parent plasmid	primers used	intermed-iate clone SDM	shuttled into *pTP05* using	binary clone
RCR3$^{N148H-Q151R}$	*pIM07*	i021 & i022	*pIM21*	*Xba*I-*Sal*I	*pIM31*
RCR3^{H267Q}	*pIM07*	i025 & i026	*pIM22*	*Xba*I-*Sal*I	*pIM32*
RCR3^{N283D}	*pIM07*	i029 & i030	*pIM23*	*Xba*I-*Sal*I	*pIM33*
RCR3^{A330S}	*pIM07*	i033 & i034	*pIM24*	*Xba*I-*Sal*I	*pIM34*
RCR3$^{H148N-R151Q}$	*pTP25*	i019 & i020	*pIM25*	*Xba*I-*Sal*I	*pIM35*
RCR3^{Q267H}	*pTP25*	i023 & i024	*pTP26*	*Xba*I-*Sal*I	*pTP36*
RCR3^{D283N}	*pTP25*	i027 & i028	*pIM27*	*Xba*I-*Sal*I	*pIM37*
RCR3^{S330A}	*pTP25*	i031 & i032	*pIM28*	*Xba*I-*Sal*I	*pIM38*
RCR3^{H148N}	*pTP25*	a001 & a002	*pAH01*	*Xba*I-*Sal*I	*pAH05*
RCR3^{R151Q}	*pTP25*	a003 & a004	*pAH02*	*Xba*I-*Sal*I	*pAH06*
RCR3^{N148H}	*pIM07*	a005 & a006	*pAH03*	*Xba*I-*Sal*I	*pAH07*
RCR3^{Q148R}	*pIM07*	a007 & a008	*pAH04*	*Xba*I-*Sal*I	*pAH08*
Epic2B^{L2V}	*pSK6.1*	a015 & a016	*pAH09*	-	-
Epic2B^{N3D}	*pSK6.1*	a017 & a018	*pAH10*	-	-
Epic2B^{K67N}	*pSK6.1*	a019 & a020	*pAH11*	-	-

lyc = S. lycopersicum,   hab = S. habrochaites,   pSK6.1-Epic2B (*Phytophthora infestans*)

4.1.7 Media

Listed below are different media used for growing pathogens.

Table 4.5 Media

Medium	recipe per litre
LB	10 g tryptone, 5 g yeast extract, 10 g NaCl and 10 g agar for solid media
NYG	5 g peptone, 3 g yeast extract, 20 ml glycerol and 10 g agar for solid media
PDA	10 g peptone, 6 g yeast extract, 40 ml glycine and 10 g agar for solid media
RSA	60 g rye grain (biological), 20 g sucrose and 15 g agar for solid media

4.1.8 Antibiotics

Listed below are antibiotics used to select positive clones and bacteria.

Table 4.6 Antibiotics

Antibiotics	stock Solution	working concentration
Ampicillin	100 mg/ml in water	100 µg/ml *E. coli* and *A. tumefaciens*
Rifampicin	100 mg/ml in methanol	50 µg/ml *A. tumefaciens*
Gentamicin	40 mg/ml in water	100 µg/ml *A. tumefaciens*
Kanamycin	50 mg/ml in water	50 µg/ml *E. coli* and *A. tumefaciens* 300 µg/ml tomato selection

4.1.9 Fungal and bacterial pathogens

Cladosporium fulvum race 5; race 2,4; race 2,5 and race 2,4,5 were kindly provided by Dr. Mattthieu Joosten (Laboratory of Phytopathology, Wageningen University, Netherlands) and maintained as 15% glycerol stock at -80°C. Spores of required fungus were cultured on PDA

plates. The oomycete *Phytophthora infestans* strains 88069 and 88069td were supplied by Dr. Sophien Kamoun (The Sainsbury Laboratory, John Innes Centre, Norwich UK).

4.1.10 Antibodies

Listed below are primary and secondary antibodies used for immunoblot detection.

Table 4.7 Antibodies

Antibody	animal	dilution	source
α-Rcr3	rabbit	1:2,000	(Rooney et al., 2005)
α-PIP1	rabbit	1:3,000	(Tian et al., 2007)
α-C14	rabbit	1:2,000	(Kaschani et al., 2010)
α-HIS	mouse	1:500	Roche
α-Rabbit-HRP	goat	1:15,000	Sigma
α-Mouse-HRP	rabbit	1:5,000	Sigma
α-Goat-HRP	rabbit	1:15,000	Sigma
Streptavidin-HRP Polymer (ultrasensitive)	N/A	1:5,000	Sigma

Table 4.8   Oligonucleotides used in this study

No.	name	sequence (5´ → 3´)	special remarks
Cloning of PIP1 and Rcr3			
r070	Sl-PIP1-f	agctccatggcttccaattttttcctcaag	full length *PIP1*
r071	Sl-PIP1-r	ccccggatcctcaagcagtagggaacgacgcaacc	
r270	Sl-PIP1His-r	ccccggatcctcagtgatggtgatggtgatgagcagtagggaacgacgcaacctttgc	full length *PIP1* rev with C-terminal His tag
r072	Sl-RCR3-f	agctccatggctatgaaagttgatttgatg	full length *Rcr3*
r073	Sl-RCR3-r	agctctcgagctatgctatgtttggataagaagac	

r271	Sl-RCR3His-r	agctctcgagctagtgatggtgatggtgatgtgctatgtttggataagaagacatc	full length *Rcr3* rev with C-terminal His tag
r110	Si-C14-f2	atggcctcgagcagctcaactctcaccatatcc	full length *C14*
r057	Si-C14-r	agctggatcctcaagaactgctcttctttcctcc	
r112	promf	ggagaggaccatttggagaggacacgt	pFK26-specific Seq. primer
r113	termr	gattagcatgtcactatgtgtgcatcc	
r114	binf	taggtttacccgccaatatatcctgtc	pTP5-specific Seq. primer
r115	binr	ttctgtcagttccaaacgtaaaacggc	
Site-directed-mutagenesis (SDM)-Rcr3 (lyc-hab)			
i019	sdm_hab1f	gtcactcaagtgaaacatcaaggtcgatgtggatgttgctgg	SDM introduces N148H-Q151R in Rcr3^{hab}
i020	sdm_hab1r	ccagcaacatccacatcgaccttgatgtttcacttgagtgac	
i021	sdm_lyc1f	gtcactcaagtgaaaaatcaaggtcaatgtggatgttgctgg	SDM introduces H148N-R151Q in Rcr3^{lyc}
i022	sdm_lyc1r	ccagcaacatccacattgaccttgatttttcacttgagtgac	
i023	sdm_hab2f	ggaatagctgctagccaagatttacagttttac	SDM introduces Q267H in Rcr3^{hab}
i024	sdm_hab2r	gtaaaactgtaaatcttggctagcagctattcc	
i025	sdm_lyc2f	ggaatagctgctagccatgatttacagttttac	SDM introduces H267Q in Rcr3^{lyc}
i026	sdm_lyc2r	gtaaaactgtaaatcatggctagcagctattcc	
i027	sdm_hab3f	ggaacttatgacggaaactgtgccgatcgaattaaccatgc	SDM introduces D283N in Rcr3^{hab}
i028	sdm_hab3r	gcatggttaattcgatcggcacagtttccgtcataagttcc	
i029	sdm_lyc3f	ggaacttatgacggatcctgtgccaatcgaattaaccatgc	SDM introduces N283D in Rcr3^{lyc}
i030	sdm_lyc3r	gcatggttaattcgattggcacaggatccgtcataagttcc	
i031	sdm_hab4f	gcataagagattctggggatccttcaggtctttgtgatatc	SDM introduces S330A in Rcr3^{hab}
i032	sdm_hab4r	gatatcacaaagacctgaaggatccccagaatctcttatgc	

i033	sdm_lyc4f	gcataagagattctgggaatcctgcaggtctttgtgatatc	SDM introduces A330S in Rcr3^{lyc}
i034	sdm_lyc4r	gatatcacaaagacctgcaggattcccagaatctcttatgc	
a001	RCR3^{H148N}f	gtcactcaagtgaaaaatcaaggtcgatgtgga	SDM introduces H148N in Rcr3^{lyc}
a002	RCR3^{H148N}r	tccacatcgaccttgattttttcacttgagtgac	
a003	RCR3^{R151Q}f	gtgaaacatcaaggtcaatgtggatgttgctgg	SDM introduces R151Q in Rcr3^{lyc}
a004	RCR3^{R151Q}r	ccagcaacatccacattgaccttgatgtttcac	
a005	RCR3^{N148H}f	gtcactcaagtgaaacatcaaggtcaatgtgga	SDM introduces N148H in Rcr3^{hab}
a006	RCR3^{N148H}r	tccacattgaccttgatgtttcacttgagtgac	
a007	RCR3^{Q151R}f	gtgaaaaatcaaggtcgatgtggatgttgctgg	SDM introduces Q151R in Rcr3^{hab}
a008	RCR3^{Q151R}r	ccagcaacatccacatcgaccttgattttttcac	
a009	Epic1^{V2L}f	tacttccagggccaactggacggcggatactcg	SDM introduces V2L in Epic1
a010	Epic1^{V2L}r	cgagtatccgccgtccagttggccctggaagta	
a011	Epic1^{D3N}f	ttccagggccaagtgaacggcggatactcgaag	SDM introduces D3N in Epic1
a012	Epic1^{D3N}r	cttcgagtatccgccgttcacttggccctggaa	
a013	Epic1^{N68K}f	agtgtcaactcggacaaggagctgggtggctgt	SDM introduces N68K in Epic1
a014	Epic1^{N68K}r	acagccacccagctccttgtccgagttgacact	
a015	Epic2B^{L2V}f	tacttccagggccaagtgaacggatactcaaag	SDM introduces V2L in Epic2B
a016	Epic2B^{L2V}r	cttttgagtatccgttcacttggccctggaagta	
a017	Epic2B^{N3D}f	ttccagggccaactggacggatactcaaagaag	SDM in introduces D3N in Epic2B
a018	Epic2B^{N3D}r	cttctttgagtatccgtccagttggccctggaa	
a019	Epic2B^{K67N}f	agcgtcaactcggacaacgagctgggcggctgt	SDM introduces N68K in Epic2B
a020	Epic2B^{K67N}r	acagccgcccagctcgttgtccgagttgacgct	
Selection of transgenic lines of PIP1 and C14			

i035	npt-II-f	agacaatcggctgctctgat	230-249
i036	npt-II-r	ccgctcagaagaactcgtca	930-948
i039	p35S-HindIII	gcgaagcttggtccccagattagcctttcaa	35S for pBINplus vector
i040	Tnos-KpnI	gcgggtacccccgatctagtaacatagatgacaccg	Tnos for pBINplus vector
i041	PIP1-Fspe	gcgactagtatggcttccaatttttcctcaag	*PIP1* for asPIP1
i042	PIP1-RBam	gcgggatcctcaagcagtagggaacgacgcaacctttgc	
	PIP1Fbam	gcgggatccatggcttccaatttttcctcaag	*PIP1* for overexpression
i050	PIP1-RspeHIS	gcaaaggttgcgtcgttccctactgctcatcaccatcaccatca ctgaactagtcgc	
Quantitative real-time PCR for transgenic tomato lines			
i056	SlAct2-SGN-U314753f	gctatccaggctgtgctttc	*SlActin2*, enclosing second intron.
i057	SlActin2-SGN-U314753r	tgctcctagcggtttcaagt	
i060	SlPIP1rtF2	cttcctcaccccaatcactc	qRT-PCR in asPIP1
i061	SlPIP1rtR2	attgcggctaacgatgagtt	
i062	SlC14rtF	gcaccacttgctgctgtatc	to test co-silencing of *C14* in asPIP1 lines
i063	SlC14rtR	ttgagcatgttccttgacga	
i066	SlRcr3rtF	ttacgcgggaggaacttatg	to test co-silencing of *Rcr3* in asPIP1 lines
i067	SlRcr3rtR	acctgaaggatccccagaat	
i072	CfAvr9-f	gagcttgctctcctaattgctactact	to detect fungus *Avr9* gene
i078	Avr9rPeter	gtagtctagcccgactcccaatc	
i074	SlPR-1a-f	tggtggttcatttcttgcaactac	Tomato *PR-1a*

i075	SlPR-1a-r	atcaatccgatccacttatcatttta	
i076	CfEcp6-f	gctcaaggttggtcagcagat	to detect fungal *Ecp6*
i077	CfEcp6-r	ttcacacctgacagatcacttatgc	
i079	Cf-GADPHf	ggaaaccggaaccgttcag	to detect fungal *GAPDH*
i080	Cf-GADPHr	tgttagtgatcccttgtgatccaa	
i081	Avr2qRTf	accgcatccgaagtaatagca	to detect fungal *Avr2*
i082	Avr2qRTr	ccagacttctccttcactttgca	
i094	clado actin Fw	acgtcaccaccttcaactcc	to detect fungal *Actin*
095	clado actin Rv	ggtgcgatgatcttgacctt	
Gene-specific primers			
r262	Rcr3^{lyc}f	gaatcagattatgaatacctaggtc	to detect *Rcr3^{lyc}*
r263	Rcr3^{pim}f	gaatcagattatgaatacctaggtg	to detect *Rcr3^{pim}*
r264	rcr3-3^{pim}f	gaatcagattatgaatacctaggtgaat	to detect *rcr3-3^{pim}*
r265	RCR3wtf	gaatcagattatgaatacctaggtgaac	to detect *Rcr3wt*
r266	Cf2-1f	gatctcattgcgatccgtata	to detect *Cf2.1*
r267	Hcr2-0Af	gatctcattgctcttcgggtg	to detect *Hcr2-0A*
r268	Hcr2rr	atagcccatcagagctgctttcc	Rev prim to detect *Cf2.1* and *Hcr2-0A*
r269	RCR3r	gctatgtttggataagaagacatc	Rev prim to detect *lyc*, *pim* allele
i037	Rcr3f1	cttgatggaattctctgaacagg	to detect *rcr3-3* from crossing experiment
i038	Rcr3f2	cgattgcaccaccaacaattatgg	to detect *rcr3-3* for seq analysis

| i046 | r154F actin tom | atgaagctcaatccaagaggggtatc | Tomato *Actin* |
| i047 | r155R actin tom | ctcctgctcatagtcaagagccac | |

4.2 Methods

4.2.1 Generate expression constructs of *PIP1* and *RCR3* alleles

Selected wild tomato species (Table 4.1) were used for cloning proteases. Seven open reading frames (ORFs, five for *PIP1* and two for *Rcr3)* have been amplified from cDNA by PCR using insert-specific primer pairs (Table 4.3). The cDNA was obtained from the leaves of BTH-treated wild tomato plants. These ORFs were cloned into *pFK26,* sequenced, and shuttled into the binary vector pTP5 as explained in Table 4.3. A Histidine-tag has been added by PCR to the C-terminus of all *Rcr3* and *PIP1* alleles to allow purification on nickel-columns. Binary vectors harboring *PIP1/Rcr3* were transformed into *Agrobacterium tumefaciens* strain GV3101. The cloning procedure of *PIP1* and *Rcr3* alleles is described in Table 4.3.

4.2.2 Plasmid DNA preparation from *E. coli* and *Agrobacterium*

Plasmid DNA was prepared using the Macherey-Nagel plasmid kit or Qiagen plasmid mini-prep kit following the manufacturer's instructions.

4.2.3 DNA digestion by restriction enzymes

Restriction digests were carried out using the appropriate enzymes and buffers according to

the manufacturers' instructions (Table 4.3). One unit enzyme was used per µg plasmid DNA, and reactions were incubated for 2 hours at the recommended temperature.

4.2.4 DNA dephosphorylation

Removal of the 5′ phosphate residue from linearised plasmid DNA was carried out to prevent the re-ligation of the vector. 2.5 µg linearised DNA was treated with one unit shrimp alkaline phosphatase (SAP, Fermentas) in SAP buffer (20 mM Tris-HCl pH 8.0, 10 mM $MgCl_2$) for 30 minutes at 37°C. The enzyme was subsequently inactivated by heating to 70°C for 10 minutes.

4.2.5 Preparation of competent *E. coli*

50 ml LB medium (Table 4.5) was inoculated with DH10B from a glycerol stock and grown overnight at 37°C, shaking at 250 rpm. Four one-liter Erlenmeyer flasks with 250 ml LB media were prepared and 2.5 ml of the starter culture was diluted in 250 ml LB media in a 1 liter flask and grown to an OD_{600} of 0.4 at 37°C, shaking at 250 rpm. The culture was cooled on ice and centrifuged at 3,000 *g* for 30 minutes at 4°C. The pellet was resuspended in 250 ml ice-cold sterile water and centrifuged 20 minutes at 3,000 g at 4°C. The pellet was resuspended again in 200 ml ice-cold water, centrifuged for 30 minutes at 3,000 g at 4°C and supernatant was discarded. At this stage, only 20 ml ice-cold water was used to resuspend the bacteria in a 50 ml falcon tube, the cells were centrifuged for 10 minutes at 2,000 g at 4°C. The pellet was resuspended 40 ml ice-cold water and centrifuged for 10 minutes at 2,000 g at 4°C. Subsequently 3.2 ml of 7% DMSO was added and the cells were resuspended and frozen in 40-50 µl aliquots in liquid nitrogen and stored at -80°C. This method was adapted from Inoue et al (1990).

4.2.6 Preparation of competent *Agrobacterium tumefaciens*

10 ml LB medium was inoculated with *A. tumefaciens* GV3101 and grown overnight at 28°C. 50 ml LB medium in a 250 ml flask was inoculated with 0.5 ml starter culture and grown at 28°C until it reached a OD_{600} of 1.2–1.5. The culture was then centrifuged at 2000 g for 10 minutes at 4°C. The pellet was washed five times with sterile ice-cold water. After the final wash the pellet was resuspended in 1 ml sterile water and transferred to a microfuge tube. The cells were pelleted at 1,000 g and the pellet was resuspended in 10% glycerol to a total volume of 400 µl. The cells were frozen at -80°C in 25 µl aliquots.

4.2.7 Transformation of *E. coli* by heat shock

Competent cells were thawn on ice, an aliquot of 50 µl of cells were gently mixed with 1 µl plasmid DNA or 10 µl ligation reaction and incubated on ice for 30 minutes. The mixture was then heat-shocked at 42°C for 1 minute and cooled on ice for one minute. 500 µl LB medium was added to the cells and then incubated at 37°C for 50-60 minutes on a rotary shaker. The transformation mixture was centrifuged for 20 seconds, the desired portion of the cells were then plated onto LB with the appropriate selective antibiotic (Table 4.6) and incubated at 37°C overnight or until colonies were visible.

4.2.8 Transformation of *E. coli* by electroporation

Electrocompetent cells were placed on ice. 40 µl of cells were transferred to a cold, 1.5 ml polypropylene tube. 1-10 µl of DNA suspension (plasmid or ligated products) was mixed gently by flicking the tube. The cell/DNA mixture was placed between the chilled electroporation cuvette placed in the safety chamber, and the electric pulse (1800V) was applied using Electroporator 2510, (Eppendorf AG, Germany). Following the pulse, the cells were immediately removed from the cuvette and mixed with 1 ml LB medium. The cells were incubated for 1 hour at 37°C shaking at 225 rpm. The cells were plated on LB medium containing desired antibiotics and kept for 14-16 hours at 37°C.

4.2.9 Transformation of *Agrobacterium* by electroporation

Electroporations were carried out using Electroporator 2510 (Eppendorf AG, Germany). 25 µl competent cells were mixed with 0.5 µl plasmid DNA in sterile water in a pre-chilled 0.15 cm electroporation cuvette and the cuvette was inserted into the cuvette holder of the electroporator so that the plastic nose of the cuvette fits into the slit of the cuvette holder. The electric pulse was applied at 1800V. After transformation, cells were transferred to 1 ml LB medium, incubated at 28°C for 1 hour then plated onto LB medium with the appropriate antibiotic and incubated at 28°C for 2 days.

4.2.10 Selection of transgenic lines of PIP1 and C14

The selection of transgenic plants of *PIP1* and *C14* were completed mainly in three steps described in details in chapter two. The primers used for selection of primary transformants are described in Table 4.8. The transcript abundance of *PIP1* in asPIP1 tomato plants have

shown in also result chapter. Following plasmids were used for the transformation; pBinPlus (*35S:PIP1-His*) for overexpressing, pBinPlus (*35S:asPIP1*) for silencing and pTP41 (*35S:C14*) (Shabab et al., 2008) for overexpression in MM-Cf0 tomato plants.

This project of generation, selection and molecular verification of the PIP1 and C14 overexpression and silent plants has been performed at The Sainsbury Laboratory, John Innes Centre, Norwich UK.

4.2.11 Tomato crosses

Tomato is a self-pollinating crop, thus emasculation is important. For the generation of tomato crosses, the immature flowers of the female parent were emasculated with forceps before the anthers began to dehisce (2-3 days before opening). Two days later took the anthers from the pollen parent and brushed inside lightly onto the stigma of the female flower to transfer pollen. Fully ripe fruit were harvested for seed collection. The seeds were removed from the fruit and incubated for 15 minutes in 50% w/v hydrochloric acid to remove any remaining fruit tissue/pulp. The seeds were then rinsed in water and incubated for a further 15 minutes in saturated Na_3PO_4 solution to remove any viral contamination. Finally the seeds were rinsed in water and dried in air.

4.2.12 Plant growth conditions

Tomato seeds were sown in EINHEIT ERDE® minitray soil and plants were grown in EINHEIT ERDE® *TYP ED73* profi substrate with fertilizer supplement RADIGEN, Germany in individual pots at 22°C during the day and 18°C during night. During the winter months 16 hours of artificial lighting was provided. For all pathogen inoculations the tomato plants were transferred in to climatic chamber at a 14-h light regime at 18°C (night) and 22°C (day).

Nicotiana benthamiana were germinated in the EINHEIT ERDE® minitray soil and grown individually in pots at 25°C during the day and 20°C at night in a containment glasshouse.

4.2.13 Preparation of genomic DNA from tomato

Plant genomic DNA was prepared using 400 µl Edward buffer (200 mM Tris pH 7.5, 250 mM NaCl, 25 mM EDTA, 0.5% SDS) to grind 100 mg fresh leaf tissue. The mixture was incubated at 65°C for 20 minutes and added to 1 volume of chloroform and gently mixed by

inverting the tubes. The tubes were centrifuged at 14,000 rpm for 10 minutes and the upper phase was transferred to a tube containing one volume of isopropanol to precipitate the DNA. After 10 minutes incubation at room temperature the DNA was pelleted by centrifugation at 14,000 rpm for 10 minutes and the pellet was washed in 70% ethanol. The DNA was dissolved in 50 µl water and stored at -20°C. This procedure yields impure DNA of sufficient quality for PCR amplification. For direct sequencing of genomic DNA, DNA was isolated using the Qiagen kit and instructions described in the manual.

4.2.14 Preparation of total RNA from plant tissue and cDNA synthesis

Total RNA was isolated from frozen leaf tissue using the RNeasy Plant Mini Kit (Qiagen) according to the manufacturer's instructions. DNA-free RNA was generated by using RNase-free endonuclease DNAse I (Roche) using buffer and RNase inhibitor as described by manufacturer. The purity and integrity of the RNA was checked by gel electrophoresis and RNA was quantified by measuring the ratio of A260 to A280 by NanoDrop. For cDNA synthesis 2 µg RNA in 8.0 µl water together with 1 µl dNTPs and 1 µl Oligo dT primers was heated to 65°C for 5 minutes to denature the RNA and cooled on ice for one minute. 4 µl RT buffer (50 mM Tris-HCl pH 8.3, 40 mM KCl, 5 mM MgCl2 10mM DTT, 0.5% Tween-20), 2 µl DTT, 1 µl RNAse inhibitor (Roche) and 1 µl Superscript II reverse transcriptase (Invitrogen) was added to a total volume of 20 µl and incubated for 60 minutes at 42°C. The reaction was stopped by heating to 72°C for 10 minutes. Synthesized cDNA was diluted and used for quantitative real time PCR or standard PCR reactions.

4.2.15 Polymerase chain reaction (PCR)

Amplification of specific DNA or cDNA fragments was carried out by PCR. Template DNA from a variety of sources was used. For plant genomic DNA 1 µl of template was used. For plasmid DNA 1 µl of a 1:50 dilution of plasmid mini-prep was used. Reaction volumes were between 20 – 50 µl containing 1 x PCR buffer (20 mM Tris-HCl pH 8.4, 50 mM KCl, 0.05% W-1), 200 µM of each dNTP, 1 µM forward and reverse primer, 2.5 unit DNA polymerase (Invitrogen, Promega, Biobudget) and 1.5 mM $MgCl_2$ for genomic DNA template and colony PCR or 0.75 mM $MgCl_2$ for all other templates. All PCR were carried out using a Bio-Rad DNA Engine Tetrad® 2 Thermal Cycler. The reaction was cycled for amplification using following program.

1	Initial denature	95°C	2:00 min
2	Denature	95°C	0:15 min
3	Annealing	55°C	0:15 min
4	Elongation	72°C	1:00 min/kb
5	Go to 2	x times (22-29 cycles)	
6	Elongation	72°C	5:00 min
7	Cooling	4°C	∞

4.2.16 Direct analysis of bacterial colonies by PCR

Direct analysis of *E. coli* and *Agrobacterium* colonies by colony PCR was carried out by substituting a small number of cells for template in a standard PCR reaction. A colony was transferred to 500 µl water and mixed by vortexing for 15 seconds. 1 µl of the diluted colony was used as a template for PCR.

4.2.17 Agarose gel electrophoresis

Agarose gel electrophoresis was used to separate and visualize DNA fragments. DNA samples were loaded in 1 x loading dye (Fermentas) into 0.8% - 1.5% (w/v) agarose gels (my-Budget Universal Agarose) in 1 x TBE buffer (45 mM Tris-borate, 1 mM EDTA) and 1 µg/ml ethidium bromide (EtBr). Electrophoresis was performed in TBE buffer at 50–100V depending on the fragment size and the separation needed. The DNA was visualized with a UV transilluminator and photographed using a Kodak EDAS290 camera system.

4.2.18 Quantitative real-time PCR (qRT-PCR)

Quantitative real-time PCR was performed using an iQ5 Real–time PCR Detection System (Bio-Rad). Hybridization mixture (IQ^{TM} SYBR® Green supermix, Bio-Rad) was used for making PCR master mixture. For qRT-PCR, 15 µl reaction volume was used containing 4 µl H_2O, 1 µl primers (Fw-Rv), 7 µl hybridization mix (buffer, $MgCl_2$, dNTPs and Taq Polymerase) and 3 µl cDNA. Following cycling protocol was used, initial denaturation at

95°C- 3 min, amplification (95°C- 10 sec, 60°C- 20 sec, 72°C- 20 sec, 40 cycles), melting curve (95°C- 3 sec, 60°C- 30 sec) and cooling 40°C- 30 sec. A set of different primer pairs were used for monitoring transcript denoted in Table 4.8. LightCycler® 480 II (Roche) was used when analyzing large set of samples with different oligonucleotide combinations at a same time to reduce the cost and input of experiment. Experiments were carried out using three independent biological samples. The threshold cycles were recorded and transcript abundance was analyzed using iQ5 Optical System Software (version 2.0) and LightCycler® 480 software version 1.5. Tomato *Actin* was used as reference.

4.2.19 Preparation and quantification of proteins from plant tissue

For total protein extraction from plant leaf tissue a 1 cm diameter leaf disc was frozen in liquid nitrogen and ground to a fine powder with two metal beads using tissue disruptor (Qiagen) with shaking frequency of 30 Hz for 1 minute. The ground tissue was resuspended in 500 µl (20 mM Tris pH: 8, 5 mM DTT), centrifuged five minutes two times at 14000 rpm at 4°C. The protein concentration was determined using the RCDC protein assay (Bio-Rad). The BSA (bovine serum albumin) standards were used for making different dilutions of 40 μl ranging 0.25-2.0 mg/ml of a of BSA stock solution (2.0 mg/ml). From the total leaf extract made at least 2 replicates of each 40 μl in 2 ml tubes following the addition of reagents A (200 µl) and B (1600 µl). Absorption was measured immediately at 750 nm using spectrophotometer and standard curve was used to calculate protein concentrations. This assay is compatible with plant samples because the measurement is done at 750 nm. At this wavelength the chlorophyll in plant samples does not absorb.

4.2.20 BTH treatment

For foliar application of the BTH, tomato plants (3-4 week-old) were sprayed with 300 μM benzothiadiazole to the leaf surface until the droplets ran off (Bion WG50 with 50% active ingredient). BTH spray treatment was repeated at 0, 2 and 4 days. The control plants were sprayed with sterile demineralized water. The tomato leaves were harvested at day 5.

4.2.21 Extraction of apoplastic fluids (AF)

AF was extracted from tomato and *N. benthamiana* leaves using a method modified from de Wit and Spikman (1982). Leaves were vacuum-infiltrated with ice-cold water, dried on tissue

paper and centrifuged at 2,500 rpm at 4°C for 10 minutes. AF was collected and stored at -20°C.

4.2.22 *Agrobacterium*-mediated transient gene expression in *N. benthamiana*

Agrobacterium strains carrying the binary vectors were grown overnight in 10 ml LB media containing 50 μg/ml kanamycin and 50 μg/ml rifampicin at 28°C shaking at 250 rpm. The culture was centrifuged at 2,500 rpm to pellet the cells, which were then resuspended in 10 mM MES pH 5.6, 10 mM $MgCl_2$ and 150 μM acetosyringone to an OD_{600} of 2.0. *Agrobacterium* culture containing the p19 silencing inhibitor (Voinnet et al., 2003) was resuspended to a final OD_{600} of 2.0. *Agrobacterium* containing PLCP binary plasmids was mixed in a 1:1 ratio (volume) with *Agrobacterium* containing p19 plasmid and incubated at room temperature for 2 hours before being infiltrated into *N. benthamiana* leaves using 1 ml syringe without needle. Leaf tissue or AF was harvested after 5 days.

4.2.23 SDS-PAGE and western blotting

Protein samples were heated in 1x loading buffer (50 mM Tris-HCl pH 6.8, 2% SDS, 10% glycerol, 100 mM DTT, bromophenol blue) for 5 minutes at 95°C, cooled and centrifuged at 14,000 rpm for 1 minute. Proteins were separated by vertical SDS-PAGE using X-Cell II Module system (Invitrogen) at 180 mA for 70-80 minutes. Gels were prepared freshly as needed and prepared according to standard procedures (Sambrook, 1989). Following electrophoresis the gel was either stained with Coomassie Blue R-250 stain (7% Acetic acid, 20% methanol, 0.25% Coomassie R-250) or proteins were transferred onto PVDF (Immobilon-P, Millipore) membrane. The membrane was moved into a 50 ml Falcon tube and blocked with 5 ml solution of 3% BSA, 1x TBS (Tris-Buffered Saline pH: 7.4) and 2% Tween-20 for 5 min with gentle agitation on a roller mixer (SRT2, Stuart). For the detection of biotinylated proteins, the membrane was incubated with streptavidin-HRP (Ultrasensitive, Sigma) at 1:3000 in the presence of 2% Tween-20 for 1 hr, and then washed five times five minutes with TBS containing 0.1% Tween-20. For the detection of nonbiotinylated proteins, the membrane was incubated with the protein-specific first antibody (Table 4.7) in 10 ml of 1 x TBS, 3% BSA and 2% Tween-20 for 1 hr, and then washed five times five minutes with TBS buffer containing 0.1% Tween-20. Next, the membrane was incubated with HRP-conjugated secondary antibody (Amersham) at 1:5000 in 10 ml of TBS-BSA and 2% Tween-

20 for 1 hr, and then washed five times five minutes with TBS buffer containing 0.1% Tween-20. Finally, HRP binding was detected by chemiluminescence (SuperSignal West Pico/Femto, Pierce), by exposing to photographic films (BioMax MR, Kodak) in the darkroom. The exposed film was developed by automatic X-ray film processor (Optimax, Protec).

4.2.24   Activity-based protease profiling and inhibition assays using DCG-04

Activity-based protein profiling was performed as described previously with minor changes (van der Hoorn et al., 2004). To assay protease activity of PIP1 or Rcr3 expressed in *N. benthamiana* leaves or AF isolated from tomato, AF was diluted into a final volume of 500 µl containing 50 mM NaAc, pH 6, 1 mM DTT and 2 µM DCG-04. For the negative control,   40 µM E-64 was added and preincubated for 30 minutes for competing DCG-04 labelling. Samples were incubated at room temperature for 5 hours on a rotary shaker. After five hours incubation, Labelled samples were mixed with 1 ml-ice cold acetone and centrifuged at 4°C for 5 minutes at 4000 rpm. Supernatant was then discarded and the pellet washed with 500 µl 70% ice-cold acetone. Pellets were dried at room temperature and resuspended in 50 µl SDS gel loading buffer. Samples were loaded onto a 12% polyacrylamide gel and proteins were transferred to PVDF membranes. The detection of biotinylated proteins is described in section 4.4.23. For inhibition assays, AF or protein extracts were preincubated for 30 minutes with pathogen derived-inhibitors such as Avr2, Epic1, Epic2B and E-64 (positive control) before adding DCG-04.

4.2.25 Pathogen assays

4.2.25.1 Tomato disease assays with the fungus *Cladosporium fulvum*

Inoculation of tomato with *C. fulvum* was performed as previously described (de Wit, 1977). The fungus *C. fulvum* race 5 was cultured on half-potato-dextrose agar (PDA) at 22°C. Conidia from three-week-old cultures on potato-dextrose agar were used for inoculation. 4-week-old tomato plants were used for inoculation. The tomato leaves were inoculated at the lower side by spraying with a conidial suspension in water (10^6 conidia/ml) using a regular plant sprayer. After drying, plants were kept in plastic cages at 100 % relative humidity. Afterwards 48 hours, relative humidity was maintained between 70-80% by opening the

transparent plastic cover. Temperature varied between 19-22C and light regime was 16 h day/8 h night. Disease progression was monitored until 14 days-post-inoculation.

4.2.25.2 Tomato disease assays with the oomycete *P. infestans*

P. infestans strains 88069 and 88069td were grown in Rye Sucrose Agar (RSA) plates for 12 days at 18°C. Sporangia were harvested from RSA plates by adding cold water to the plates and zoospores were collected after 3 hours of incubation at 4°C. Six-week-old tomato leaves were drop-inoculated with a solution of 10^6 zoospores/ml. Droplets of 10 μl were applied onto abaxial sides of -detached leaves on wet paper towels. Three droplets per leaf with a total of 24 droplets on total eight leaves per box were inoculated. Infected leaves were exposed to UV light at 4, 5, 6 and 8 days-after-inoculation (dpi) and disease progression was documented for necrosis and hyphal growth using microscope with identical setting for all the time points. Digitalized leaf images were loaded in Image J (1.45M) software (http://rsbweb.nih.gov/ij/) and leaf lesion area was measured in mm^2. Finally, the lesion growth rate (LGR) was calculated by subtracting the lesion area of the previous day. Significance level was calculated using SPSS statistical software.

Table 4.9   *P. infestans pathogenicity assays*

Summary of *Phytophthora infestans* disease assay on detached tomato leaves

	Infection 1	Infection 2	Infection 3	Infection 4
P. Infestans (strains)	88069	88069	88069, Td tom	Td tom
No. of plates	5	5	4	1
No. of leaves	8(40x)	8(40x)	8(32)	8(8)
Environment	growth chamber 18 °C	growth chamber 18°C	lab~20-25 °C	lab~20-25 °C
Data documentation	4-7dpi	3-6dpi	4-8dpi	10dpi
Methods	digital camera	digital camera microscope(GFP2)	microscope(DSR) microscope(GFP2)	microscope(DSR) microscope(GFP2)

References

Asai T., Tena G., Plotnikova J., Willmann M.R., Chiu W.-L., Gomez-Gomez L., Boller T., Ausubel F.M., Sheen J. (2002) MAP kinase signalling cascade in Arabidopsis innate immunity. Nature 415:977-983.

Avrova A.O., Stewart H.E., De Jong W., Heilbronn J., Lyon G.D., Birch P.R.J. (1999) A Cysteine Protease Gene Is Expressed Early in Resistant Potato Interactions with *Phytophthora infestan*. Molecular Plant-Microbe Interactions 12:1114-1119.

Bent A.F., Mackey D. (2007) Elicitors, Effectors, and *R* Genes: The New Paradigm and a Lifetime Supply of Questions. Annual Review of Phytopathology 45:399-436.

Boller T., Felix G. (2009) A Renaissance of Elicitors: Perception of Microbe-Associated Molecular Patterns and Danger Signals by Pattern-Recognition Receptors. Annual Review of Plant Biology 60:379-406.

Bolton M.D., Van Esse H.P., Vossen J.H., De Jonge R., Stergiopoulos I., Stulemeijer I.J.E., Van Den Berg G.C.M., Borrás-Hidalgo O., Dekker H.L., De Koster C.G., De Wit P.J.G.M., Joosten M.H.A.J., Thomma B.P.H.J. (2008) The novel *C. fulvum* lysin motif effector Ecp6 is a virulence factor with orthologues in other fungal species. Molecular Microbiology 69:119-136

Bond T.E.T. (1938) Infection experiments with *C. fulvum* cooke and related species. Annals of Applied Biology 25:277-307.

Bozkurt T.O., Schornack S., Win J., Shindo T., Ilyas M., Oliva R., Cano L.M., Jones A.M.E., Huitema E., van der Hoorn R.A.L., Kamoun S. (2011) *Phytophthora infestan* effector AVRblb2 prevents secretion of a plant immune protease at the haustorial interface. Proceedings of the National Academy of Sciences 108:20832-20837.

Brömme D. (2001) Papain-like Cysteine Proteases, Current Protocols in Protein Science, John Wiley & Sons, Inc.

Caldwell K.S., Michelmore R.W. (2009) *Arabidopsis thaliana* Genes Encoding Defense Signaling and Recognition Proteins Exhibit Contrasting Evolutionary Dynamics. Genetics 181:671-684.

Charrier B., Scollan C., Ross S., Zubko E., Meyer P. (2000) Co-silencing of homologous transgenes in tobacco. Molecular Breeding 6:407-419.

Chichkova N.V., Shaw J., Galiullina R.A., Drury G.E., Tuzhikov A.I., Kim S.H., Kalkum M., Hong T.B., Gorshkova E.N., Torrance L., Vartapetian A.B., Taliansky M. (2010) Phytaspase, a relocalisable cell death promoting plant protease with caspase specificity. EMBO J 29:1149-1161.

Chinchilla D., Zipfel C., Robatzek S., Kemmerling B., Nurnberger T., Jones J.D.G., Felix G., Boller T. (2007) A flagellin-induced complex of the receptor FLS2 and BAK1 initiates plant defense. Nature 448:497-500.

Chisholm S.T., Coaker G., Day B., Staskawicz B.J. (2006) Host-Microbe Interactions: Shaping the Evolution of the Plant Immune Response. Cell 124:803-814.

Chung E.-H., da Cunha L., Wu A.-J., Gao Z., Cherkis K., Afzal A.J., Mackey D., Dangl J.L. (2011) Specific Threonine Phosphorylation of a Host Target by Two Unrelated Type III Effectors Activates a Host Innate Immune Receptor in Plants. Cell Host & Microbe 9:125-136.

Dangl J.L., Jones J.D.G. (2001) Plant pathogens and integrated defence responses to infection. Nature 411:826-833.

de Jonge R., Peter van Esse H., Kombrink A., Shinya T., Desaki Y., Bours R., van der Krol S., Shibuya N., Joosten M.H.A.J., Thomma B.P.H.J. (2010) Conserved Fungal LysM Effector Ecp6 Prevents Chitin-Triggered Immunity in Plants. Science 329:953-955.

de Wit P.J.G.M. (1977) A light and scanning-electron microscopic study of infection of tomato plants by virulent and avirulent races of *C. fulvum*. European Journal of Plant Pathology 83:109-122.

Desveaux D., Singer A.U., Wu A.-J., McNulty B.C., Musselwhite L., Nimchuk Z., Sondek J., Dangl J.L. (2007) Type III Effector Activation via Nucleotide Binding, Phosphorylation, and Host Target Interaction. PLoS Pathog 3:e48.

Dixon M.S., Golstein C., Thomas C.M., van der Biezen E.A., Jones J.D.G. (2000) Genetic complexity of pathogen perception by plants: The example of *Rcr3*, a tomato gene required specifically by *Cf-2*. Proceedings of the National Academy of Sciences 97:8807-8814.

Dixon M.S., Hatzixanthis K., Jones D.A., Harrison K., Jones J.D.G. (1998) The Tomato *Cf-5* Disease Resistance Gene and Six Homologs Show Pronounced Allelic Variation in Leucine-Rich Repeat Copy Number. The Plant Cell Online 10:1915-1926.

Dixon M.S., Jones D.A., Keddie J.S., Thomas C.M., Harrison K., Jones J.D.G. (1996) The Tomato *Cf-2* Disease Resistance Locus Comprises Two Functional Genes Encoding Leucine-Rich Repeat Proteins. Cell 84:451-459

Dodds P.N., Rathjen J.P. (2010) Plant immunity: towards an integrated view of plant–pathogen interactions. Nat Rev Genet 11:539-548.

Dou D., Kale S.D., Wang X., Chen Y., Wang Q., Wang X., Jiang R.H.Y., Arredondo F.D., Anderson R.G., Thakur P.B., McDowell J.M., Wang Y., Tyler B.M. (2008) Conserved C-Terminal Motifs Required for Avirulence and Suppression of Cell Death by *Phytophthora sojae* effector Avr1b. The Plant Cell Online 20:1118-1133.

Drake R., John I., Farrell A., Cooper W., Schuch W., Grierson D. (1996) Isolation and analysis of cDNAs encoding tomato cysteine proteases expressed during leaf senescence. Plant Molecular Biology 30:755-767.

Drenth J., Jansonius J.N., Koekoek R., Swen H.M., Wolthers B.G. (1968) Structure of Papain. Nature 218:929-932.

Felix G., Duran J.D., Volko S., Boller T. (1999) Plants have a sensitive perception system for the most conserved domain of bacterial flagellin. The Plant Journal 18:265-276.

Flor H.H. (1956) The complementary genic systems in flax and flax rust. Molecular Genetic Medicine 8, 29-54.

Göhre V., Spallek T., Häweker H., Mersmann S., Mentzel T., Boller T., de Torres M., Mansfield J.W., Robatzek S. (2008) Plant Pattern-Recognition Receptor FLS2 Is Directed for Degradation by the Bacterial Ubiquitin Ligase AvrPtoB. Current Biology 18:1824-1832.

Gómez-Gómez L., Boller T. (2000) FLS2: An LRR Receptor–like Kinase Involved in the Perception of the Bacterial Elicitor Flagellin in Arabidopsis. Molecular Cell 5:1003-1011.

Greenbaum D., Medzihradszky K.F., Burlingame A., Bogyo M. (2000) Epoxide electrophiles as activity-dependent cysteine protease profiling and discovery tools. Chemistry & amp; Biology 7:569-581.

Haas B.J., Kamoun S., Zody M.C., Jiang R.H.Y., Handsaker R.E., Cano L.M., Grabherr M., Kodira C.D., Raffaele S., Torto-Alalibo T., Bozkurt T.O., Ah-Fong A.M.V., Alvarado L., Anderson V.L., Armstrong M.R., Avrova A., Baxter L., Beynon J., Boevink P.C., Bollmann S.R., Bos J.I.B., Bulone V., Cai G., Cakir C., Carrington J.C., Chawner M., Conti L., Costanzo S., Ewan R., Fahlgren N., Fischbach M.A., Fugelstad J., Gilroy E.M., Gnerre S., Green P.J., Grenville-Briggs L.J., Griffith J., Grunwald N.J., Horn K., Horner N.R., Hu C.-H., Huitema E., Jeong D.-H., Jones A.M.E., Jones J.D.G., Jones R.W., Karlsson E.K., Kunjeti S.G., Lamour K., Liu Z., Ma L., MacLean D., Chibucos M.C., McDonald H., McWalters J., Meijer H.J.G., Morgan W., Morris P.F., Munro C.A., O'Neill K., Ospina-Giraldo M., Pinzon A., Pritchard L., Ramsahoye B., Ren Q., Restrepo S., Roy S., Sadanandom A., Savidor A., Schornack S., Schwartz D.C., Schumann U.D., Schwessinger B., Seyer L., Sharpe T., Silvar C., Song J., Studholme D.J., Sykes S., Thines M., van de Vondervoort P.J.I., Phuntumart V., Wawra S., Weide R., Win J., Young C., Zhou S., Fry W., Meyers B.C., van West P., Ristaino J., Govers F., Birch P.R.J., Whisson S.C., Judelson H.S., Nusbaum C. (2009) Genome sequence and analysis of the Irish potato famine pathogen *Phytophthora infestan*. Nature 461:393-398

Halterman D.A., Chen Y., Sopee J., Berduo-Sandoval J., Sánchez-Pérez A. (2010) Competition between *Phytophthora infestan*Effectors Leads to Increased Aggressiveness on Plants Containing Broad-Spectrum Late Blight Resistance. PLoS ONE 5:e10536.

Harrak H., Azelmat S., Baker E.N., Tabaeizadeh Z. (2001) Isolation and characterization of a gene encoding a drought-induced cysteine protease in tomato (*Lycopersicon esculentum*). Genome 44:368-374.

Hayashi F., Smith K.D., Ozinsky A., Hawn T.R., Yi E.C., Goodlett D.R., Eng J.K., Akira S., Underhill D.M., Aderem A. (2001) The innate immune response to bacterial flagellin is mediated by Toll-like receptor 5. Nature 410:1099-1103.

Heath M.C. (2000) Nonhost resistance and nonspecific plant defences. Current Opinion in Plant Biology 3:315-319.

Hogenhout S.A., Bos J.I.B. (2011) Effector proteins that modulate plant–insect interactions. Current Opinion in Plant Biology 14:422-428.

Hörger A. (2011) Evolution of disease resistance genes in wild tomato species. In Section of Evolutionary Biology, vol. PhD. Munich: Ludwig-Maximilians-University.

Jia Y., McAdams S.A., Bryan G.T., Hershey H.P., Valent B. (2000) Direct interaction of resistance gene and avirulence gene products confers rice blast resistance. EMBO J 19:4004-4014.

Jones J.D.G., Dangl J.L. (2006) The plant immune system. Nature 444:323-329.

Joosten M., de Wit P. (1999) The Tomato–*C. fulvum* interaction: A Versatile Experimental System to Study Plant-Pathogen Interactions. Annual Review of Phytopathology 37:335-367.

Kamoun S. (2007) Groovy times: filamentous pathogen effectors revealed. Current Opinion in Plant Biology 10:358-365.

Kamoun S., Smart C.D. (2005) Late Blight of Potato and Tomato in the Genomics Era. Plant Disease 89:692-699.

Kaschani F., Shabab M., Bozkurt T., Shindo T., Schornack S., Gu C., Ilyas M., Win J., Kamoun S., van der Hoorn R.A.L. (2010) An Effector-Targeted Protease Contributes to Defence against *Phytophthora infestan* and Is under Diversifying Selection in Natural Hosts. Plant Physiology 154:1794-1804.

Kim H.-S., Desveaux D., Singer A.U., Patel P., Sondek J., Dangl J.L. (2005) The *Pseudomonas syringae* effector AvrRpt2 cleaves its C-terminally acylated target, RIN4, from Arabidopsis membranes to block RPM1 activation. Proceedings of the National Academy of Sciences of the United States of America 102:6496-6501.

Krüger J., Thomas C.M., Golstein C., Dixon M.S., Smoker M., Tang S., Mulder L., Jones J.D.G. (2002) A Tomato Cysteine Protease Required for *Cf-2*-Dependent Disease Resistance and Suppression of Autonecrosis. Science 296:744-747.

Lazarovits G., Higgins V.J. (1976) Histological comparison of *C. fulvum* race 1 on immune, resistant, and susceptible tomato varieties. Canadian Journal of Botany 54:224-234.

Lipka U., Fuchs R., Kuhns C., Petutschnig E., Lipka V. (2010) Live and let die – Arabidopsis nonhost resistance to powdery mildews. European Journal of Cell Biology 89:194-199.

Lipka V., Kwon C., Panstruga R. (2007) SNARE-Ware: The Role of SNARE-Domain Proteins in Plant Biology. Annual Review of Cell and Developmental Biology 23:147-174.

Mackey D., Belkhadir Y., Alonso J.M., Ecker J.R., Dangl J.L. (2003) Arabidopsis RIN4 Is a Target of the Type III Virulence Effector AvrRpt2 and Modulates RPS2-Mediated Resistance. Cell 112:379-389.

Mackey D., Holt Iii B.F., Wiig A., Dangl J.L. (2002) RIN4 Interacts with *Pseudomonas syringae* Type III Effector Molecules and Is Required for RPM1-Mediated Resistance in Arabidopsis. Cell 108:743-754.

Mészáros T., Helfer A., Hatzimasoura E., Magyar Z., Serazetdinova L., Rios G., Bardóczy V., Teige M., Koncz C., Peck S., Bögre L. (2006) The Arabidopsis MAP kinase kinase MKK1 participates in defence responses to the bacterial elicitor flagellin. The Plant Journal 48:485-498.

Meyers B.C., Kozik A., Griego A., Kuang H., Michelmore R.W. (2003) Genome-Wide Analysis of NBS-LRR–Encoding Genes in Arabidopsis. The Plant Cell Online 15:809-834.

Misas-Villamil J.C., van der Hoorn R.A.L. (2008) Enzyme–inhibitor interactions at the plant–pathogen interface. Current Opinion in Plant Biology 11:380-388.

Nakazato T., Warren D.L., Moyle L.C. (2010) Ecological and geographic modes of species divergence in wild tomatoes. American Journal of Botany 97:680-693.

Nimchuk Z., Eulgem T., Holt III B.F., Dangl J.L. (2003) Recognition and response in the plant immune system. Annual Review of Genetics 37:579-609.

Nurnberger T., Lipka V. (2005) Non-host resistance in plants: new insights into an old phenomenon. Molecular Plant Pathology 6:335-345.

Ortlund E.A., Bridgham J.T., Redinbo M.R., Thornton J.W. (2007) Crystal Structure of an Ancient Protein: Evolution by Conformational Epistasis. Science 317:1544-1548.

Petutschnig E.K., Jones A.M.E., Serazetdinova L., Lipka U., Lipka V. (2010) The Lysin Motif Receptor-like Kinase (LysM-RLK) CERK1 Is a Major Chitin-binding Protein in *Arabidopsis thaliana* and Subject to Chitin-induced Phosphorylation. Journal of Biological Chemistry 285:28902-28911.

Rairdan G., Moffett P. (2007) Brothers in arms? Common and contrasting themes in pathogen perception by plant NB-LRR and animal NACHT-LRR proteins. Microbes and Infection 9:677-686.

Rehmany A.P., Gordon A., Rose L.E., Allen R.L., Armstrong M.R., Whisson S.C., Kamoun S., Tyler B.M., Birch P.R.J., Beynon J.L. (2005) Differential Recognition of Highly Divergent Downy Mildew Avirulence Gene Alleles by *RPP1* Resistance Genes from Two Arabidopsis Lines. The Plant Cell Online 17:1839-1850.

Richau K.H., Kaschani F., Verdoes M., Pansuriya T.C., Niessen S., Stüber K., Colby T., Overkleeft H.S., Bogyo M., Van der Hoorn R.A.L. (2012) Subclassification and Biochemical Analysis of Plant Papain-Like Cysteine Proteases Displays Subfamily-Specific Characteristics. Plant Physiology 158:1583-1599.

Rooney H.C.E., van't Klooster J.W., van der Hoorn R.A.L., Joosten M.H.A.J., Jones J.D.G., de Wit P.J.G.M. (2005) Cladosporium Avr2 Inhibits Tomato *Rcr3* Protease Required for *Cf-2*-Dependent Disease Resistance. Science 308:1783-1786.

Sambrook J., Fritsch, E.F., and Maniiatis, T. (1989) Moloecular cloning: A Laboratory manual. (NY: Cold Spring Harbor Laboratory).

Schaffer M.A., Fischer R.L. (1988) Analysis of mRNAs that Accumulate in Response to Low Temperature Identifies a Thiol Protease Gene in Tomato. Plant Physiology 87:431-436.

Schornack S., van Damme M., Bozkurt T.O., Cano L.M., Smoker M., Thines M., Gaulin E., Kamoun S., Huitema E. (2010) Ancient class of translocated oomycete effectors targets the host nucleus. Proceedings of the National Academy of Sciences 107:17421-17426.

Schulze-Lefert P., Panstruga R. (2011) A molecular evolutionary concept connecting nonhost resistance, pathogen host range, and pathogen speciation. Trends in Plant Science 16:117-125.

Schwessinger B., Zipfel C. (2008) News from the frontline: recent insights into PAMP-triggered immunity in plants. Current Opinion in Plant Biology 11:389-395.

Shabab M., Shindo T., Gu C., Kaschani F., Pansuriya T., Chintha R., Harzen A., Colby T., Kamoun S., van der Hoorn R.A.L. (2008) Fungal Effector Protein AVR2 Targets Diversifying Defense-Related Cys Proteases of Tomato. The Plant Cell Online 20:1169-1183.

Shindo T., Van Der Hoorn R.A.L. (2008) Papain-like cysteine proteases: key players at molecular battlefields employed by both plants and their invaders. Molecular Plant Pathology 9:119-125.

Song J., Win J., Tian M., Schornack S., Kaschani F., Ilyas M., van der Hoorn R.A.L., Kamoun S. (2009) Apoplastic effectors secreted by two unrelated eukaryotic plant pathogens target the tomato defense protease Rcr3. Proceedings of the National Academy of Sciences 106:1654-1659.

Takken F.L.W., Albrecht M., Tameling W.I.L. (2006) Resistance proteins: molecular switches of plant defence. Current Opinion in Plant Biology 9:383-390.

Taylor M.A.J., Baker K.C., Briggs G.S., Connerton I.F., Cummings N.J., Pratt K.A., Revell D.F., Freedman R.B., Goodenough P.W. (1995) Recombinant pro-regions from papain and papaya proteinase IV are selective high affinity inhibitors of the mature papaya enzymes. Protein Engineering 8:59-62.

Thordal-Christensen H. (2003) Fresh insights into processes of nonhost resistance. Current Opinion in Plant Biology 6:351-357.

Tian M., Benedetti B., Kamoun S. (2005) A Second Kazal-Like Protease Inhibitor from *Phytophthora infestan* Inhibits and Interacts with the Apoplastic Pathogenesis-Related Protease P69B of Tomato. Plant Physiology 138:1785-1793.

Tian M., Huitema E., da Cunha L., Torto-Alalibo T., Kamoun S. (2004) A Kazal-like Extracellular Serine Protease Inhibitor from *Phytophthora infestan* Targets the Tomato Pathogenesis-related Protease P69B. Journal of Biological Chemistry 279:26370-26377.

Tian M., Win J., Song J., van der Hoorn R., van der Knaap E., Kamoun S. (2007) A *Phytophthora infestan* Cystatin-Like Protein Targets a Novel Tomato Papain-Like Apoplastic Protease. Plant Physiology 143:364-377.

van den Burg H.A., Harrison S.J., Joosten M.H.A.J., Vervoort J., de Wit P.J.G.M. (2006) *C. fulvum* Avr4 Protects Fungal Cell Walls Against Hydrolysis by Plant Chitinases Accumulating During Infection. Molecular Plant-Microbe Interactions 19:1420-1430.

van der Hoorn R.A.L., Kamoun S. (2008) From Guard to Decoy: A New Model for Perception of Plant Pathogen Effectors. The Plant Cell Online 20:2009-2017.

van der Hoorn R.A.L., Leeuwenburgh M.A., Bogyo M., Joosten M.H.A.J., Peck S.C. (2004) Activity Profiling of Papain-Like Cysteine Proteases in Plants. Plant Physiology 135:1170-1178.

van der Linde K., Hemetsberger C., Kastner C., Kaschani F., van der Hoorn R.A.L., Kumlehn J., Doehlemann G. (2012) A Maize Cystatin Suppresses Host Immunity by Inhibiting Apoplastic Cysteine Proteases. The Plant Cell Online.

van Esse H.P., van't Klooster J.W., Bolton M.D., Yadeta K.A., van Baarlen P., Boeren S., Vervoort J., de Wit P.J.G.M., Thomma B.P.H.J. (2008) The *C. fulvum* Virulence Protein Avr2 Inhibits Host Proteases Required for Basal Defense. The Plant Cell Online 20:1948-1963.

van Loon L.C., Rep M., Pieterse C.M.J. (2006) Significance of Inducible Defense-related Proteins in Infected Plants. Annual Review of Phytopathology 44:135-162.

Vleeshouwers V.G.A.A., Raffaele S., Vossen J.H., Champouret N., Oliva R., Segretin M.E., Rietman H., Cano L.M., Lokossou A., Kessel G., Pel M.A., Kamoun S. (2011) Understanding and Exploiting Late Blight Resistance in the Age of Effectors. Annual Review of Phytopathology 49:507-531.

Voinnet O., Rivas S., Mestre P., Baulcombe D. (2003) An enhanced transient expression system in plants based on suppression of gene silencing by the p19 protein of tomato bushy stunt virus. The Plant Journal 33:949-956.

Wang Z., Gu C., Colby T., Shindo T., Balamurugan R., Waldmann H., Kaiser M., van der Hoorn R.A.L. (2008) [beta]-Lactone probes identify a papain-like peptide ligase in Arabidopsis thaliana. Nat Chem Biol 4:557-563.

Xia Y., Suzuki H., Borevitz J., Blount J., Guo Z., Patel K., Dixon R.A., Lamb C. (2004) An extracellular aspartic protease functions in Arabidopsis disease resistance signaling. EMBO J 23:980-988.

Yamada K., Matsushima R., Nishimura M., Hara-Nishimura I. (2001) A Slow Maturation of a Cysteine Protease with a Granulin Domain in the Vacuoles of Senescing Arabidopsis Leaves. Plant Physiology 127:1626-1634.

Zipfel C., Kunze G., Chinchilla D., Caniard A., Jones J.D.G., Boller T., Felix G. (2006) Perception of the Bacterial PAMP EF-Tu by the Receptor EFR Restricts Agrobacterium-Mediated Transformation. Cell 125:749-760.
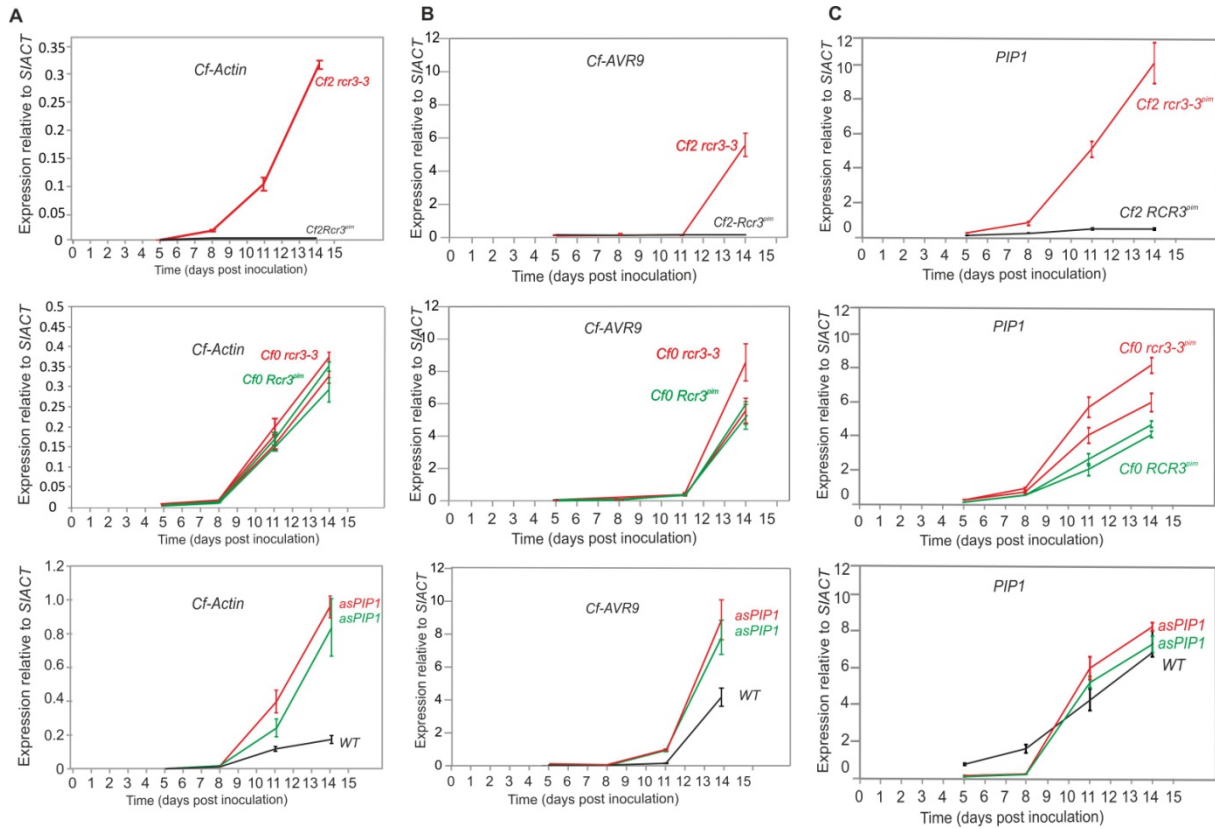
Figure S1 | Transcript levels of *C. fulvum Actin, Avr9* and tomato *PIP1*

Transcript levels relative to tomato actin (*SlACT*) were determined by quantitative real-time PCR on cDNA isolated at various time after inoculation. Relative transcript levels were measured for *C. fulvum Actin* (A) *C. fulvum AVR9* (B) and tomato *PIP1* (C), for *Cf2/RCR3*pim vs. *Cf2/rcr3-3*pim (top), *Cf0/RCR3*pim and *Cf0/rcr3-3*pim (middle) and *asPIP1* and *WT* (bottom). Bar represent the standard error of three leaflets taken from three plants at each time point analyzed. This experiment was repeated three times with similar results.

	Day 4-5		Day 6-8	
	P value	Significant (P<0.05)	P value	Significant (P<0.05)
Cf2/RCR3^{pim} vs. Cf2/rcr3-3^{pim}	0.000308358	Yes	0.010140297	Yes
Cf2/RCR3^{pim} vs. Cf0/RCR3^{pim}	0.659010372	No	0.29211038	No
Cf2/RCR3^{pim} vs. Cf0/rcr3-3^{pim}	0.090679458	No	0.405761111	No
Cf2/rcr3-3^{pim} vs. Cf0/RCR3^{pim}	0.011832972	Yes	0.045578745	Yes
Cf2/rcr3-3^{pim} vs. Cf0/rcr3-3^{pim}	0.279884813	No	0.102167756	No
Cf0/RCR3^{pim} vs. Cf0/rcr3-3^{pim}	0.03296539	Yes	0.02071878	Yes

Figure S2 | ANOVA analysis of lesion growth area

Statistically significance of the lesion growth rate between treatments upon *P. infestans* inoculation assay. Eight comparisons of four genotypes were made for six data sets in the day post inoculation 4-6 and 6-8. *P*-values were obtained by student T-test and values less than 0.05 were considered to be statistically significant by subtracting the lesion size measured at one day earlier from the next day.
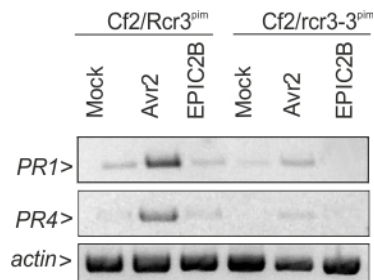
Figure S3 | Unlike Avr2, Epic2B does not induce the expression of *PR1* in

Cf2/Rcr3^{pim} tomato

RT-PCR analysis of pathogenesis-related *PR1* gene in tomato after infiltration with purified Avr2 and Epic2B. Total RNA isolated from infiltrated leaves of *Cf2/Rcr3^{pim}* and *Cf2/rcr3–3^{pim}* tomato was used in RT-PCR amplifications. Amplification of tomato *actin* was used as constitutive controls to determine the relative expression of the *PR1* genes.
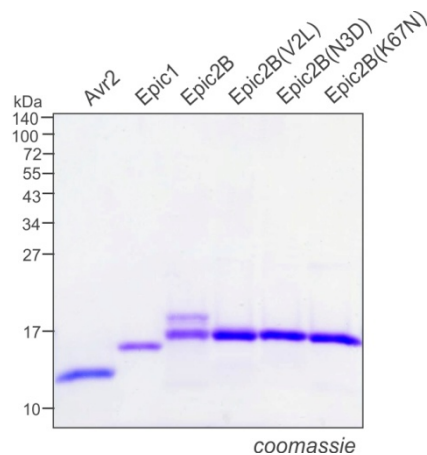

Figure S4 | Purified FLAG-tagged Avr2, Epics and Epic2B mutant proteins

FLAG-tagged affinity purified using anti-FLAG resin are shown. FLAG-tagged Avr2, Epic1, Epic2B and 3x Epic2B mutants were expressed in *E. coli,* supernatant were collected, and protein expression was evaluated by Western blot and analyzed on 15-17 % SDS/PAGE gel followed by coomassie. The size (kDa) of the molecular weight markers is shown on the left.
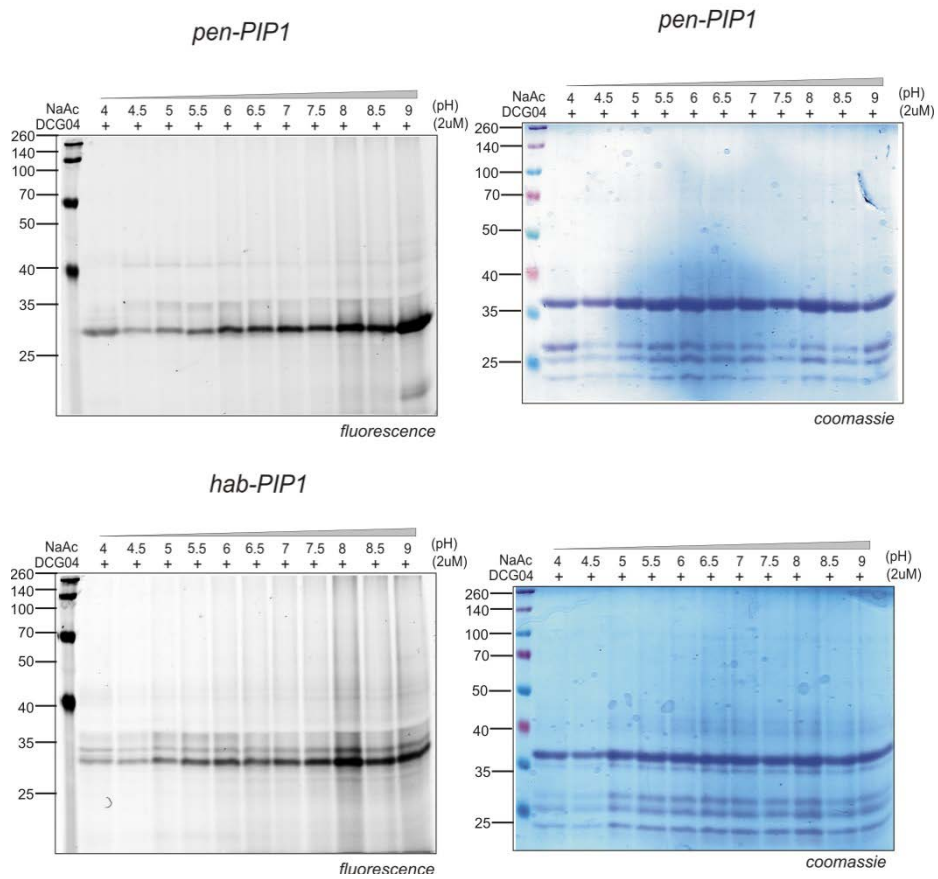
Figure S5 | Labeling of PIP1 at different pH

Transiently overexpressed PIP1 by agroinfiltration in *N. benthamiana* (apoplastic fluid) was labeled at different pH values for two hours and separated on 12% SDS/PAGE gel following fluorescent scanning.

Acknowledgment:

First of all Thank to Allah Almighty who blessed me with courage and power to complete this thesis. And all respect to Holy Prophet Hazrat Muhammad (PBUH) for paving us on the right path with the essence of faith in Allah.

I would like to express my warmest thanks to my supervisor **Dr. Renier van der Hoorn** who extended all facilities and provided inspiring guidance for the successful completion of my research work. I deem it as my privilege to work under his guidance. I appreciate all his contributions of time and ideas to make my Ph.D., experienced, productive and stimulating. I am especially thankful for his help in critically reading and correction of this thesis.

I would like to thank **Prof. Dr. Paul Schulze-Lefert**, for accepting me as a PhD student at MPIPZ. I would like to thank **Prof. Dr. Ulf-Ingo Flügge**, **Prof. Dr. Ute Höcker**, **Dr. Matthieu Joosten** (Wageningen University, The Netherlands) and Dr. Imre Somssich for kindly joining my Ph.D. thesis committee.

Collective and individual acknowledgments are also owed to my colleagues at MPIPZ. Thanks to past and present group members **Farnusch, Christian, Takayuki, Kerstin, Adriana, Johanna, Leonard, Aimone, Haibin, Tram, Oscar, Gerald, Joji** and **Nikola** for good time, moods and fruitful discussions related to science and beyond science. I am grateful to **Selva Kumari** for her help in green house, encouraging discussions, entertaining, and also nice time in Cologne. I feel tremendously lucky to have had the opportunity to work with **Anja Hörger**. I am grateful to her for the thoughtful comments and wonderful suggestions during thesis writing.

I owe my gratitude to **Dr. Sophien Kamoun**, The Sainsbury Laboratory (TSL), John Innes Centre, Norwich, UK; it is a pleasure to collaborate with him. All lab fellows at TSL in particular, thanks goes to **Joe, Tolga, Sebastian** and **Liliana** who introduced me world of *P. infestans*.

I am particularly grateful to **Astrid Oehl** and **Karin Davidson** for growing more than 2000 tomato plants in green house throughout this project.

Erklärung

Köln, 2012

Ich versichere, dass ich die von mir vorgelegte Dissertation selbständig angefertigt, die benutzen Quellen und Hilfsmittel vollständig angegeben und die Stellen der Arbeit- einschließlich Tabellen, Karten und Abbildungen -, die anderen Werken mit Wortlaut oder dem Sinn nach entnommen sind, in jedem Einzelfall als Entlehnung kenntlich gemacht habe; dass diese Dissertation noch keiner anderen Fakultät oder universität zur Prüfung vorgelegen hat; dass sie noch nicht veröffentlicht worden ist, sowie dass ich eine solche Veröffentlichung vor Abschluss des Promotionsverfahrens nicht vornehmen werde. Die Bestimmungen der Promotionsordnung sind mir bekannt. Die von mir vorgelegte Dissertation ist von Prof. Dr. Paul Schulze-Lefert betreut worden.

Max-Planck Institut für Pflanzenzüchtungsforschung,

Köln, 16 Juni 2014 _____

Muhammad Ilyas

Lebenslauf

Persönliche Daten:

Vorname:	Muhammad
Nachname:	Ilyas
Anschrift:	Max Planck Institut für Pflanzenzüchtung
	Carl-von-Linne Weg 10, D-50829 Köln, Deutschland
Büro:	+49 221 5062 276
E-Mail:	ilyas@mpipz.mpg.de

Ausbildung:

April 2008- Juni 2014   PhD student (DAAD fellowship)

Max Planck Institute for Plant Breeding Research

Cologne Germany.

Abschlussarbeit:

"*The role of papain-like cysteine proteases of tomato in pathogen* defense.*"*

Dez 2002-März 2004 M.Sc. (Hons) Agriculture (Plant Breeding and Genetics)

University of Agriculture Faisalabad, Pakistan

Abschlussarbeit: "*Cloning and transformation of replicase gene of cotton leaf curl virus DNA-A under cassava vein mosaic virus (CsVMV) promoter*".

Publikationen:

1. Ilyas, S., **Ilyas, M**., Van der Hoorn, R. A. L., and Mathur, S. **(2013)** Selective conjugation of proteins in mining the active proteome through click-functionalized magnetic nanoparticles. **ACS Nano** 7, 9655-9663.

2. Hörger A. C., **Ilyas, M**., Stephan, W., Tellier, A., Van der Hoorn, R. A.L and Laura E. Rose. **(2012)** Balancing selection at the tomato RCR3 gene family maintains variation in strength of pathogen defense. **PLoS Genetics** 8, e1002813.

3. Lozano-Torres, J., Wilbers, Ruud H. P., Gawronski, P., Boshoven, J., van't Klooster, J. W., H., Baranowski, L., **Ilyas, M**., Van der Hoorn, R. A.L., Schots, A., de Wit, Pierre J. G. M., Bakker, J., Goverse, A., and Smant G. **(2012)** Dual Cf-2-mediated resistance in tomato requires a common virulence target of two plant pathogens. **Proc. Natl. Acad. Sci. USA** 109, 10119-10124.

4. Bozkurt, T., Schornack, S., Win, J., Shindo, T., **Ilyas, M.**, Oliva, R., Cano, L., Jones, A. M. E., Huitema, E., Van der Hoorn, R. A. L, and Sophien Kamoun**, (2011)** *Phytophthora infestans effector AVRblb2 prevents focal secretion of a plant immune protease. **Proc. Natl. Acad. Sci. USA** 108, 20832-20837.*

5. Kaschani, F., Shabab, M., Bozkurt, T., Shindo, T., Schornack, S., Gu, C., **Ilyas, M.**, Win, J., Kamoun, S., and Van der Hoorn, R. A. L. **(2010)** *An effector-targeted protease contributes to defense against Phytophthora infestans and is under diversifying selection in natural hosts.* **Plant Physiol.** 154, 1794-1804.

6. Van der Hoorn, R. A. L., Gu, C**., Ilyas, M.,** Kolodziejek, I., Kumari, S., Misas- Villamil, J. C., Pruzinska, A., Richau, K., Shabab, M., Shindo, T., Wang, Z. and Kaschani, F. (2010) *Mining the active proteome in plant-pathogen interactions.* In: Biology of Plant-Microbe Interactions, Volume 7. H. Antound, T. Avis, L. Brisson, D. Prevost, and M. Trepanier, eds. International Society for Molecular Plant-Microbe Interactions, St. Paul, MN.

7. Song, J., Win, J., Tian, M., Schornack, S., Kaschani, F., **Ilyas, M.**, Van der Hoorn, R. A. L., and Kamoun, S. **(2009)** *Apoplastic effectors secreted by two unrelated eukaryotic plant pathogens target the tomato defense protease RCR3.* **Proc. Natl. Acad. Sci. USA** 106, 1654-1659.

8. **Ilyas, M.**, Naveed, M., Khan, T, M and Khan, I, A. **(2007)** *Combining Ability Studies in Some Quantitative and Qualitative Traits of Gossypium hirsutum* L. **Journal of Agriculture & Social Sciences**, 03-02-39-42.

9. Naveed, M., Mukhtar, N., Farooq, J., **Ilyas, M.**, and Islam, N, U. **(2006)** *Evaluation of some new strains of Gossypium hirsutum* L. *for yield stability across environments.* **Journal of Agriculture & Social Sciences**, 02-01-17-19.

10. Mukhtar, N., Azhar, F, M., Naveed, M., and **Ilyas, M. (2005)** *Effect of combining ability on Intra-hirsutum variation in seed cotton yield and its components.* **The Indus Cottons**, Vol.2, No.3, 172-177.

Wissenschaftliche Leistungen:

1. Botaniker Tagung Conference 18-23 September 2011- Berlin- Germany **2011**

2. 2nd PhD Retreat in Plant Sciences at Max Planck Institute for Plant Breeding Research, Cologne Germany, 15-17 April 2010 **(won 1st poster prize- EMBO Journal Subscription for year 2010-11)**

3. Chemical Proteomics Meeting Leiden the Netherlands at Leiden Institute of Chemistry, Gorlaeus Laboratories, 1-2 October **2009**

4. IS-MPMI international congress, Quebec, Canada, 19-23 July **2009**

5. 5th Solanaceae Genome Workshop 'SOL2008' Cologne Germany, 12-16 October **2008**